AFWAL-TR-88-4085

DTIC FILE COPY

AD-A197 834

COMPOSITE CURING PROCESS NONDESTRUCTIVE EVALUATION

P.W. Harruff, R.L. Levy, R.T. Harrold, Z.N. Sanjana and S. Schwab
McDonnell Douglas Corporation
McDonnell Aircraft Company
P.O. Box 516, St. Louis, MO 63166

June 1988

Final Report for Period September 1985 - December 1987

Approved for Public Release: Distribution Is Unlimited

MATERIALS LABORATORY
AIR FORCE WRIGHT AERONAUTICAL LABORATORIES
Air Force Systems Command
Wright-Patterson Air Force Base, Ohio 45433-6533

NOTICE

When Government drawings, specifications, or other data are used for any purpose other than in connection with a definitely Government-related procurement, the United States Government incurs no responsibility or any obligation whatsoever. The fact that the Government may have formulated or in any way supplied the said drawings, specifications, or other data, is not to be regarded by implication, or otherwise in any manner construed, as licensing the holder, or any other person or corporation; or as conveying any rights or permission to manufacture, use, or sell any patented invention that may in any way be related thereto.

This report has been reviewed by the Office of Public Affairs (ASD/PA) and is releasable to the National Technical Information Service (NTIS). At NTIS, it will be available to the general public, including foreign nations.

This technical report has been reviewed and is approved for publication.

JOSEPH A. MOYZIS, JR.
Technical Area Manager
Nondestructive Evaluation Branch
Metals and Ceramics Division
FOR THE COMMANDER

D. M. FORNEY, JR., Chief
Nondestructive Evaluation Branch
Metals and Ceramics Division

If your address has changed, if you wish to be removed from our mailing list, or if the addressee is no longer employed by your organization please notify AFWAL/MLLP, Wright-Patterson AFB, OH 45433-6533 to help us maintain a current mailing list.

Copies of this report should not be returned unless return is required by security considerations, contractual obligations, or notice on a specific document.

UNCLASSIFIED
SECURITY CLASSIFICATION OF THIS PAGE

REPORT DOCUMENTATION PAGE

1a. REPORT SECURITY CLASSIFICATION UNCLASSIFIED	1b. RESTRICTIVE MARKINGS
2a. SECURITY CLASSIFICATION AUTHORITY	3. DISTRIBUTION / AVAILABILITY OF REPORT Approved for Public Release; distribution is unlimited
2b. DECLASSIFICATION / DOWNGRADING SCHEDULE	
4. PERFORMING ORGANIZATION REPORT NUMBER(S)	5. MONITORING ORGANIZATION REPORT NUMBER(S) AFWAL-TR-88-4085
6a. NAME OF PERFORMING ORGANIZATION McDonnell Douglas Aircraft Company 6b. OFFICE SYMBOL (If applicable) MCAIR/MDRL	7a. NAME OF MONITORING ORGANIZATION Materials Laboratory (AFWAL/MLLP) Air Force Wright Aeronautical Laboratories
6c. ADDRESS (City, State, and ZIP Code) P. O. Box 516 St. Louis, MO 63166	7b. ADDRESS (City, State, and ZIP Code) Wright-Patterson AFB, OH 45433-6533
8a. NAME OF FUNDING / SPONSORING ORGANIZATION 8b. OFFICE SYMBOL (If applicable)	9. PROCUREMENT INSTRUMENT IDENTIFICATION NUMBER F33615-85-C-5024
8c. ADDRESS (City, State, and ZIP Code)	10. SOURCE OF FUNDING NUMBERS PROGRAM ELEMENT NO. 62102F; PROJECT NO. 2418; TASK NO. 02; WORK UNIT ACCESSION NO. 28

11. TITLE (Include Security Classification)
Composite Curing Process Nondestructive Evaluation

12. PERSONAL AUTHOR(S)
P.W. Harruff, R.L. Levy, R.T. Harrold, Z.N. Sanjana, S. Schwab

13a. TYPE OF REPORT	13b. TIME COVERED	14. DATE OF REPORT (Year, Month, Day)	15. PAGE COUNT
Final	FROM 9/85 TO 12/87	June 1988	122

16. SUPPLEMENTARY NOTATION

(Key words)

17. COSATI CODES			18. SUBJECT TERMS (Continue on reverse if necessary and identify by block number)
FIELD	GROUP	SUB-GROUP	
11	04		Composite, Cure Cycle, Monitoring Techniques, Cure Parameter, Cure Sensor, Fluorescence Optrode, Acoustic Waveguide, Pressure Sensor, Data Presentation. (JES)
14	02		

19. ABSTRACT (Continue on reverse if necessary and identify by block number)

The objective of this program was to develop nondestructive evaluation techniques that can be used for in-process monitoring of the 350°F carbon/epoxy cure cycle. The techniques developed should have the capability of measuring composite material properties that can be used as a real time measure of the state of composite cure.

Fluorescence Optrode and Acoustic Waveguide sensors were selected for development as cure-monitoring techniques. Miniature pressure sensors were also evaluated for tracking laminate resin hydrostatic pressures. Development efforts undertaken to establish optimum sensor responses, evaluate sensor-laminate interface methods, establish factory-capable data acquisition and presentation systems, determine sensor response-material property relationships, and demonstrate sensor capability for monitoring typical autoclave composite cure cycles are described. Results of development and demonstration tasks are discussed with respect to current and future application to cure-monitoring technology.

20. DISTRIBUTION / AVAILABILITY OF ABSTRACT	21. ABSTRACT SECURITY CLASSIFICATION
☐ UNCLASSIFIED/UNLIMITED ☐ SAME AS RPT. ☒ DTIC USERS	UNCLASSIFIED

22a. NAME OF RESPONSIBLE INDIVIDUAL	22b. TELEPHONE (Include Area Code)	22c. OFFICE SYMBOL
Dr. J. Moyzis	(513) 255-5309	AFWAL/MLLP

DD FORM 1473, 84 MAR — 83 APR edition may be used until exhausted. All other editions are obsolete.

SECURITY CLASSIFICATION OF THIS PAGE
UNCLASSIFIED

SUMMARY

The objective of this program was to identify, develop and evaluate new in-process monitoring techniques for the cure of 350°F curing carbon/epoxy composite materials.

Current manufacturing practices for high quality composite structures are characterized by high cost learning curves, labor-intensive procedures and lack of in-process control of cure cycles. Ongoing processing science programs have been successful in achieving a fundamental understanding of composite curing processes. However, no satisfactory method has been found for real-time monitoring and control of the cure cycle. The work funded under this program was meant to develop new nondestructive evaluation (NDE) techniques, and to evaluate the potential of these systems for real-time cure monitoring and control.

Two sensor systems, fluorescence optrode cure sensor (FOCS) and acoustic waveguide (AWG), were selected based upon laboratory tests that indicated their sensitivity to changes occurring during the cure of epoxy resins. The use of miniature pressure sensors was evaluated for in-process cure pressure monitoring and to help predict void formation. The following program approach was followed: (1) establish optimum sensor performance for cure monitoring; (2) determine the relationship of sensor responses to resin properties during composite cure cycles; (3) establish degree of reproducibility; and (4) demonstrate the capability for control of autoclave curing of composites.

The cure-monitoring capability of the FOCS, which was developed at McDonnell Douglas, is based upon the viscosity/degree-of-cure dependence of resin fluorescence. A second-generation FOCS, which simultaneously measures resin fluorescence intensity and wavelength, was used to monitor the cure of AS4/3501-6 laminates. A tool-mounted optrode and data acquisition system were developed that are capable of use in composite manufacturing. Hardware and software systems were improved to achieve higher sensitivity.

The AWG system, developed by Westinghouse, monitors acoustic waves which are transmitted along waveguides in the curing resin and attenuated to varying degrees due to changes in the surrounding medium. Various materials were evaluated for the waveguide itself. The effects of laminate configuration and voids upon sensor response were studied. It was found that the shape and attenuation of the response signal curve was dependent upon carbon fiber orientations within the vicinity of the waveguide. Voids within a laminate appeared to result in increased attenuation. In both neat resin and carbon/epoxy cure cycles, the signal response curves pinpoint the resin gelation event and show some correlation with degree of cure.

The effect of location of miniature pressure sensors within the laminate was evaluated. Significant differences in resin hydrostatic pressure were found to result from layup variations as well as location.

Sensor responses were monitored during isothermal cures of AS4/3501-6 laminates and results compared statistically with changes in resin viscosity and degree-of-cure as predicted by a computer model. Mathematical relationships between FOCS signal profiles and material properties were established,

although there was significant data scatter. There was even more scatter in the AWG-monitored isothermal cures, and direct mathematical relationships between sensor response and material properties data were not evident. However, an event that probably relates to resin gelation was identified reproducibly.

A series of seven laminates was cured in a laboratory autoclave, with both FOCS and AWG sensors installed, to demonstrate the ability to follow material property changes through a variety of different cure cycles. AWG signal responses were highly attenuated in the autoclave environment; excessive signal loss resulted in an inability to monitor cure parameters. Correlation between FOCS signal profiles and material properties was similar to that obtained in laboratory runs.

Results of laboratory experiments demonstrated the feasibility of the AWG system for following resin cures; however, implementation into autoclave cure environments was not achieved due to hardware-induced attentuation of sensor signals. The effects of carbon/epoxy laminate variables also need to be defined. The ability to detect the resin gelation event was strongly indicated.

The FOCS system can be successfully interfaced with autoclave cure environments. Although the ability to follow cure cycles was demonstrated, additional efforts are necessary to reduce data scatter and define sensor data/material properties relationships before FOCS can be used for production cure control.

It is recommended that further research be conducted to better understand the material property relationships inherent in the FOCS and AWG cure-monitoring concepts. In addition, further work should be undertaken to identify and eliminate sources of attenuation of the acoustic signal.

PREFACE

This report was prepared by Mr. Paul W. Harruff (McDonnell Aircraft Company), Dr. Ram L. Levy and Dr. Scott Schwab (McDonnell Douglas Research Laboratories), Mr. Ronald T. Harrold and Mr. Zal N. Sanjana (Westinghouse Electric Company, Research and Development Center), who are co-authors. Work was performed under Contract Number F33615-85-C-5024 by McDonnell Douglas Corporation, McDonnell Aircraft Company and McDonnell Douglas Research Laboratories divisions, St. Louis Missouri. Major subcontract efforts were performed by Westinghouse R&D Center, Pittsburgh, Pennsylvania. Mr. Paul M. Stifel was Program Manager for McDonnell Aircraft Co. The work was administered under the direction of the Air Force Wright Aeronautical Laboratories/Materials Laboratory. Dr. Joseph Moyzis (AFWAL/MLLP) was the Air Force Project Engineer. The program was conducted during the period of 13 September 1985 through 12 December 1987.

Additional contributions to the work effort were made by Wilbur O. Feldmeier, Kevin P. Kepley, George Koons, Andrew R. Mallow, Michael K. Mohesky, Bruce D. West and Paul J. Zucker, all of McDonnell Aircraft Company.

Production of reports was ably performed by Ms. Jan D. Grammer.

TABLE OF CONTENTS

TABLE OF CONTENTS (Continued)

TABLE OF CONTENTS (Continued)

LIST OF FIGURES

LIST OF FIGURES (Continued)

LIST OF FIGURES (Continued)

LIST OF FIGURES (Continued)

LIST OF FIGURES (Continued)

LIST OF FIGURES (Continued)

LIST OF FIGURES (Concluded)

1.0 INTRODUCTION

1.1 BACKGROUND

The increasing use of composite materials in advanced aircraft structure has been restrained by the high cost of skill-craft methods for manufacturing these structures. Manufacturing processes are characterized by high-labor content, high-cost learning curves, and the lack of adequate in-process monitoring and control. This latter deficiency has made it necessary to take an empirical approach toward curing composite materials in typical autoclave cure cycles. Factors that have an effect upon achieving acceptable quality in the cured structure are typically averaged into selected cure cycles, and conservative methods have been adopted to offset potentially degrading conditions. This approach invariably increases processing costs and may even result in a less than optimum envelope of performance properties.

The need for in-process monitoring of the critical material parameters, with a view toward eventual control and optimization of cure schedules, has been widely recognized. The Air Force Materials Laboratory has directed a number of processing science programs toward the objective of achieving a fundamental understanding of the composite curing process. Results of these efforts have been successful in characterizing and modeling the material and processing factors that can be addressed in efforts to optimize cure cycles. However, the implementation of this knowledge into real-time control requires a means for in-process sensing of material changes and conversion of this information into control of the processing parameters. A number of nondestructive evaluation (NDE) techniques exist that can be used as in-process monitoring tools, but none of these have been shown to give the real-time, sensor-output/material-property correlations that will be required to provide a basis for cure cycle control. Ongoing programs, such as the Computer Aided Curing of Composites (CACC) program (Reference 1) at McDonnell Aircraft Company are concentrating on the use of ultrasonics and micro-dielectrometry techniques to monitor the properties of the curing resins, and miniature pressure transducers (Reference 2) to measure resin hydrostatic pressure.

The work reported herein was undertaken to identify and develop new nondestructive evaluation methods for in-process monitoring of composite material parameters that are considered to be significant for control of the composite cure process.

1.2 TECHNICAL APPROACH

Two sensor systems, the Fluorescence Optrode Cure Sensor (FOCS) and Acoustic Waveguide (AWG), were selected for development and evaluation. Both of these systems have shown, in laboratory environments, the capability of following the cure of some epoxy resins. The program efforts undertaken to develop and demonstrate their capability for in-process monitoring and potential for real-time cure control consisted of three tasks:

Task I - Technique Development and Evaluation
Task II - Develop a Final Demonstration Plan
Task III - Demonstration of Process Monitoring

The plan for Task I is outlined in Figure 1. The most relevant material parameters for correlation with cure cycle sensor monitoring were selected. These included viscosity, degree-of-cure and void content. Since void formation during the cure cycle is dependent upon temperature and hydrostatic resin pressure during the pre-gelation cure stage, thermocouple and miniature pressure sensors were utilized for monitoring these parameters as indicated by the experimental requirements.

Hercules 3501-6 epoxy resin, a basic system used for many current composite aircraft structural applications, was used for all laboratory investigations and final in-process monitoring demonstration cure cycles. Production carbon/epoxy unidirectional tape prepreg (AS4/3501-6) was used for laminate cure cycles.

Major subtasks under Task I involved sensor development and evaluation of sensor-response/material-property correlations:

- o Qualitative analysis of sensor responses relative to selective cure parameters - neat resin and/or carbon/epoxy laminates
- o Optimization of sensor signal output and method for incorporation of the sensor into laminate cure environments
- o Evaluation of pressure sensor capability to track internal resin hydrostatic pressures during pre-gelation and solid cure-state conditions
- o Development and refinement of hardware and software for signal acquisition, data processing and presentation
- o Quantitative analysis of sensor output and correlation with model data representing material cure parameters

The data for viscosity and degree-of-cure, which were the parameters selected for comparing with sensor signal profiles, were taken from the model tables established in the CACC program. These data were generated for the specific batch of 3501-6 resin used in this program, based upon the viscosity and kinetic submodels and temperature-time profile input data from the sensor cure-monitoring experiments.

The output from Task I efforts were used to prepare the sensor-laminate interface methods for demonstration of laminate cure-monitoring in Task III. Task II efforts consisted of the generation and Air Force approval of the Final Experimental Plan (Figure 2(a)). The plan encompassed determination of the scope of Task III experiments, selection and location of sensors within the laminates to be cured, cure conditions to be monitored, methods for data collection and analysis and selection of methods to compare sensor data output with laminate properties.

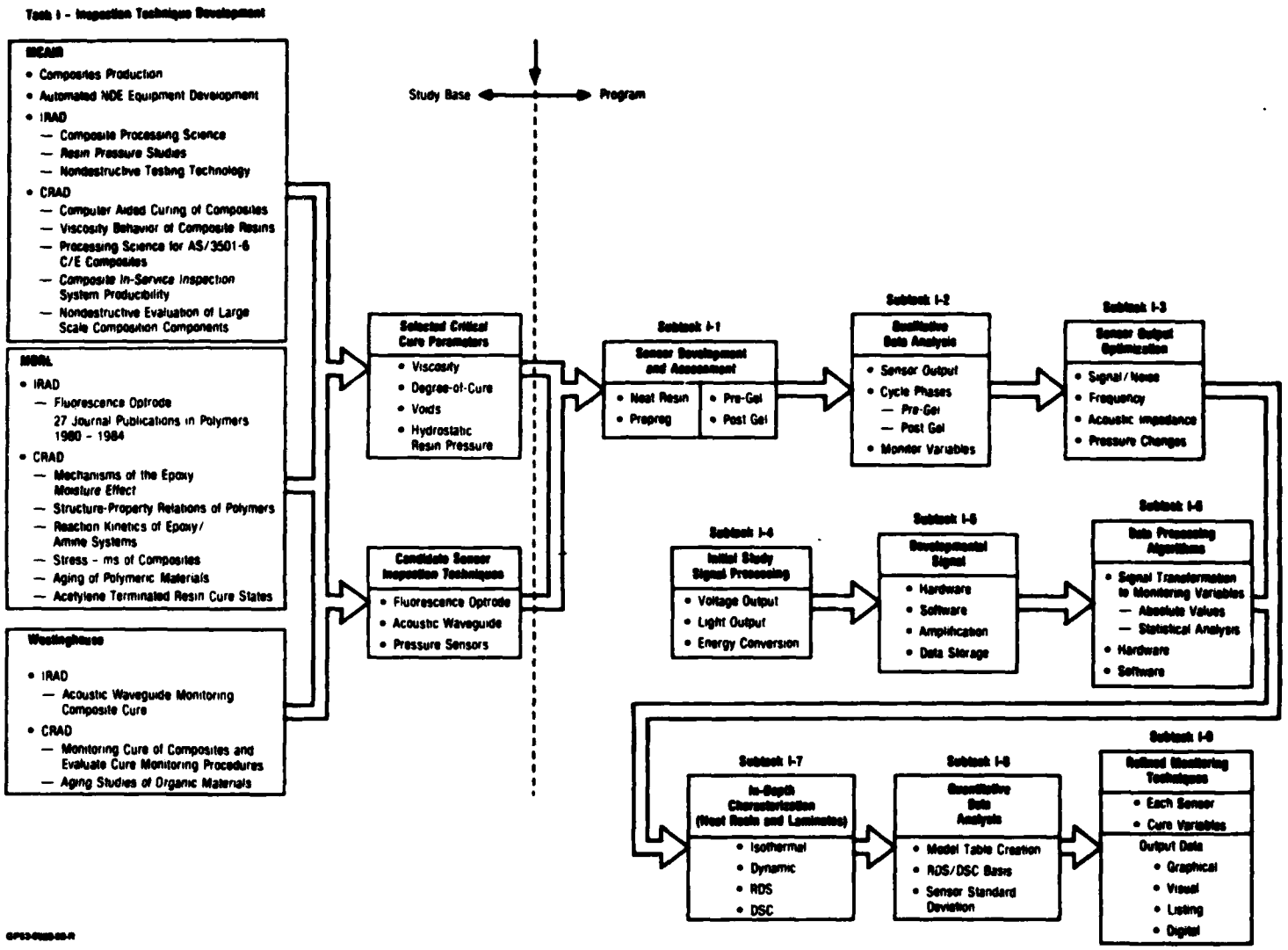

Figure 1. Task I Development and Evaluation of Sensor Techniques

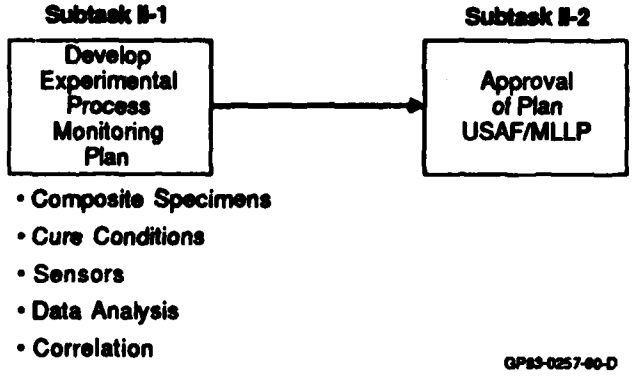

Figure 2a. Task II Develop and Document a Final Experimental Plan

The approach for Task III is outlined in Figure 2(b). A series of laminates was cured in a laboratory autoclave, with sensors positioned to provide the critical response data required for real-time in-process monitoring and correlation with material property parameters. Laminates were of sufficient thickness (~0.21 inch) and size (18x24 or 18x12 inches) to represent typical production aircraft structural parts. Various cure cycles were selected to represent a wide range of cure parameters. Resultant cure cycle sensor profiles were evaluated to verify the results of Task I development efforts, to determine the capability of the sensor systems to operate in a realistic manufacturing environment, and to assess the correlation of sensor output data with model predictions of in-process material property changes and final laminate properties. Laminate properties considered to be most relevant were degree-of-cure and anomalous conditions such as voids.

1.3 PROGRAM ACTIVITIES

Development of the FOCS system was carried out at McDonnell Douglas Research Laboratories (MDRL). Laboratory development of AWG was conducted at Westinghouse R&D Center. Evaluation of miniature pressure sensor capability, and all of the Task III laminate fabrication and evaluation efforts were conducted by McDonnell Aircraft Engineering Laboratories, with participation of MDRL and Westinghouse in analysis of results.

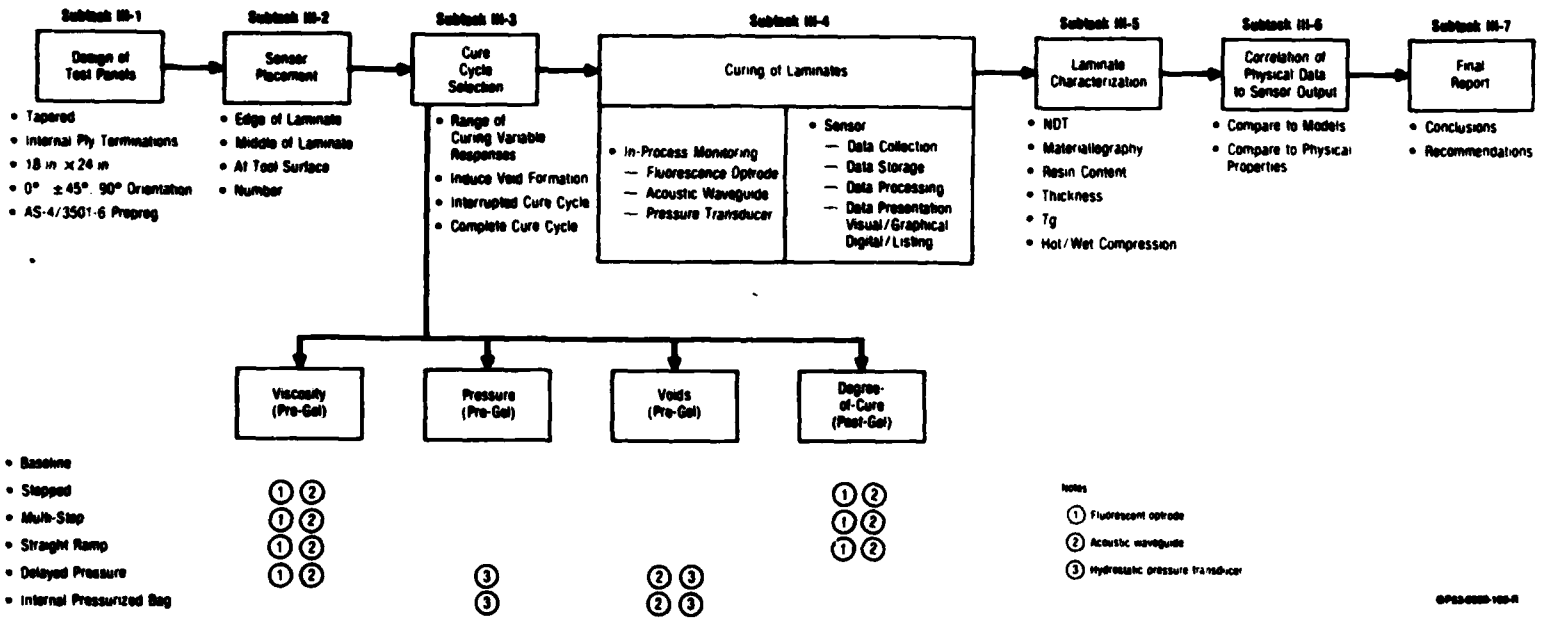

Figure 2b. Task III Demonstration of Process Monitoring

2.0 DEVELOPMENT OF FLUORESCENCE OPTRODE CURE SENSOR (FOCS)

2.1 BACKGROUND AND THEORY

A novel cure sensor concept called "Fluorescence Optrode Cure Sensor" was developed at McDonnell Douglas Research Laboratories (MDRL) in 1983-85 (References 3 through 7). The purpose of this development was to explore the potential of a new technology to provide a reliable low cost alternative to the dielectric and acoustic cure monitoring techniques, neither of which has been proven successful for application in routine manufacturing of composites. The principle of FOCS operation is based upon the combination of fiber-optic fluorometry (FOF) and a viscosity/degree-of-cure dependence of the epoxy resin fluorescence. It represents the first nondielectrometric and nonacoustic cure sensor concept to be introduced in the last 10 years. Due to its relatively recent introduction, study of the FOCS has been considerably less extensive in comparison to the dielectrometric and acoustic (ultrasonic) sensors.

2.1.1 Viscosity Dependent Fluorescence - The fluorescence quantum yields, Φ_f, of certain compounds exhibit a strong dependence on the viscosity of the medium. It was known as early as 1913 that some dyes which do not fluoresce in ordinary solvents will, however, fluoresce strongly in viscous media such as glycerol at low temperatures. A number of studies on the viscosity-dependent fluorescence (VDF) of various compounds have appeared (References 8-10). Despite these and other studies, however, the VDF phenomenon had remained obscure and its potential unexplored. Loutfy (Reference 11) was the first to exploit the VDF effect for monitoring polymerization reactions.

Viscosity-dependent fluorescence (VDF) is typically observed in cases where the low fluorescence yield exhibited by a compound in ordinary low-viscosity solvents is due to fast nonradiative deactivation (relaxation) of the excited state by intramolecular torsional motions. When such torsional motions become progressively more inhibited in media of higher viscosities, the fluorescence yield rapidly increases.

The quantitative relationship between the fluorescence quantum yield, Φ_f, the absolute temperature, T, and the viscosity of the medium, η, has been empirically determined for a diphenyl methane probe (Auramine-O) by Oster and Nashijima (Reference 8) to be

$$\frac{1}{\Phi_f} = 1 + \frac{1^{\tau}}{\tau_2} + a\ \tau_1\ (\frac{T}{\eta})$$

where τ_1 is the intrinsic lifetime of the fluorescence and τ_2 is the lifetime for internal conversion by vibrational processes (but not by torsional/rotational processes). Subsequently, Forster and Hoffman (Reference 9) have shown that the relationship between Φ and η can be described by

$$\Phi_f = C\eta^{2/3}$$

for a triphenyl methane probe. These expressions demonstrate that quantitative relationships between the fluorescence and the viscosity, η, can be established for a broad range of viscosities. Thus, the local viscosity

of a medium containing a VDF probe can be determined from measurements of T and ϕ_f, provided all error-contributing factors are properly accounted for or eliminated. In practical terms this means that where the identity and the behavior of a particular VDF probe are known the viscosity of the medium containing the probe can be monitored by fluorescence measurements.

2.1.2 Fiber-Optic Fluorometry (FOF) - Fiber-optic waveguides provide excellent means for delivering excitation energy to fluorescing media in remote, hostile, or inaccessible environments, such as in reactors or plant streams, and for guiding the emitted fluorescence back to a detector or a spectrometer.

Measurements of fluorescence via fiber-optic waveguides, i.e., fiber-optic fluorometry (FOF), provide opportunities for innovation in sensor development and remote monitoring of fluid streams. Examples of such FOF-based innovations can be found in T. Hirschfeld's pioneering work of the early 1980s (Reference 12). The FOCS is also an example of an FOF based innovation. Fiber optic fluorometry differs from conventional fluorometry only in the optics used to deliver excitation and to separate the collected fluorescence radiation from the light reflected back into the detector via the waveguide. However, FOF provides several important advantages over conventional methods:

- o permits in-situ measurement of fluorescence in remote, hostile environments
- o provides immunity to electromagnetic interferences
- o can easily be multiplexed, permitting monitoring of many sites with a single fluorometer
- o has a potential for low cost applications

These advantages of FOF play an important role in the potential use of the FOCS for monitoring the resin fluorescence during cure in an autoclave. The unique capabilities of a photodiode array-based spectrofluorometer, with its associated computer hardware and MDRL-developed software used in the FOCS, go beyond the capabilities of existing FOF systems; this FOCS system represents an advancement in the state of the art.

2.1.3 Origin of the Epoxy VDF Behavior - The viscosity-dependent fluorescence (VDF) of the Ciba-Geigy MY720 epoxy resin, a major ingredient of Hercules 3501-6 formulation, was first observed by MDRL in 1983 (Reference 3). In addition, it was observed that the purified main constituent of the MY720 resin, N,N-tetraglycidyl diaminodiphenyl methane (TGDDM), also exhibits the VDF behavior. These observations, combined with the well known fact that Auramine-O, a compound with a molecular structure similar to that of TGDDM, also exhibits VDF, led to the tentative conclusion that TGDDM monomer itself exhibits VDF. In subsequent experiments, however, evidence was obtained which conclusively indicated that the primary source of the epoxy resin fluorescence originates in one or more of the resin impurities or synthesis by-products present in the MY720 resin. A series of liquid chromatography experiments to separate, isolate and identify the resin constituents responsible for the VDF behavior were performed during the early stages of this contract. Although an understanding of the dependence of VDF upon resin

constituency will be important to the application of FOCS to the cure-monitoring of 3501-6 resin, further efforts were outside the scope of this contract.

2.2 CURE-MONITORING HARDWARE

2.2.1 FOCS System Hardware - The evolutionary development of the FOCS includes two distinctly different systems:

a. first generation FOCS

b. second generation FOCS

The first generation FOCS (Reference 6) is based upon use of a simple fiber-optic fluorometer (FOF) that utilizes band-pass filters to separate the excitation and emission beams. It is capable of monitoring only changes in the intensity of the epoxy fluorescence. This hardware was not used for any of the cure monitoring experiments performed under this contract.

The observation in 1984 of substantial shifts in the wavelength of the fluorescence emission maximum during cure presented an opportunity to enhance the performance of the FOCS by developing a second generation system (References 5 and 7) capable of monitoring the changes in both intensity and wavelength during cure. A working breadboard FOCS system that can monitor these two parameters was assembled and tested during the period immediately preceding the initiation of this contract. The FOCS breadboard system was designated "second generation" because of its additional capability. The main components of the initial breadboard of the second generation FOCS are shown schematically in Figure 3. It consists of a helium-cadmium (HeCd) laser excitation source (Omnichrome Model 439) which provides 5 mW output power at 442 nm, a geometric coupler, a polychromator (J-Y Model HR-320), and an optical multichannel analyzer (Princeton Applied Research OMA II). The geometric coupler (Reference 12) permits focusing of the excitation laser beam onto the optical fiber through a narrow hole in a folding mirror and separation of the returning fluorescence, which propagates along the same fiber, by the difference in divergence between the input and output beams. Most of the returning wide angle fluorescence beam impinges on the folding mirror and is focused by a relay lens on the slit of the polychromator which disperses the fluorescence by wavelength. The entire fluorescence emission spectrum is thus continuously observed by the vidicon detector of the OMA II (or other photodiode array detector systems). Determination of the fluorescence intensity and the wavelength of maximum emission (λmax) for each cure time increment is accomplished by performing a third order polynomial curve fit on the 200-250 data points that represent the fluorescence emission band and extracting the desired parameters by appropriate computer processing of the data.

2.2.1.1 Improved Optical Configuration - During some of the isothermal cure cycles at 180°C (356°F) and 120°C (248°F) (Section 2.5) highly unusual sudden increases and fluctuations of the FOCS intensity signal were observed (Figure 4). These signal fluctuations were traced to large laser power output fluctuations (known to precede laser tube failure). These observations underscored the need to modify the optical layout of the FOCS so that the effect of such power fluctuations is eliminated. To accomplish

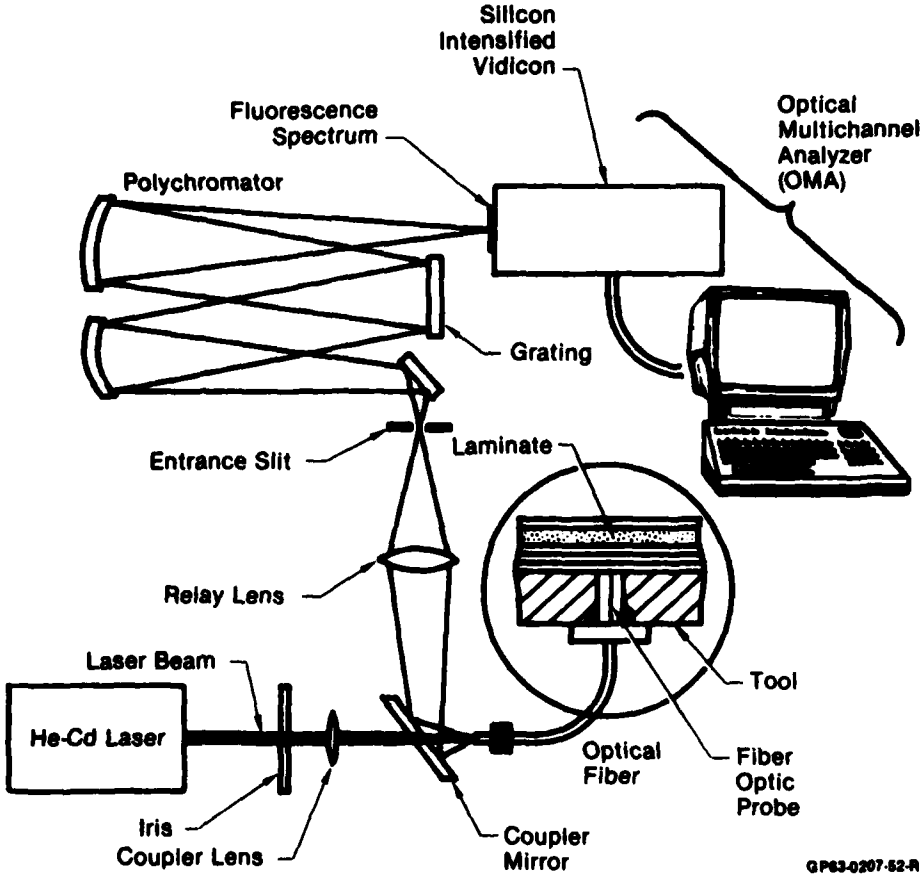

Figure 3. Second-Generation FOCS Breadboard System Capable of Monitoring Fluorescence Intensity and Wavelength

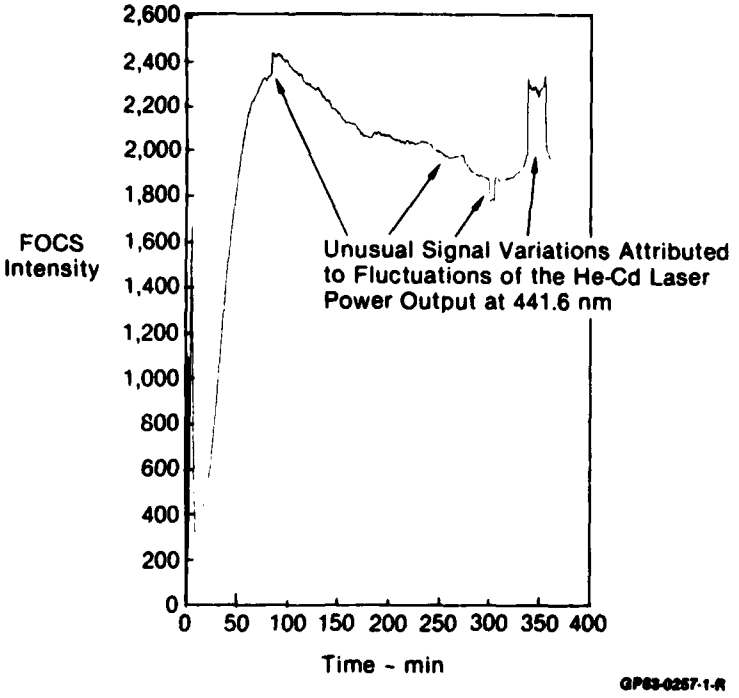

Figure 4. FOCS Intensity Signal Profile Recorded During 180°C (356°F) Isothermal Cure of AS4/3501-6 Laminate

this, a laser power meter (Spectra Physics Model 404) was incorporated into the system as shown in Figure 5. The output of the laser power meter is connected to the OSMA (OMA) photodiode array controller, where it is incrementally recorded and subsequently used for source compensation. The modified optical layout affects the FOCS signal profiles only to the extent that it corrects for laser fluctuations and assures that the deleterious effect of laser power fluctuations is eliminated.

Compensation is performed in the following manner: the response time of the source compensation photodetector is adjusted to be comparable to the total integration time of the photodiode array by adding the appropriate RC circuit to the photodetector's amplifier. This insures that the source compensation reading reflects the average laser power over the entire 30 second integration time of the array. Figures 6 and 7 illustrate how the source compensation eliminates the noise and distortion caused by laser power fluctuations. Figure 6, an uncompensated FOCS intensity profile for 120°C (248°F) isothermal cure, shows several intensity "spikes" during the cure. However, once the compensation curve has been applied (Figure 7), the spikes disappear and the profile has a slightly different and more correct shape.

2.2.2 Laboratory Microautoclave - The testing of the FOCS system, the study of the factors affecting its performance and the development of optrode-laminate interface required monitoring of many cure cycles. Autoclave cure conditions were simulated in a laboratory "microautoclave" shown in Figure 8. Small AS4/3501-6 composite laminates were cured in the

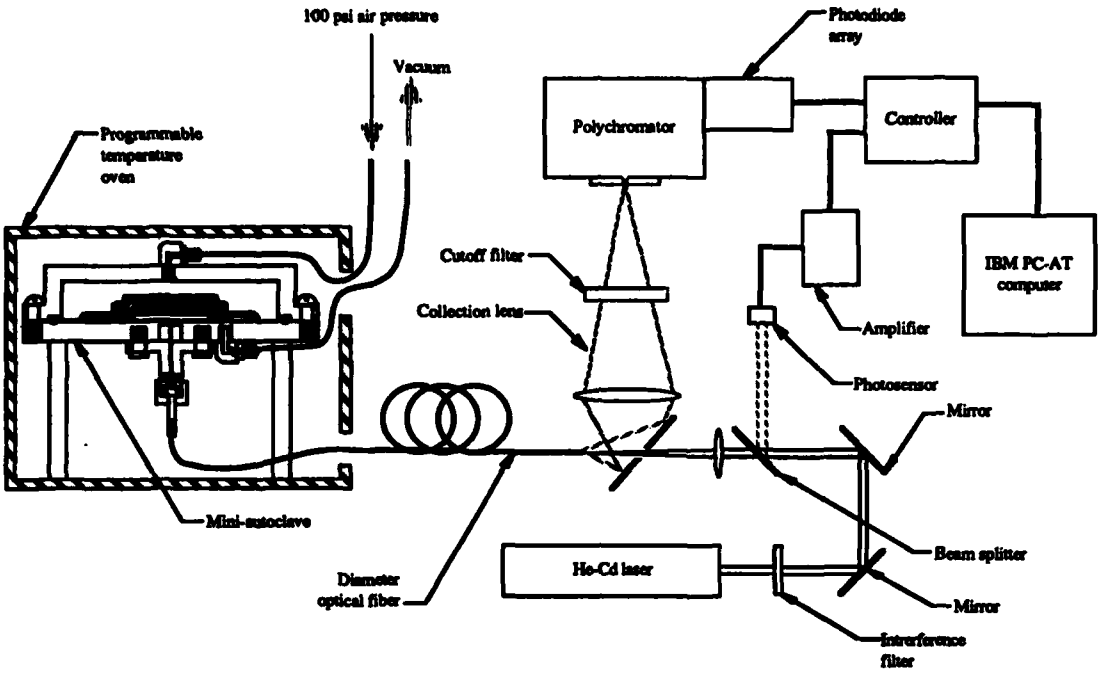

Figure 5. Second-Generation FOCS Optical Layout With Source Compensation Connected to Laboratory "Mini-Autoclave".

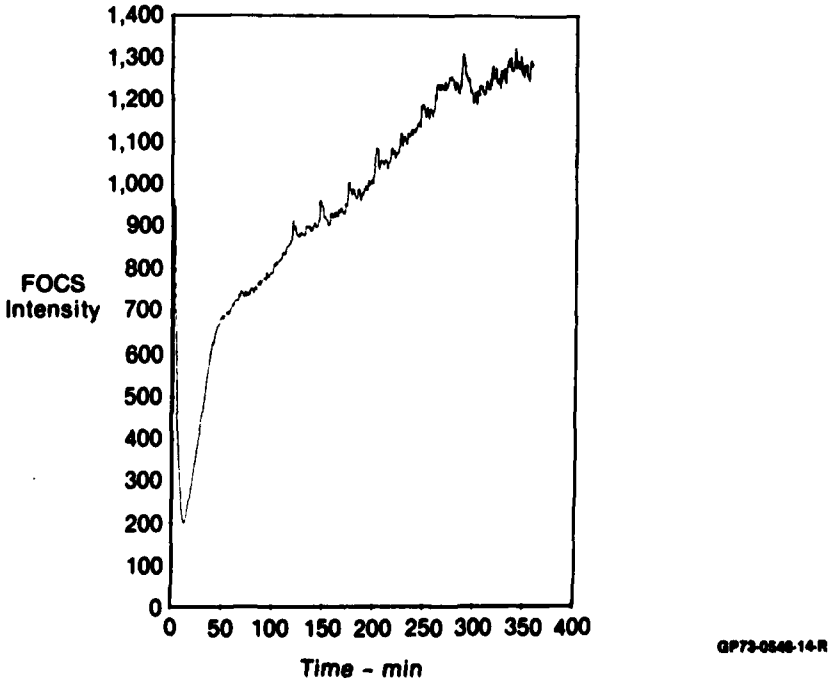

Figure 6. Uncompensated FOCS Intensity Signal Profile Recorded During 120°C (248°F) Isothermal Cure of AS4/3501-6 Laminate

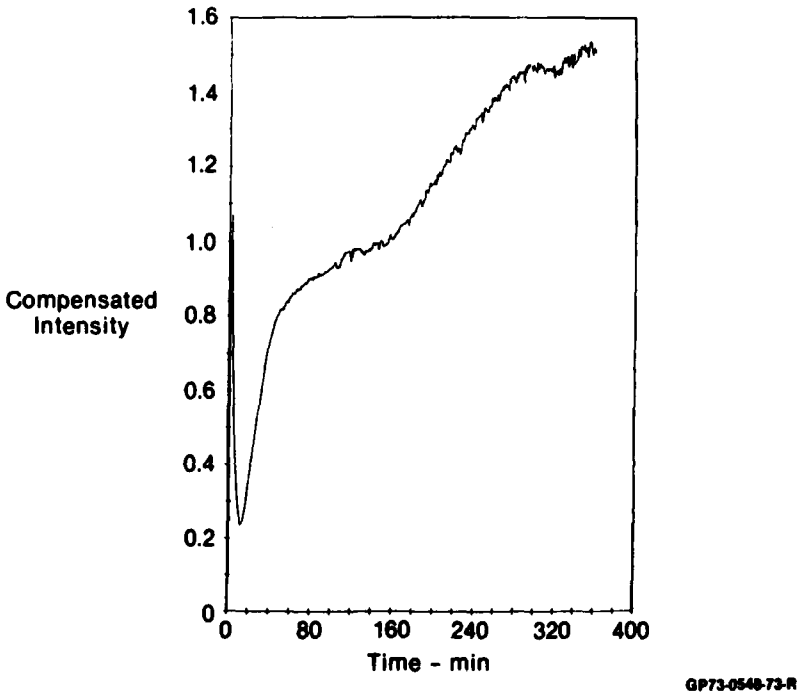

Figure 7. Compensated FOCS Intensity Signal Profile Recorded During 120°C (248°F) Isothermal Cure of AS4/3501-6 Laminate

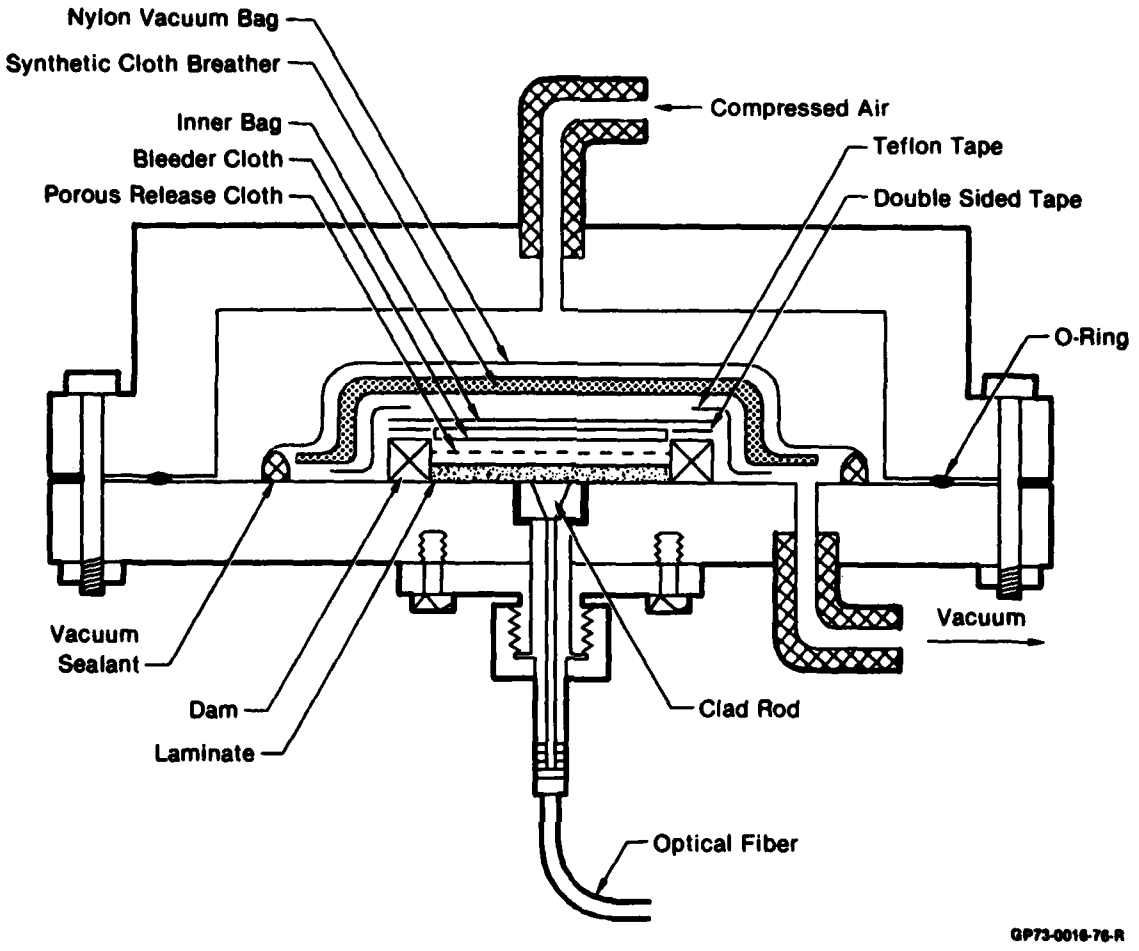

Figure 8. Micro-Autoclave System and Lay-Up Arrangement for Monitoring Curing of Carbon/Epoxy Laminates With the Fluorescence Optrode Cure Sensor

microautoclave by placing the unit inside a programmable temperature-controlled oven, so that the vacuum, pressure, temperature and bleed control conditions were the same as would be achieved in a larger autoclave. This microautoclave was used for all of the development cure cycles and the isothermal calibration cure-monitoring runs reported (Section 2.5.1). The "resin-cavity" configuration for the optrode laminate interface (Figure 9) was also developed using this microautoclave.

2.2.3 Tool-Mounted Optrode (TMO) - All cure-monitoring experiments described in this report were conducted with a "tool-mounted" optrode sensor arrangement. In this type of arrangement the sensor (optrode) is mounted on the tool and comes in contact with the laminate via an optrode-laminate interface. Tool-mounted sensors do not interfere with the laminate lay-up work and minimize sensor installation labor cost. The use of TMO-based FOCS in composite manufacturing would be as simple as the use of tool-mounted thermocouples.

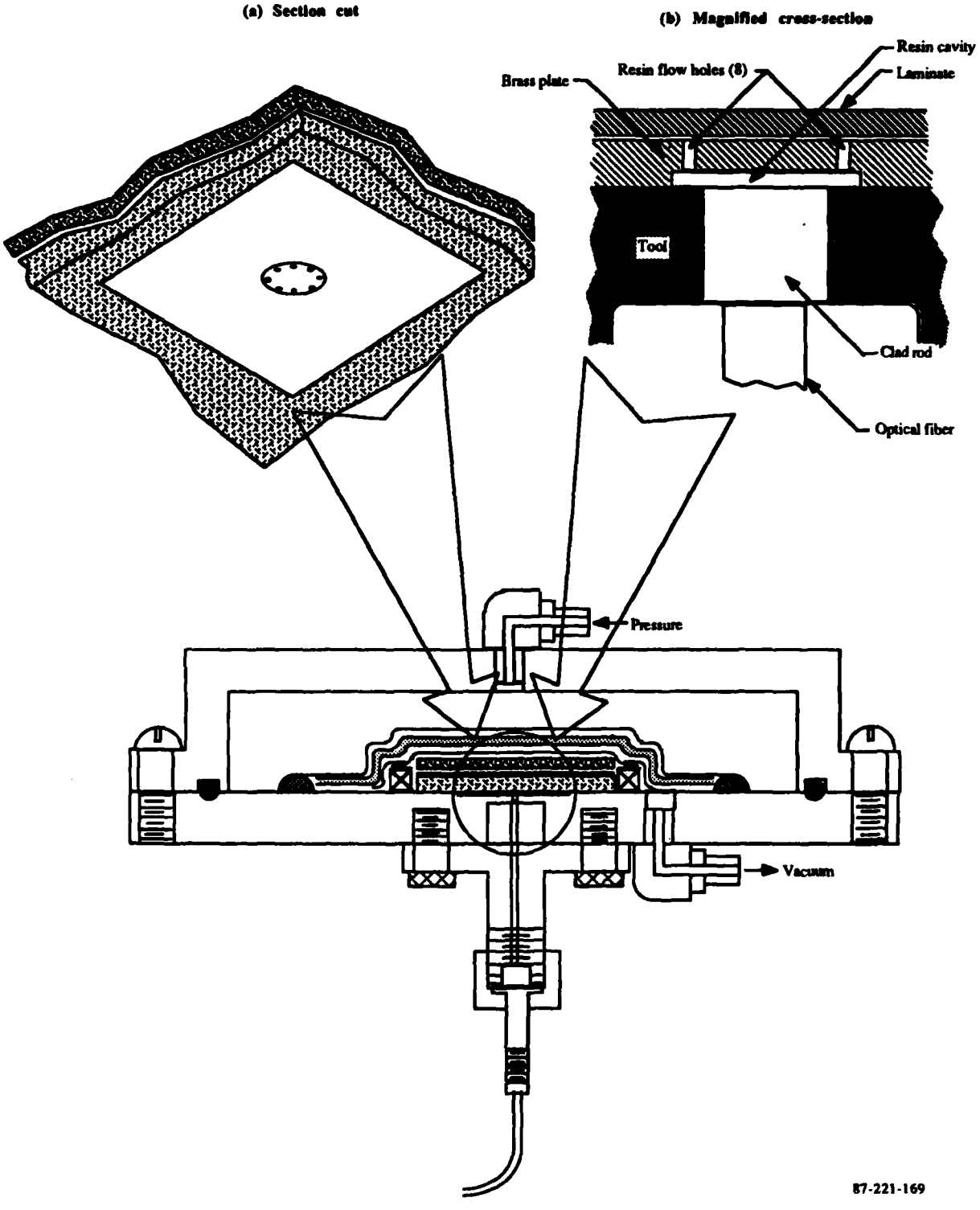

Figure 9. Schematic of Laboratory "Resin Cavity" Optrode-Laminate Interface

2.2.4 Optimization of the Optrode-Laminate Interface - During the sensor development, qualitative data analysis and sensor output optimization tasks of this program, it became obvious that the configuration of the optrode-laminate interface is critical to the reproducibility and patterns of the FOCS signal profiles.

The evolutionary development of the optrode-laminate interface resulted in a design that was called the "resin cavity" configuration, shown in Figure 9. This interface was modified somewhat for the large cure plate that was used to fabricate Task III laminates in the larger autoclave, as shown in Figures 10 and 11. The principal differences between the laboratory and the final autoclave process versions of the "resin cavity" interface design are in the size of the resin-flow holes, 0.028 inch for the process version and 0.014 inch for the laboratory version, and in the fact that in the process version the interface is recessed into the tool surface. In both versions a 0.01 inch thick Teflon spacer, which is the most critical component of the interface, creates the resin cavity.

All of the isothermal cure cycles reported in Section 2.5.1 of this report were performed with the laboratory version of the optrode-laminate interface. In addition, a number of exploratory cure cycles were monitored with the laboratory version of the resin cavity interface configuration. In all of the cure monitoring runs performed with the laboratory version of the "resin cavity" configuration, the interface performed as expected. However, during the Task III laminate cure cycles, the resin cavity did not fill completely with the resin in some of the seven runs, resulting in lower signal levels.

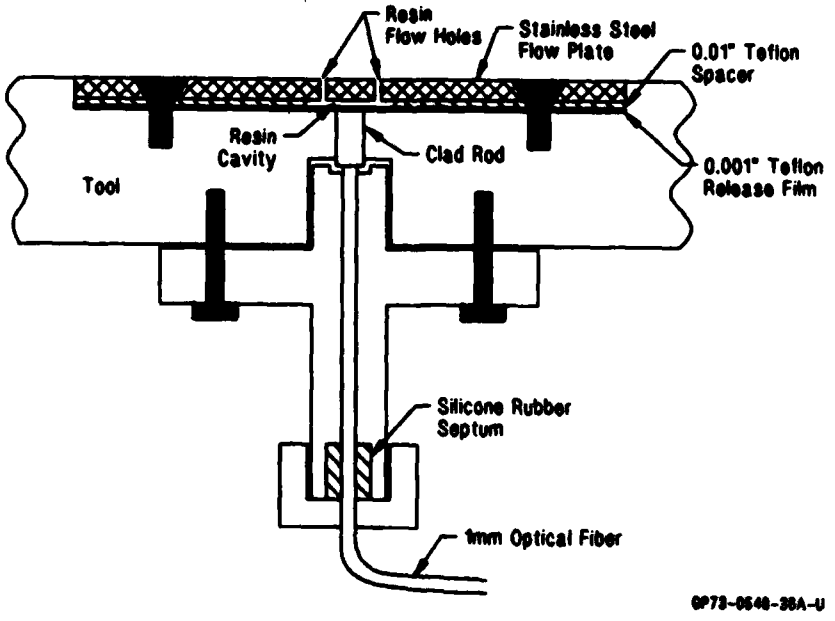

Figure 10. Optrode-Laminate Interface – Final Production Tool Configuration

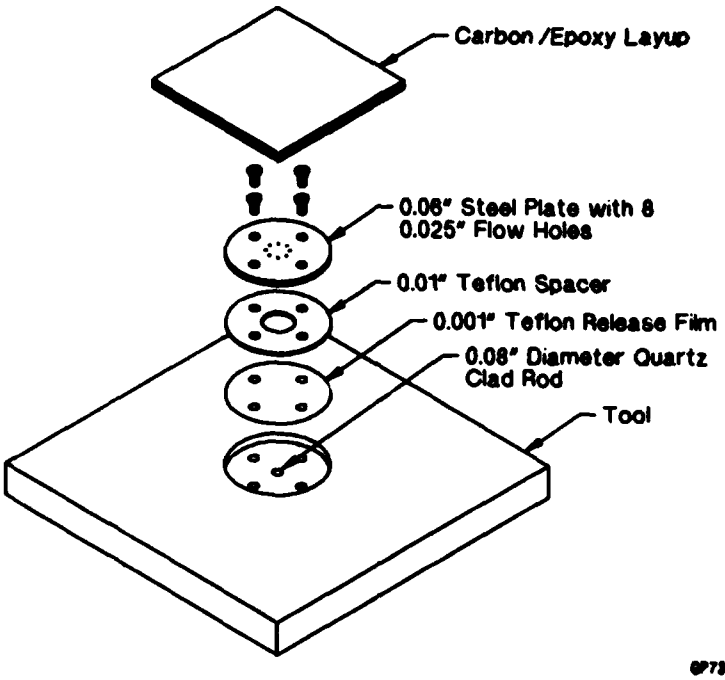

Figure 11. Elements of Final Production Tool Optrode – Laminate Interface

2.3 ORIGIN AND CHARACTERISTICS OF THE FOCS SIGNAL PROFILES

Approximately 100 individual cure cycles of AS4/3501-6 laminates were monitored with the FOCS system during the course of this contract. Considerable information on the patterns of the FOCS intensity and wavelength signal profiles was accumulated from these cure cycles. This cumulative information permits certain observations and generalizations to be made on the origin and the characteristics of the FOCS intensity and wavelength signal profiles.

2.3.1 FOCS Intensity Signal - Changes in the fluorescence intensity during cure follow changes in the resin viscosity up to gelation. Fluorescence intensity continues to change beyond gelation at a rate that is related to the rate of cure. In fact, under standard step cure cycle conditions, the profile of fluorescence intensity as a function of cure time follows the pattern of the profile of viscosity as a function of cure time obtained under the same conditions with a Rheometrics dynamic mechanical spectrometer. Furthermore, the dynamic mechanical spectrometer ceases to provide the viscosity/degree-of-cure information early in the cure cycle (i.e., when the cure state approaches gelation), whereas FOCS signals continue to follow the curing to completion.

2.3.2 FOCS Wavelength Signal - Changes in the fluorescence maximum wavelength (λmax) as a function of temperature and degree-of-cure produce a highly characteristic signal profile which is reproducible and also reveals the main chemorheological events, such as minimum viscosity and the gelation

event, with either reversal of the direction of the signal change or with a distinct change of slope. The molecular origin of the changes in λmax is complex in this case because both the dielectric environment and the mobility of the dipoles surrounding the fluorescent molecules change during cure. Therefore, the models employed for the analysis of the dependence of λmax upon the dielectric properties of the solvent or the medium surrounding these molecules cannot be applied to this case.

Changes in the FOCS fluorescence wavelength signal during the early stages of cure appear to be strongly dependent on the "freshness" of the prepreg material and the total time the material has been kept at room temperature prior to initiation of the cure cycle. It is possible that the ability to detect these conditions with the FOCS could be exploited as an early indicator of the condition of the prepreg material at the onset of curing. However, additional experiments which are specifically designed to explore this aspect of the FOCS wavelength signal would be needed.

2.3.3 Factors Affecting the FOCS Signal Profiles and Their Reproducibility - The observed FOCS signal profiles are affected primarily by the cure-induced changes in the epoxy resin. However, other experimental variables also contribute to the overall appearance and reproducibility of the FOCS signal profiles. The following sections describe the main variables and how they affect the signal profiles.

2.3.3.1 Inner-Filter Effects - The absorption of the fluorescence excitation and emission by the specimen is referred to as the "inner-filter" effect; this effect has been treated in the literature (References 13 and 14). The inner-filter effect reduces the signal levels and distorts the emission spectrum. The effect is more pronounced in right-angle fluorescence measurements than in the "front face" configuration, in which the fluorescence is viewed from the same direction as the excitation beam, which is the case with the FOCS.

The magnitude of the inner-filter effect with the FOCS depends strongly on the thickness of the resin layer viewed by the optrode and becomes pronounced only during the late stages of cure, when the absorbance of the resin at 441.6 nm increases. A particularly pronounced impact of the inner-filter effect on the intensity signal profile of the FOCS is observed when the optrode monitors curing of the neat Hercules 3501-6 resin. The mathematical corrections for inner-filter effects assume a constant absorbance of the specimen; in our case the absorbance of the resin at the excitation-light wavelength is a function of the degree-of-cure and, therefore, does not lend itself to the existing treatments.

The magnitude of the inner-filter effect is strongly influenced by the extent of thermo-oxidative reactions which accompany curing reactions when oxygen is present. Therefore, run-to-run variations in the level of oxygen in the resin can produce variations in the magnitude of the inner-filter effect and thus affect the reproducibility of the FOCS signal profiles.

2.3.3.2 Laser Beam Power - The intensity of the fluorescence excitation beam, i.e., the HeCd laser beam power, was found to affect the FOCS signal profiles. Those profiles obtained with 1.0 mW laser power delivered to the resin showed increased inner-filter effect for the FOCS intensity profile and considerably larger wavelength shifts in comparison to the profiles obtained with 0.1 mW laser power. Since the magnitude of the wavelength shifts is also affected by the inner-filter effect it was concluded that the effect of the laser power is manifested through the inner filter effect.

Visual inspection of the cured resin monitored with 1.0 mW excitation light shows darkening of the resin in the 0.04 inch (1 mm) diameter spot where the laser beam illuminates the resin, whereas no such darkening is observed in the cured resin monitored with 0.1 mW power. The observed darkening of the resin is a strong indication of enhanced photo-oxidative (and thermo-oxidative) reactions taking place, thus causing enhanced inner-filter effect, when the resin is illuminated with excitation beam of higher power.

2.3.3.3 Thickness of the Resin Layer - The FOCS intensity signal is proportional to the thickness of the resin layer found in the "resin cavity" of the optrode-laminate (OL) interface. Therefore, any experimental factor that might cause run-to-run variations in the thickness of the resin "viewed" by the optrode would affect the reproducibility of the results. Such differences could, for instance, occur if the Teflon spacer used in the OL interface to produce the resin cavity is not properly seated or if the resin cavity is not completely filled with resin. The effective thickness of the resin viewed by the optrode could also be affected by formation of bubbles in the light path. During the FOCS monitoring of isothermal cure cycles with the laboratory microautoclave, no variation of the resin layer thickness was observed.

2.4 SIGNAL PROCESSING AND OUTPUT

The initial step in the measurement of fluorescence intensity and λmax with the FOCS is based on signal-averaged (coadded) recording of the epoxy fluorescence emission spectrum by the intensified photodiode array detector, which is part of the FOCS system. After each signal-averaging fluorescence measurement interval (usually 30 seconds), the raw fluorescence intensity versus wavelength spectrum recorded by the photodiode array is transmitted in digital form via an IEEE 488 link to the IBM PC-AT for signal processing. The raw fluorescence emission band data residing in the PC-AT undergoes a rapid curve fitting. A FORTRAN program written specifically for the FOCS fits a third-order polynomial function to the spectrum and finds both its maximum emission intensity and the corresponding wavelength at the maximum (λmax). These two outputs are then plotted against time on the CRT for the entire length of the cure cycle, giving the operator a graphical representation of the progression of the cure. The cure temperature, decoded from a digital temperature indicator, is updated and displayed for each time interval. In addition, a factor proportional to the HeCd laser power used for source compensation (see Section 2.2.1.1) is also displayed. All important parameters, i.e., time, cure temperature, FOCS intensity, FOCS wavelength and laser power factor, are written to a tabular ASCII file which is available for immediate or for future manipulation. All entry lines to

this tabular file could be transmitted as soon as they are generated to the autoclave control or the cure optimizing computer used in the computer aided curing of composites.

2.5 SENSOR RESPONSE/MATERIAL PROPERTY RELATIONSHIPS

2.5.1 Monitoring of Isothermal Cures - A series of laminate cure cycles was completed for statistical analysis of sensor repeatability and for correlation with material property data obtained under the same time-temperature conditions. Four cures of AS4/3501-6 prepreg material run at 120°C (248°F) and four at 180°C (356°F) in the laboratory microautoclave were monitored with FOCS. These two temperatures correspond to the two hold temperatures of the typical step-cure cycle to be used for Task III laminates. Additional isothermal cures, one each at several temperatures [80°C (176°F), 100°C (212°F), 140°C (284°F), 160°C (320°F) and 200°C (392°F)], were also monitored to establish the statistical effect of temperature upon sensor response.

The superimposed FOCS intensity signal profiles versus time, recorded during four separate isothermal cure cycles of AS4/3501-6 laminates at 120°C (248°F), are shown in Figure 12. The superimposed FOCS wavelength (λmax) signal profiles for the same cure cycles are shown in Figure 13.

The superimposed FOCS intensity signal-time profiles recorded during four separate isothermal cure cycles of AS4/3501-6 laminates at 180°C (356°F), are shown in Figure 14, and the corresponding λmax signal-time profiles for the same cure cycles are shown in Figure 15.

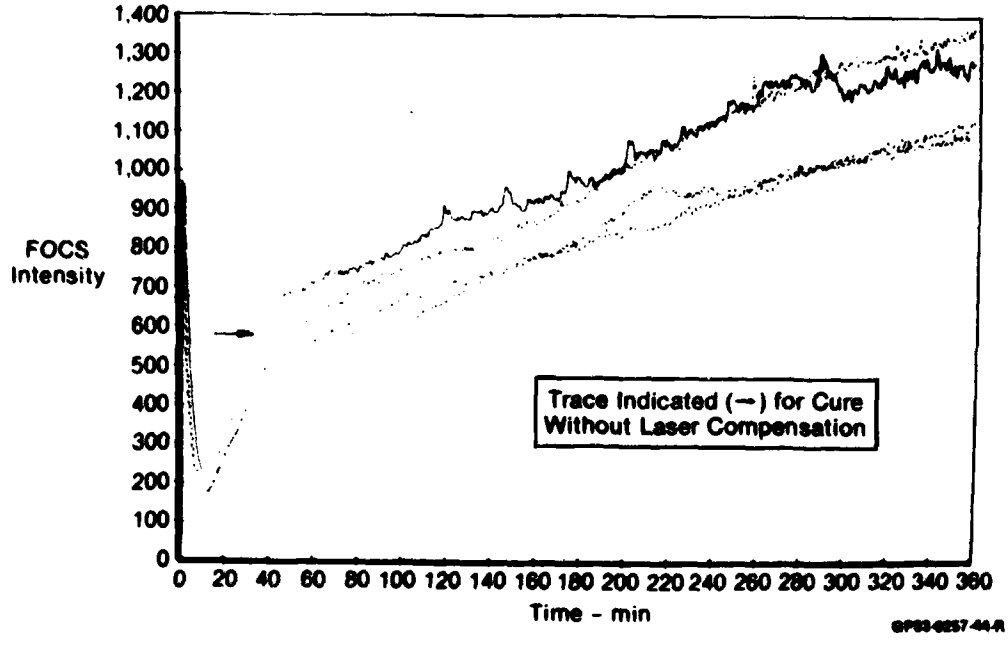

Figure 12. Four FOCS Intensity Signal Profiles for 120°C (248°F) Isothermal Cures

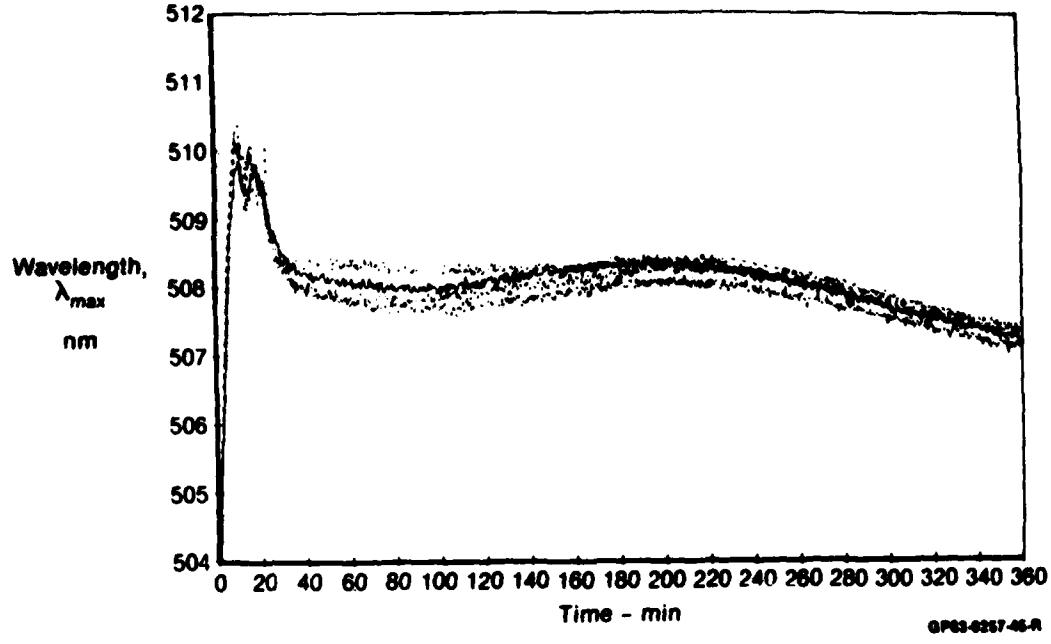

Figure 13. Four FOCS Wavelength Signal Profiles for 120°C (248°F) Isothermal Cures

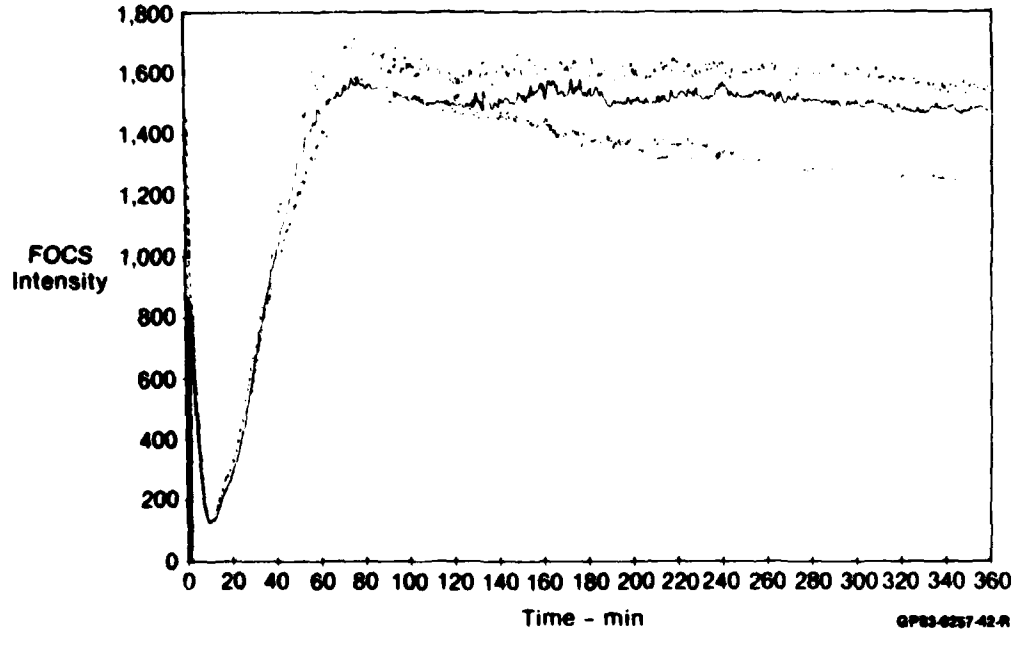

Figure 14. Four FOCS Intensity Signal Profiles for 180°C (356°F) Isothermal Cures (AS4/3501-6)

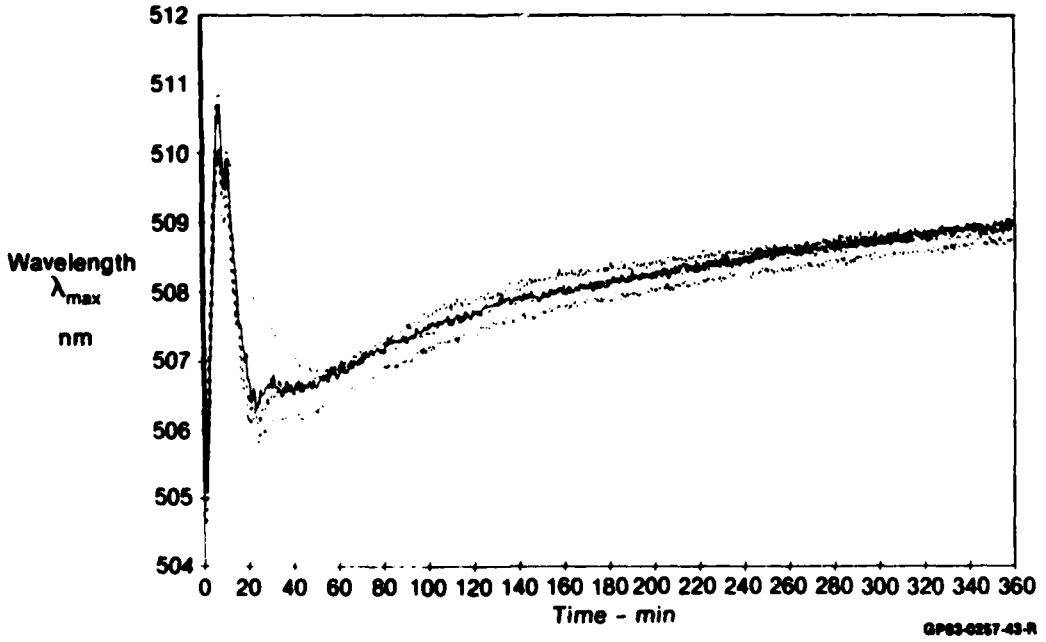

Figure 15. Four FOCS Wavelength Signal Profiles for 180°C (356°F) Isothermal Cures (AS4/3501-6)

2.5.2 Statistical Analysis of Isothermal Cure Response Data - The objectives of this task were to establish the reproducibility of the FOCS system as used to follow epoxy cure reactions and to determine the degree of correlation at various temperatures between sensor responses and known cure parameters such as changes in viscosity (η) and degree-of-cure (α). These parameters have been determined for the cure reactions of the 3501-6 epoxy resin system in the Computer-Aided Curing of Composites (CACC) program (Reference 1), in which the curing conditions of temperature, time and kinetic models are inputs, and η and α are outputs. Model tables for η and α were developed for the specific batch of 3501-6 resin in the prepreg used for these laminates; a description of these resin characterization data is given in Section 4.

2.5.2.1 Reproducibility of Isothermal Cure Data - Data from the four replicate trials made at 120°C (248°F) and four trials made at 180°C (356°F) were first inspected to determine degree of reproducibility of the relationships between sensor response and the viscosity and degree-of-cure changes calculated from the resin cure models. Then, empirical relationships between each of the 4-trial sensor response data and these cure parameters were established.

Two FOCS output functions were monitored and plotted against calculated viscosity and degree-of-cure profiles: wavelength at maximum intensity (λmax) and maximum intensity. Figures 16 through 20 show these relationships for isothermal cures at 120°C (248°F) and 180°C (356°F). Visual inspection of the data in these figures indicated that the patterns were not identical, i.e., not repeatable in a statistical sense. Repeatability means that the

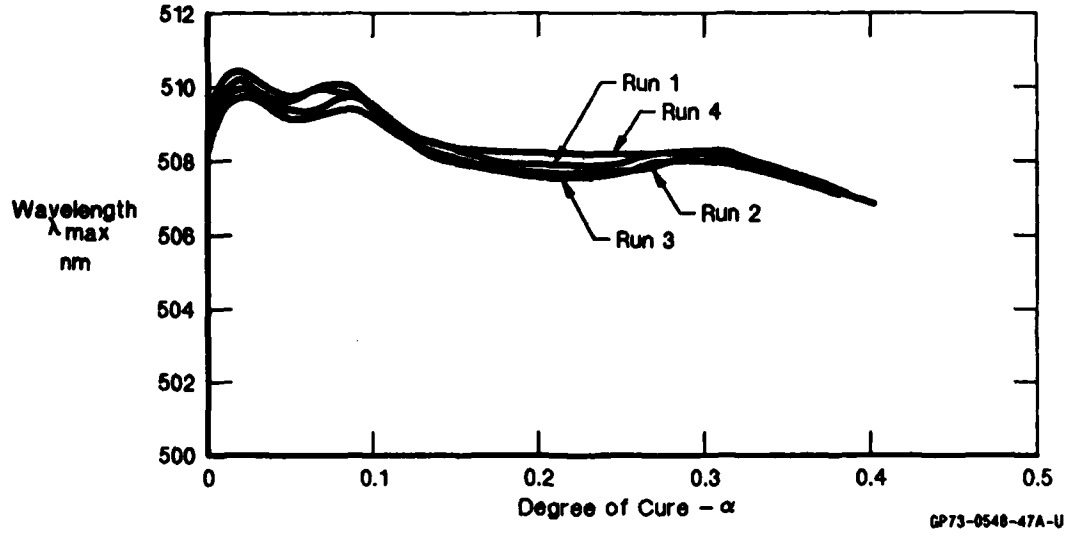

Figure 16. Correlation Between FOCS Wavelength and Degree of Cure for 120°C (248°F) Isothermal Cures

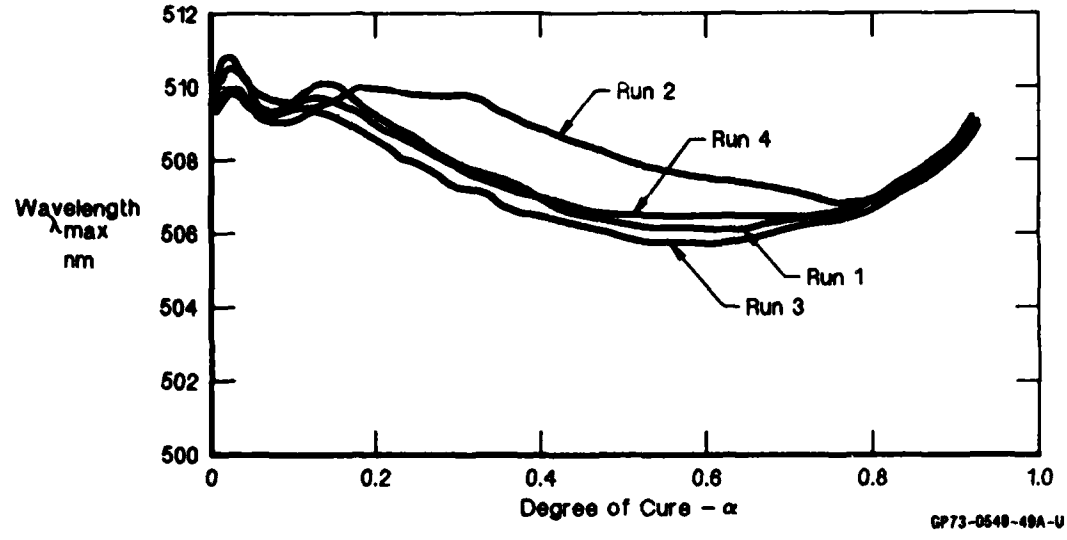

Figure 17. Correlation Between FOCS Wavelength and Degree of Cure for 180°C (356°F) Isothermal Cures

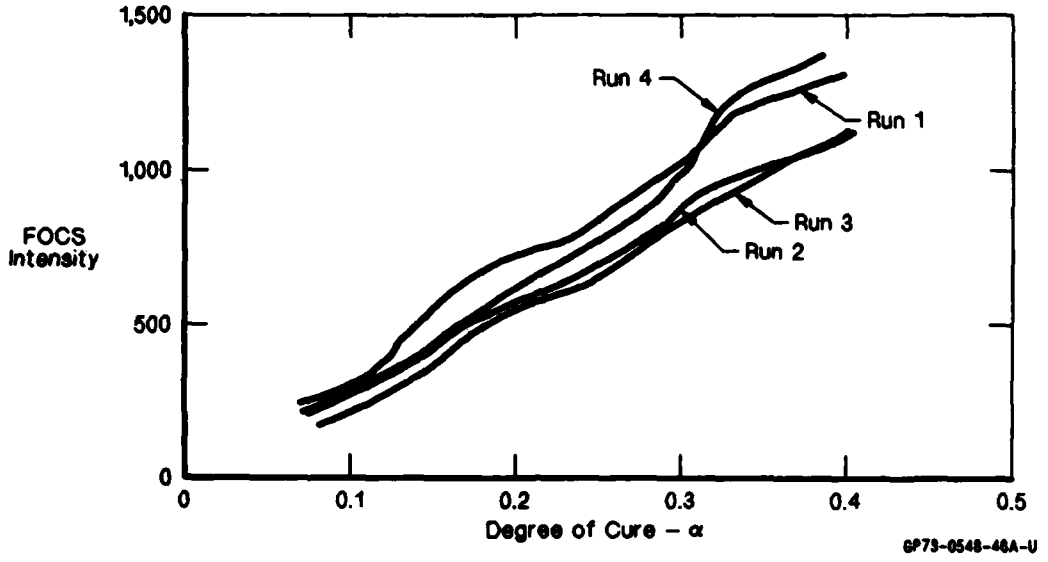

Figure 18. Correlation Between FOCS Intensity and Degree of Cure for 120°C (248°F) Isothermal Cures

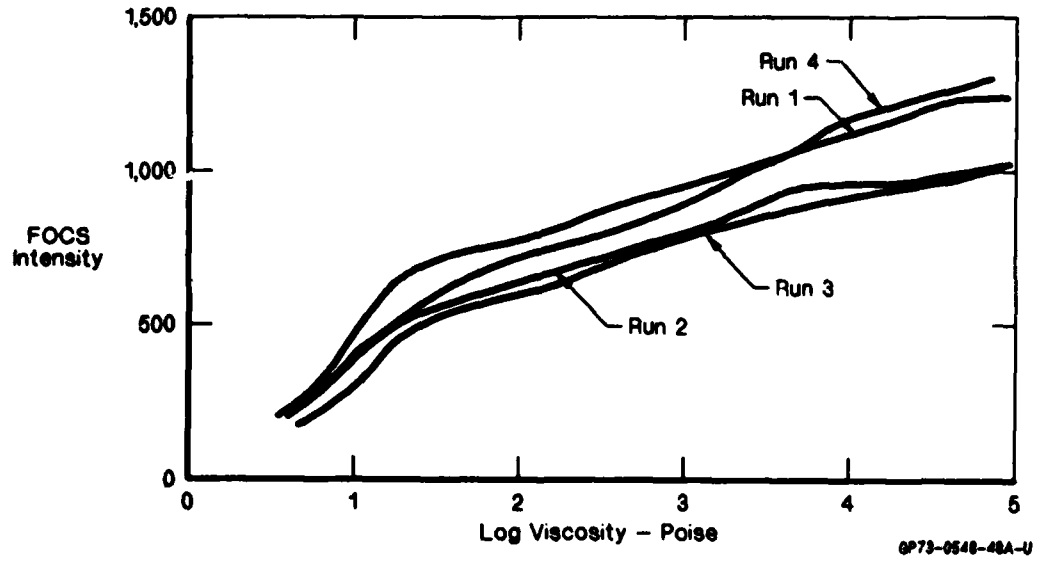

Figure 19. Correlation Between FOCS Intensity and Viscosity for 120°C (248°F) Isothermal Cures

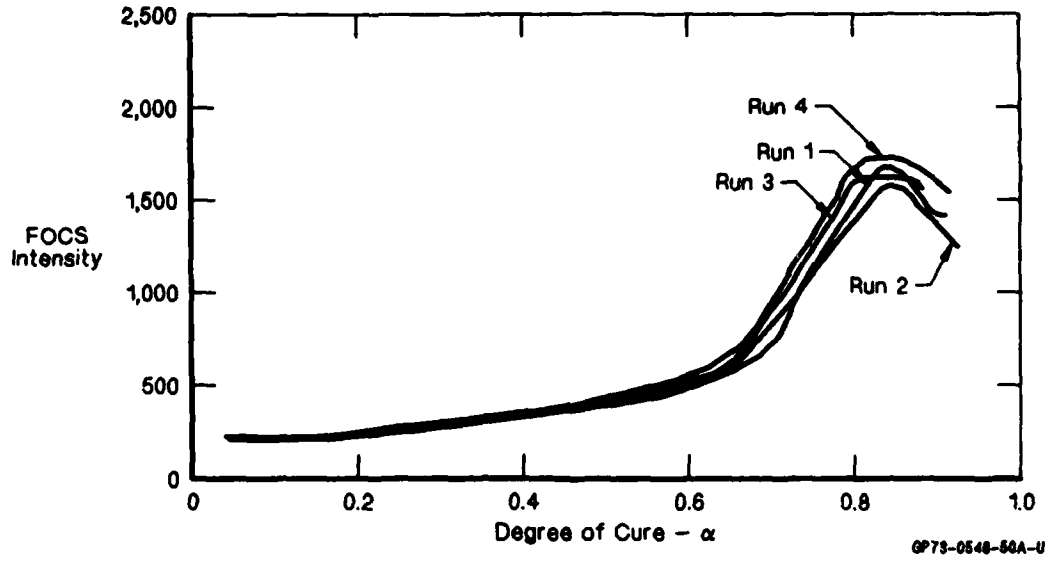

Figure 20. Correlation Between FOCS Intensity and Degree of Cure for 180°C (356°F) Isothermal Cures

same relationship exists for each of the repeated trials. Statistical tests can be used to determine if, in light of the variation of individual observations about their respective relationships, these relationships could be considered to be the same. Since the data in most cases show a high degree of scatter and divergency and obvious lack of repeatability, these statistical tests were deemed to be unnecessary.

Empirical relationships were, however, developed using the statistical principle of least squares to estimate the coefficients of the model. Where applicable, data from all four trials at each temperature were combined when performing these calculations. The resultant line can be thought of as describing the general relationships between FOCS responses and η or α. The variation about this general relationship line is attributed to variations within a particular trial and to variations in the trial-to-trial relationship.

2.5.2.2 Analysis of Wavelength Response - The relationship between wavelength at maximum emission (λmax) and degree-of-cure at 120°C (248°F), Figure 16, shows that there is relatively little change in response as α increases, although all four runs shown the same trends during this pre-gelation cure stage. Corresponding curves of λmax versus viscosity (η) were not plotted; wavelength responses were even less sensitive to viscosity changes, even over a four-decade change in η. Wavelength response is, therefore, not a predictor of degree-of-cure or viscosity changes at this temperature.

At 180°C (356°F), the relationship between λmax and α (Figure 17) was somewhat more pronounced. A reversal of the pattern occurs at about $\alpha = 0.8$, beyond which there appears to be a higher degree of repeatability and a positive correlation with α. A profile of the FOCS wavelength response

versus time during the late stages of cure for one of the four 180°C (356°F) isothermal cure cycles is shown in Figure 21. The corresponding curve for degree-of-cure (α) is superimposed for comparison. The obvious correlation during the late stages of cure is also shown for all four runs in Figure 22, which is an expansion of this area taken from Figure 17. In Figure 22, the range of α is shown from 0.82 to 0.95. For the four replicate trials, the linear relationships in this range between wavelength and α were calculated using least squares regression techniques. It is not known whether these mathematical differences in predicted degree-of-cure from run to run are attributable solely to the random variation of system response or to a small degree of non-repeatability among the four trials.

2.5.2.3 Analysis of FOCS Intensity Response - Analysis of the intensity signal as a sensor response parameter was more successful, even though there were divergences in some of the repeat trial curves (Figures 18 through 20). It should be noted that sensor data obtained during the first 15 minutes were not used, because the initial heatup to isothermal test temperature resulted in erratic response data.

Analysis of raw data points for the 120°C (248°F) trials (Figures 18 and 19), which reveal the scatter bands for each run, showed little overlap from run to run. It can be concluded that there are other factors operative from trial-to-trial that were more influential than basic experimental error. Therefore, the four trials can not be considered to have generated identical relationships. Mathematical relationships for these runs, using averaged data points from all four runs, were established. Using the equations to predict degree-of-cure from FOCS intensity responses, within 95 percent

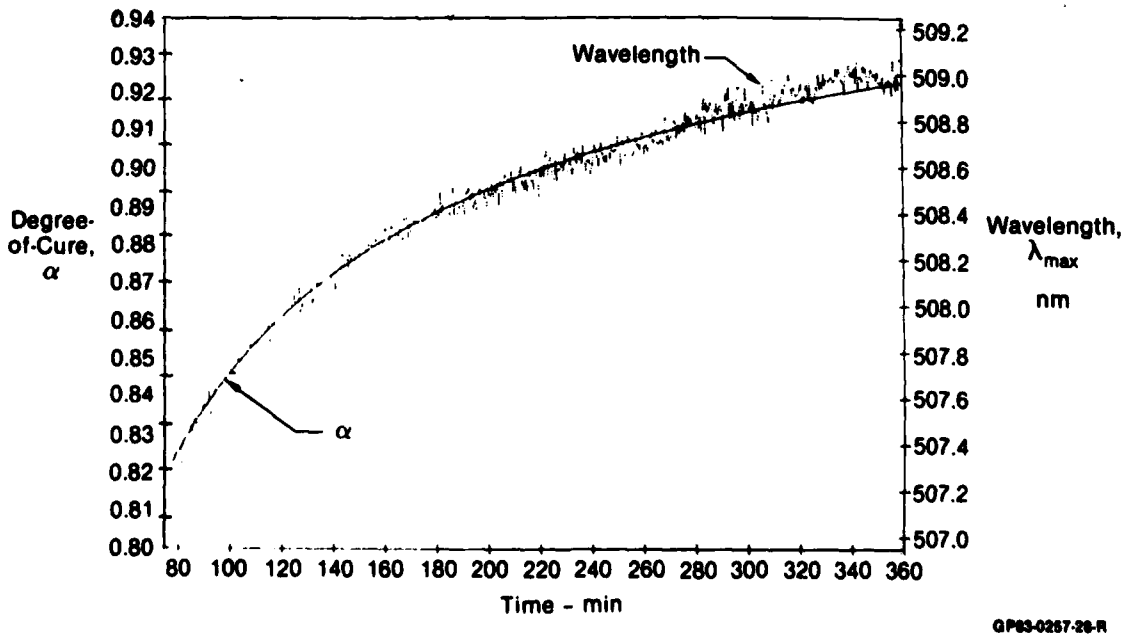

Figure 21. Correlation of Degree-of-Cure (α) for Late Stages of Cure With FOCS Wavelength Signal for 180°C (356°F) Isothermal Cure

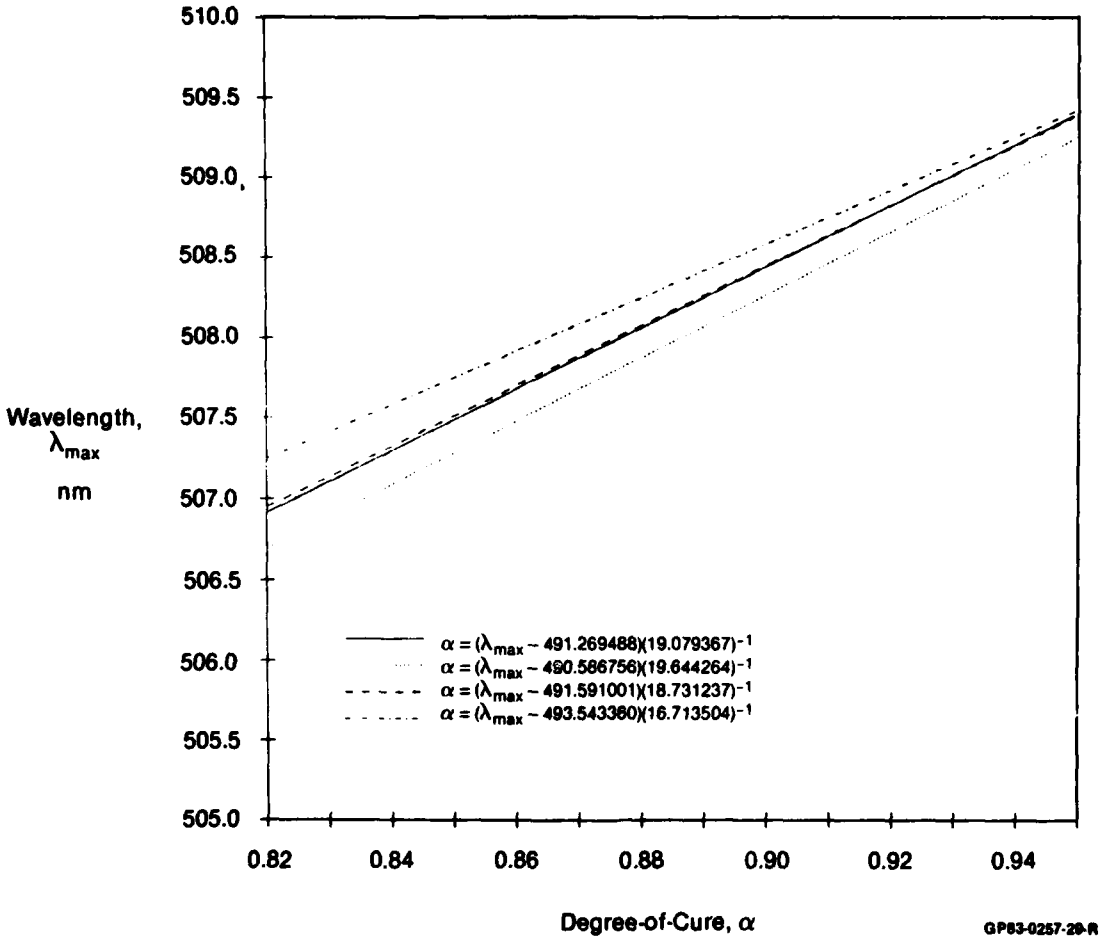

Figure 22. FOCS Wavelength Response/Degree-of-Cure (α) Relationships for Four 180°C (356°F) Isothermal Cures During Late Cure Stages

confidence limits, it was determined that at the early cure stage predicted α could vary as much as 30 percent in the α = 0.15 range and 35 percent in the α = 0.35 range. The corresponding viscosity predictions could vary from, for example, 6 to 28 poise in early cure stage and by 2.5 orders of magnitude at higher viscosities. It is obvious that the predictive level for both α and η is low as these parameters increase.

The relationship between maximum intensity and α at 180°C (356°F) for the four trials is shown in Figure 20. For statistical analysis purposes, data for α > 0.8 were discarded; it is believed that the slope reversals more likely reflect equipment-related causes than changes in the sensor response-material property relationship. Within the remaining range of values, this relationship is much more reproducible than those observed during the 120°C (248°F) trials. Using the combined data from the four trials, a fourth degree polynomial was derived:

$$\alpha = 0.722 + 0.102 \times 10^{-3} (MI-900) - 0.525 \times 10^{-10} (MI-900)^2 + 0.525 \times 10^{-11} (MI-900)^3 - 0.766 \times 10^{-14} (MI-900)^4,$$

where MI = maximum FOCS intensity units

This equation, which expresses the relationship of α between 0.3 and 0.8 based upon FOCS intensity at 180°C (356°F), has a coefficient of determination and a standard error of estimate equal to 0.98 and 0.017, respectively. Using this equation, approximately 95 percent prediction limits are about $\pm$0.07 about the calculated degree-of-cure.

2.5.2.4 Effect of Temperature upon FOCS Intensity Response - The temperature at which the 3501-6 cure is performed has a significant effect upon the relationships between FOCS intensity and both of the cure parameters - viscosity (η) and degree-of-cure (α). The relationships are shown in Figures 23 and 24, respectively.

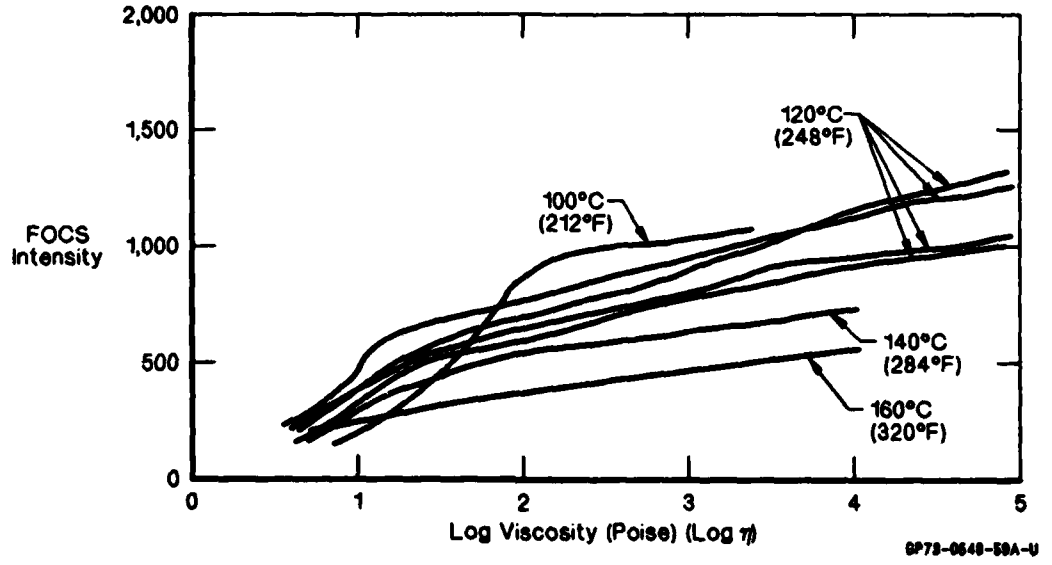

Figure 23. Effect of Temperature of Isothermal Cure of 3501-6 Upon FOCS Intensity - Viscosity Relationship

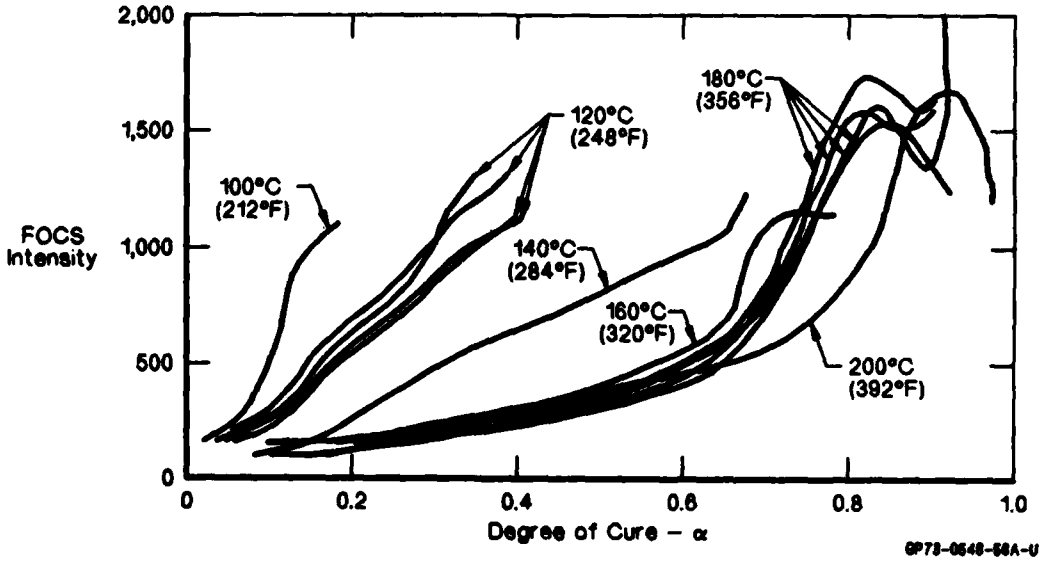

Figure 24. Effect of Temperature of Isothermal Cure of 3501-6 Upon FOCS Intensity - α Relationship

There appears to be a lesser temperature effect in the maximum intensity - η relationship. With the exception of the 100°C (212°F) curve, the rate of change in maximum intensity versus η decreased with an increase in temperature. However, if the three temperatures not tested for repeatability [100°C (212°F), 140°C (284°F) and 160°C (320°F)] were to show the same degree of scatter as the relationships at 120°C, much overlapping could be expected. As a result, it would be questionable that a maximum intensity-viscosity-temperature relationship could be defined that would accurately predict viscosity from maximum intensity changes over a wide temperature range that would be typical for cure of a composite material.

Rate of change in maximum intensity versus α (Figure 24) also decreases as cure temperature increases. These rate changes decrease rapidly from 100°C (212°F) to 160°C (320°F), but above this temperature there appears to be little temperature effect at values of $\alpha < 0.65$. Since the curves at the higher α values (>0.80) are distorted, probably due to mechanical changes within the sensor or resin system, the effect of temperature upon the maximum intensity - α relationship is difficult to predict.

Since FOCS response to changes in η and α are dependent upon the temperature imposed upon the system, the response patterns will be different for each different time-temperature profile used to cure the resin. The lack of repeatability in the FOCS response-resin property relationships will make it difficult to develop the temperature correction factors that are needed to generalize the mathematical relationship across the entire spectrum of temperatures that will be encountered in practice.

2.5.3 Discussion of Results - The optimization of the optrode-laminate interface described in Section 2.2.4 and the provision for compensation of the fluctuations in the intensity of the excitation light described in Section 2.2.1.1 provide conditions for improved FOCS performance. It is quite possible that further improvements of the FOCS performance can be achieved through additional refinements of the optrode-laminate interface.

All of the FOCS intensity signals for the 120°C (248°F) and 180°C (356°F) isothermal cure cycles initially follow the expected signal profile patterns of decrease with heat up portion of the cure cycle followed by an increase resulting from cure-induced increase of the viscosity. The point of minimum viscosity is easily and accurately observed in all runs.

The reproducibility of the isothermal runs at 120°C (248°F) and 180°C (356°) are discussed in Section 2.5.2.1. The observation of differences between the minimum FOCS intensity signal values for the 120°C (248°F) run (Figure 12) suggests either inhomogeneous distribution of the curing agent or catalyst in the resin or inhomogeneous distribution of the compounds responsible for the viscosity-dependent fluorescence of the resin. The wider scatterband of the intensity signals during the later stages of cure for both the 120°C (248°F) and the 180°C (356°F) runs can also be attributed to such inhomogeneity in the resin which, of course, could be indicative of actual differences in the epoxy networks resulting from these separate cure cycles.

As discussed in 2.5.2.2, a linear relationship exists between λmax and degree-of-cure for $\alpha > 0.8$ in the 180°C (356°F) cure cycles (Figure 22). However, α never reaches 0.8 in the 120°C (245°F) runs; the λmax - α relationship in these lower ranges is complex and not well understood.

3.0 DEVELOPMENT OF ACOUSTIC WAVEGUIDE (AWG) CURE SENSOR

3.1 BACKGROUND AND THEORY

Acoustic waves travel by molecular interaction. Therefore, they are sensitive to minute changes in the material elastic constants, temperature, density, viscosity, porosity, crystal size and orientation. In view of this, it is not surprising that ultrasonic wave propagation through a resin can yield information about the curing process. However, the practical application of ultrasonics to the curing process has been restricted. Physical difficulties have been experienced in coupling the ultrasonic transducers to the resin. Signal-to-noise ratios have been reduced by the dispersion and scattering of the acoustic beam as it traverses a specimen, making the interpretation of results difficult. In some cases access to the curing material is complicated by a hostile environment and confined space.

These problems have been reduced considerably by integrating acoustic waveguides into the resin (References 15 through 19). The waveguide material can be, e.g., epoxy reinforced glass, carbon or aramid fibers. An acoustic wave transmitted along a buried waveguide 0.04 inch in diameter is not subject to dispersion or alignment problems. These devices are very sensitive to changes during material cure because sound escapes from the waveguide to the resin dependent on the relative acoustic impedances of the waveguide and host material. Consequently, the acoustic waveguide cure sensor (AWG) can readily monitor viscosity changes within a curing resin. The sensor output can also be interpreted to pinpoint gelation of the resin, where the change in form of the epoxy from a liquid to a rubbery gel is accompanied by large changes in both the acoustic impedance and acoustic wave velocity. It is reasonable to assume that the ability to detect changes in elastic properties of the host material, after gelation, will provide a reasonable measure of the degree-of-cure in relation to time and temperature. Consequently, it follows that data analyzed with respect to temperature should yield approximate values for activation energies and chemical reaction rates.

3.2 STUDY OF 3501-6 NEAT RESIN CURE

3.2.1 Experimental Apparatus for Acoustic Waveguide Cure Monitoring of Resins and Composites - The experimental apparatus used for laboratory development of acoustic waveguide cure monitoring of resin and composites is outlined in the schematic, Figure 25. A Wavetek 191 pulse function generator is used to excite the transmitting acoustic transducer (~70-~80 kHz resonant frequency) with 32 cycle sine wave pulsed wavetrains. These wavetrains are from one volt to 15 volt peak value and are repeated 150 times per second. A square wave can be substituted for the sine wave if necessary. The transmitted signal is displayed on a Tektronix 7844 dual beam oscilloscope together with the signal received from the waveguide. The received signal appears as a modulated envelope of signals. The wave transit time along the waveguide can also be obtained from the oscilloscope record. A television camera and monitor and a VCR are used for recording the signals appearing on the oscilloscope screen. This is valuable for playback and analysis of rapidly changing signals, particularly near gelation. The video camera is shown in Figure 26.

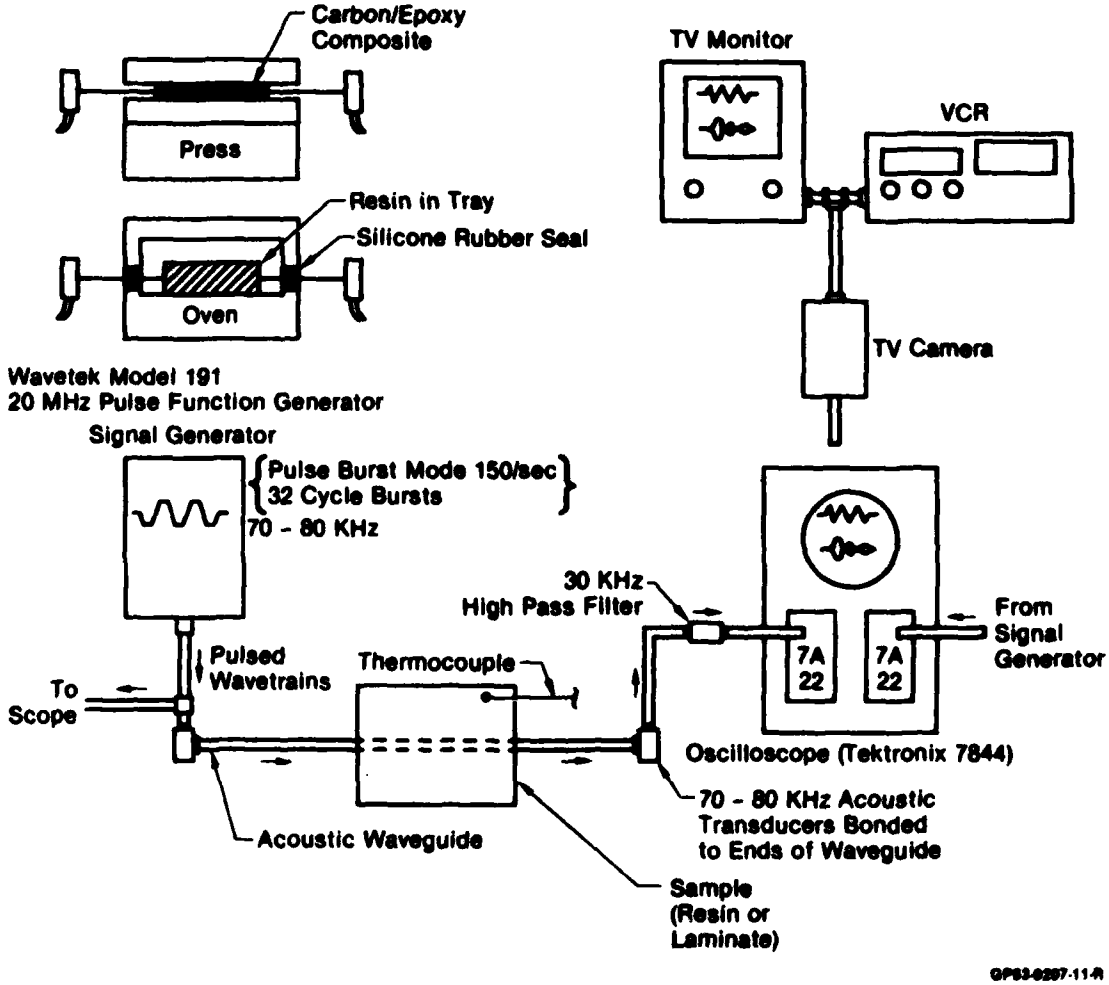

Figure 25. Schematic of Instrumentation and Systems Used for Acoustic Waveguide Monitoring of Resin and Carbon/Epoxy Composite

GP83-0307-12-R

Figure 26. Video Camera Used to Record and Playback the Oscilloscope Signal During AWG Cure Monitoring

For experimental work, data are manually recorded from the oscilloscope and are entered into a spread-sheet program (Supercalc-3) on an Apple IIe coupled to the HP7470 plotter from which data plots are generated.

3.2.2 Neat Resin (3501-6) Curing Experiments

3.2.2.1 Experiment Description - Figure 27 shows a 6 1/2 inch x 6 1/2 inch pan with 3501-6 resin after a curing experiment was completed. The acoustic waveguide of 0.06 inch diameter glass/polyester material running through the resin is shown bonded to the two acoustic transducers. Silicone rubber isolators were tested and found satisfactory to isolate the waveguide from the pan containing the resin and from the oven walls. A microdielectrometer sensor buried in the resin can also be seen. Figure 28 shows the experimental setup with the signal generator and oscilloscope for the acoustic measurements, the Wizard temperature controller and strip chart to control and monitor oven and resin temperatures, and the microdielectrometer used to measure simultaneously the dielectric properties of 3501-6 resin during cure. About 200 gms of resin were used, with the resin depth in the pan of about 0.14 inch.

3.2.2.2 Test Result (AWG-01) - Figures 29 through 32 present the sonic output, transit time and loss factor as a function of time during the experiment. The resin temperature profile is also presented in Figures 29 through 31.

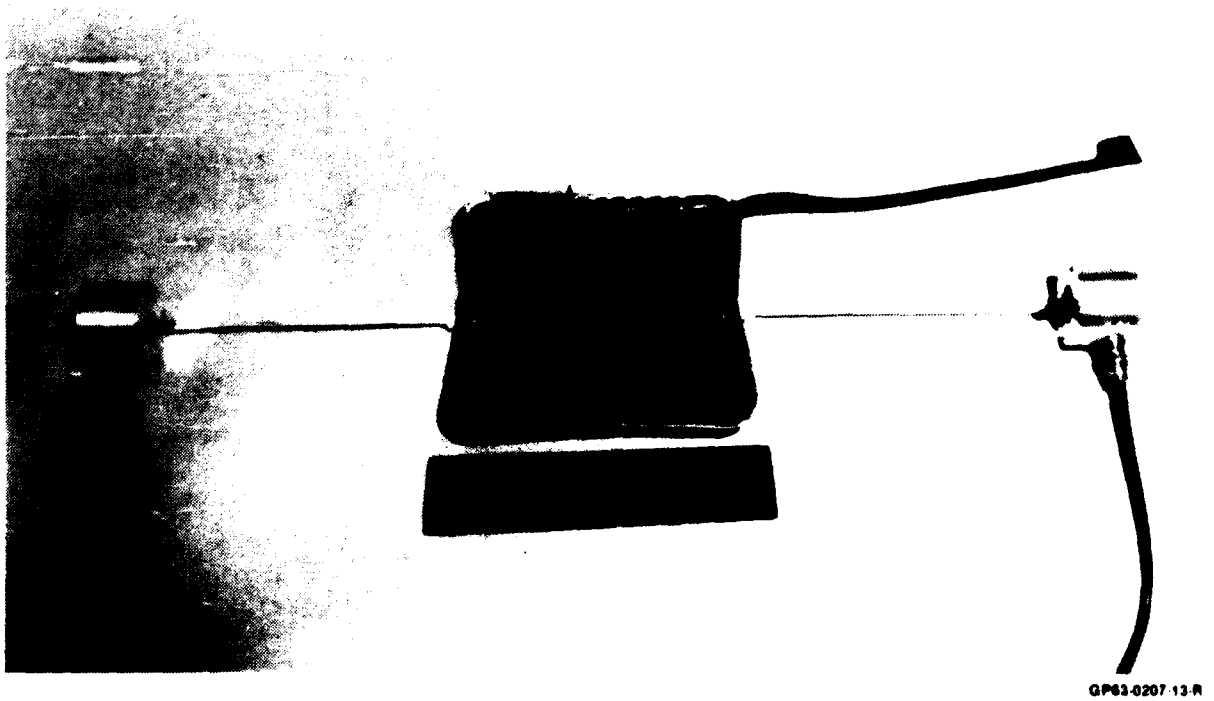

GP83-0207-13-R

Figure 27. Resin Cure Monitoring Experiment With AWG

GP83-0207-14-R

Figure 28. Overall View of Experimental Setup for AWG Cure Monitoring

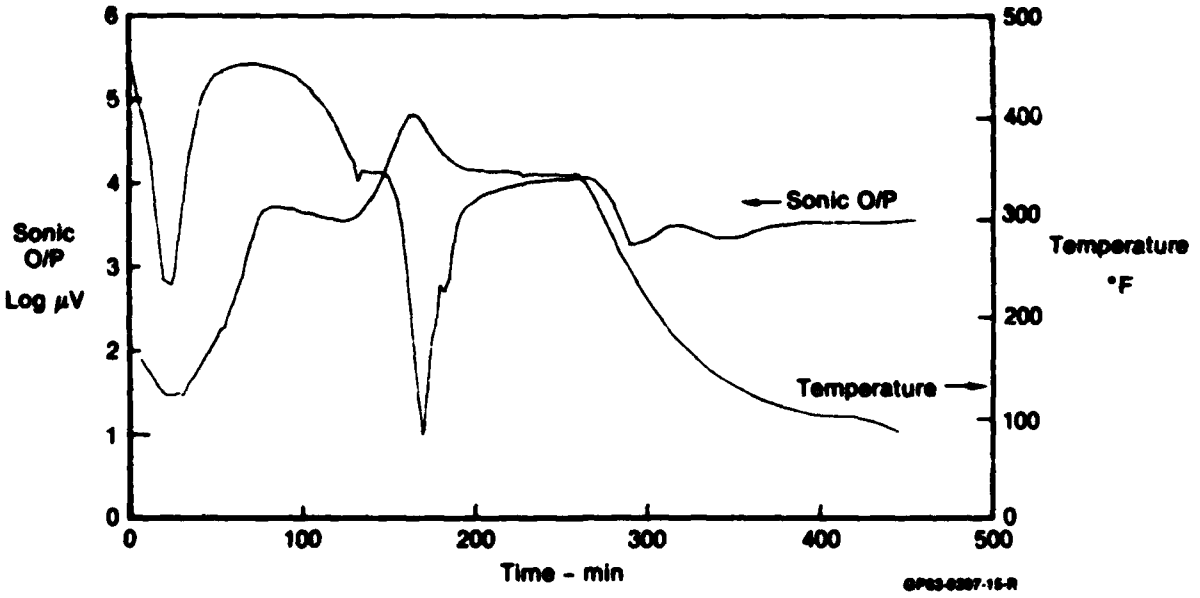

Figure 29. AWG Response and Temperature Profile for Oven Cure of 3501-6 Neat Resin (AWR01)

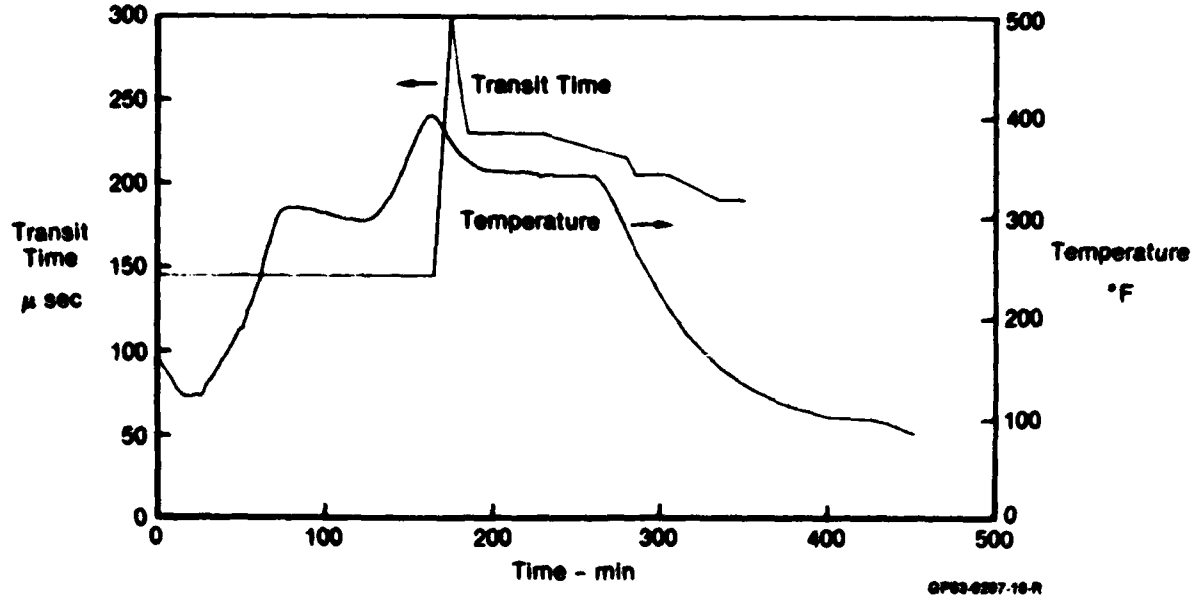

Figure 30. AWG Wave Transit Time and Temperature Profile for Oven Cure of 3501-6 Neat Resin (AWR01)

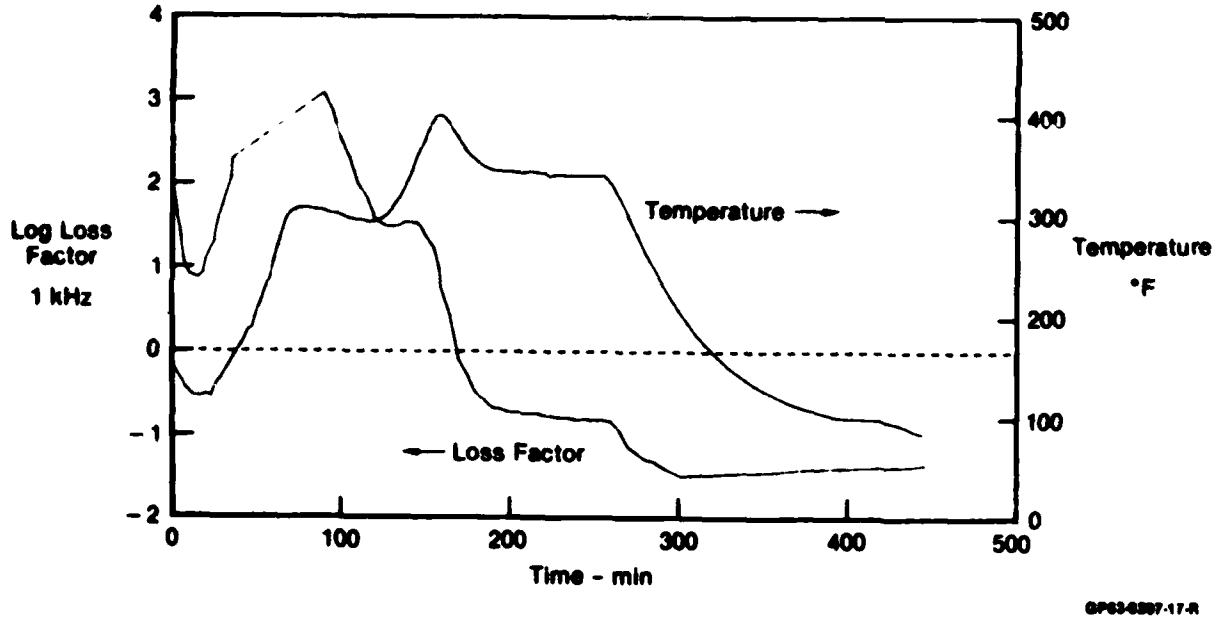

Figure 31. Dielectrometer Loss Factor and Temperature Profile for Oven Cure of 3501-6 Neat Resin (AWR01)

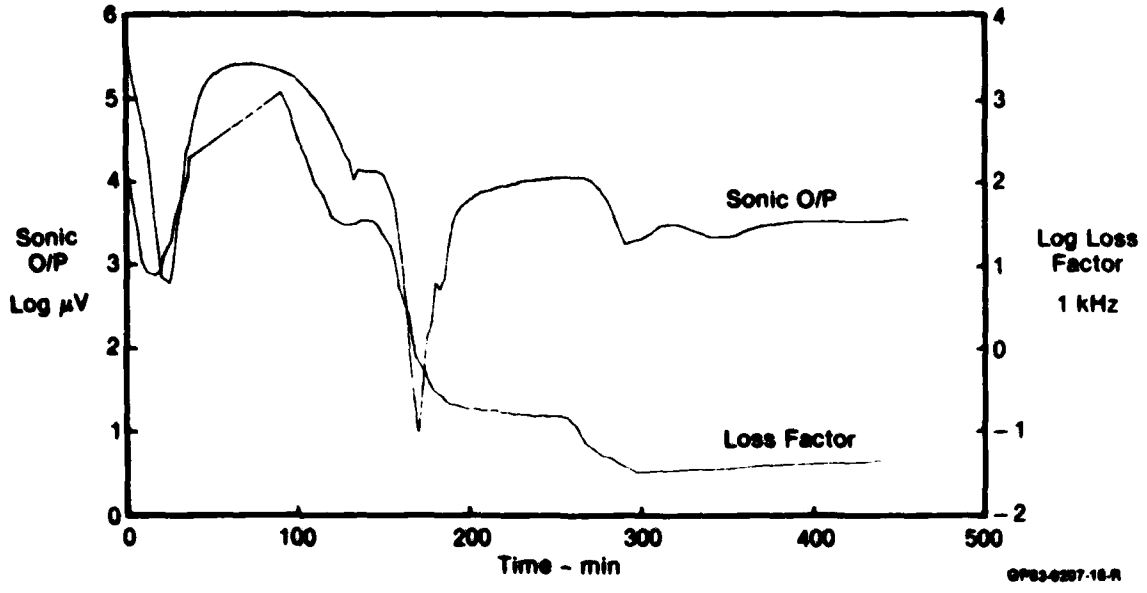

Figure 32. Comparison of Dielectrometer Loss Factor and AWG Response During Oven Cure of 3501-6 Neat Resin (AWR01)

The resin temperature overshot initially on reaching the 360°F setpoint level and was cut back manually by about 20°F. The peak was due to a set point of 370°F instead of 360°F and to a resin exotherm, which is normally expected for this mass (200 gms) of resin.

The sonic output (Figure 29) shows the typical response with changing viscosity. Response increases as the temperature is raised to the 270°F hold temperature. Then, as the chemical reaction increases the viscosity, the sonic output decreases. As the cure proceeds, the output drops rapidly to about 10 μV yielding a total voltage change of about 4 decades. The minimum of output at 170 minutes represents gelation (liquid to rubbery gel transition). In the plot of transit time as a function of time during cure (Figure 30), it can be seen that there is a sudden increase in transit time coincident with the minimum acoustic signal (at gelation). This sudden decrease in acoustic wave velocity occurs because, at gelation, most of the acoustic wave is travelling in the resin layer adjacent to the waveguide surface (slow velocity of ~2000 m/s) instead of inside the acoustic waveguide (faster velocity of ~4000 m/s).

3.2.2.3 Correlation of AWG Results with Dielectrometry - Simultaneous measurements of AWG and automatic dielectrometry loss factor for neat resin are compared in Figure 32. There is good correlation between the two sets of data, with both sensors detecting the onset of gelation near 80 minutes into the cure cycle and responding similarly to viscosity changes until gelation at 170 minutes. The AWG is more precise in pinpointing gelation. Several experiments were performed on neat resin with the AWG embedded in the resin, with essentially identical results, indicating good reproducibility.

3.3 STUDY OF CARBON/EPOXY LAMINATE CURE

3.3.1 Carbon/Epoxy (AS4/3501-6) Prepreg Experiments - In using the AWG to monitor the cure of prepreg, a balanced layup of forty plies, 12 inch x 12 inch, of unidirectional prepreg tape was used, with fibers oriented 0/90° and the two 90° plies adjacent to the centrally located waveguide parallel to each other. A standard step cure cycle was employed with the prepreg in a press maintained at 50 psig pressure (Figure 25). The waveguide material was the same as used in neat resin experiments. The AWG and microdielectrometer response data again exhibited good correlation (Figure 33). The acoustic data profile is similar to that found for the neat resin, except that it is not biased by the strong exotherm. Figure 34 clearly shows the ability of the waveguide sensor sonic output to follow the staging and cure of the prepreg resin, with a sharp minimum in sonic output at or near gelation. Increase in the output with increasing degree of cure after gelation is also noted. In addition, the time at which gelation occurs is pinpointed by a large increase in the acoustic wave transit time (Figure 35). A typical AWG-monitored cure of AS4/3501-6 is shown in Figure 36; numerous similar cure profiles were obtained during the development efforts.

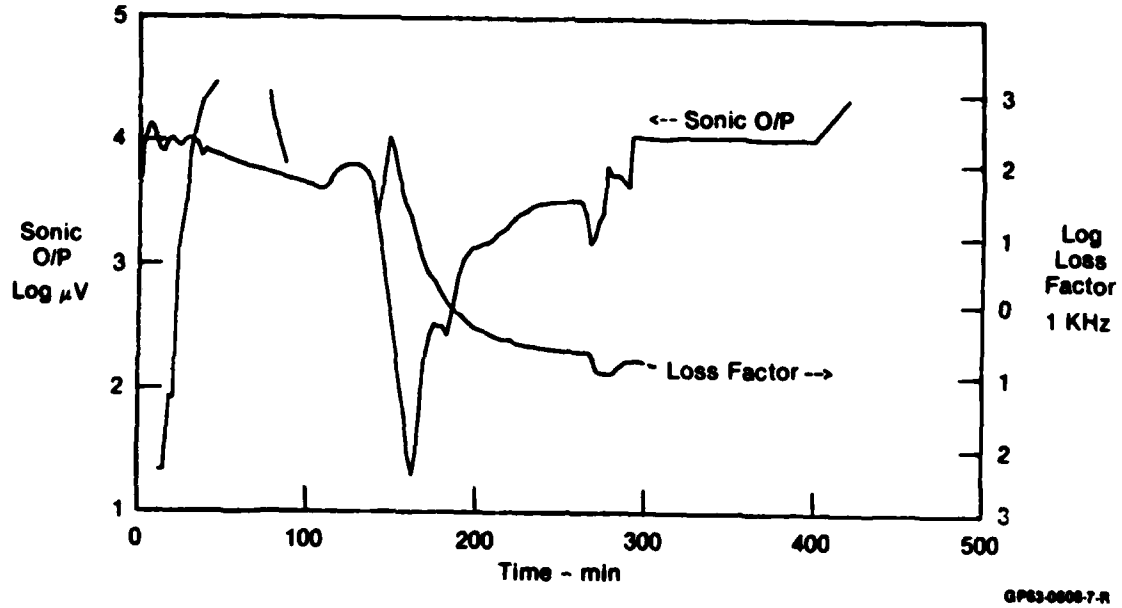

Figure 33. Comparison of Dielectrometer Loss Factor and AWG Response During Press Cure (50 PSIG) of AS4/3501-6 Prepreg (AWG05)

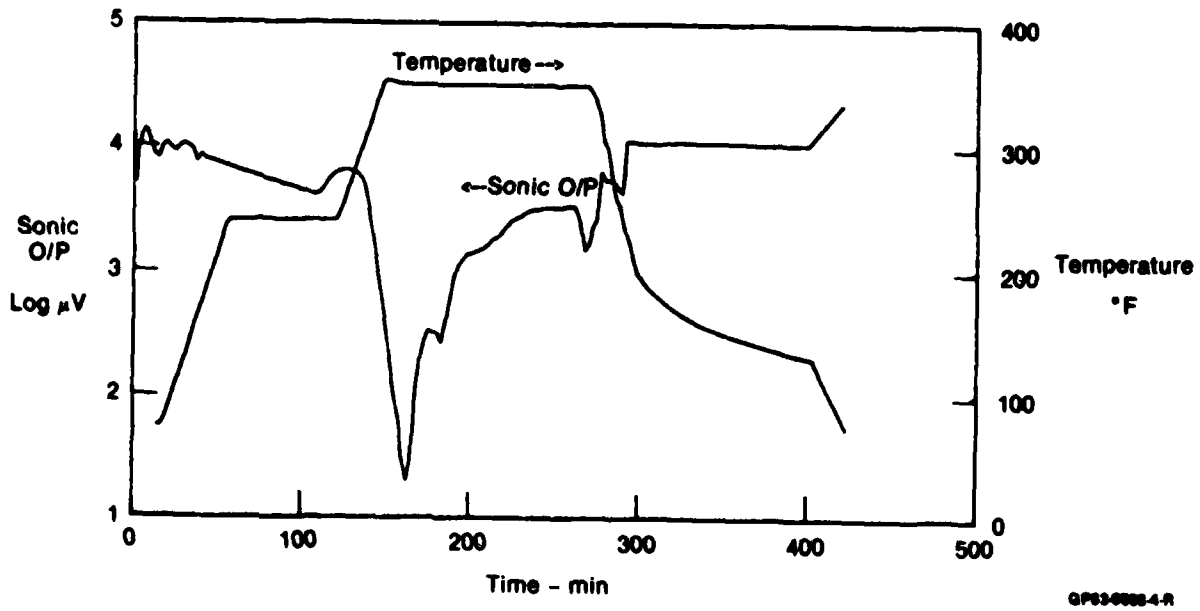

Figure 34. AWG Response and Temperature Profile for Press Cure (50 PSIG) of AS4/3501-6 Prepreg (AWG05)

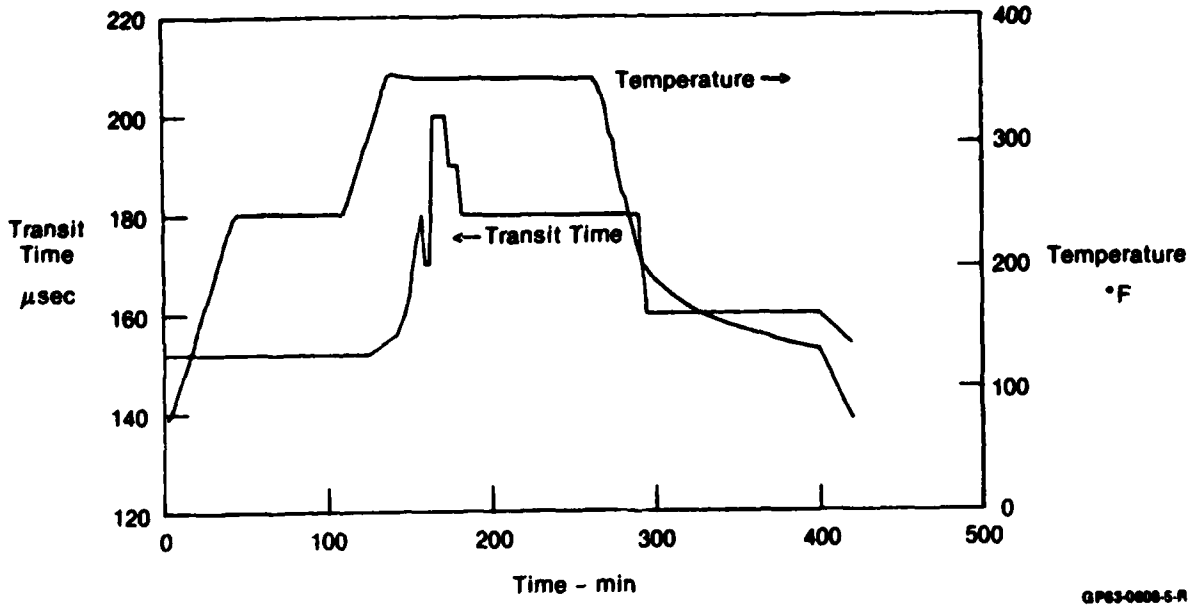

Figure 35. AWG Wave Transit Time and Temperature Profile for Press Cure (50 PSIG) of AS4/3501-6 Prepreg (AWG05)

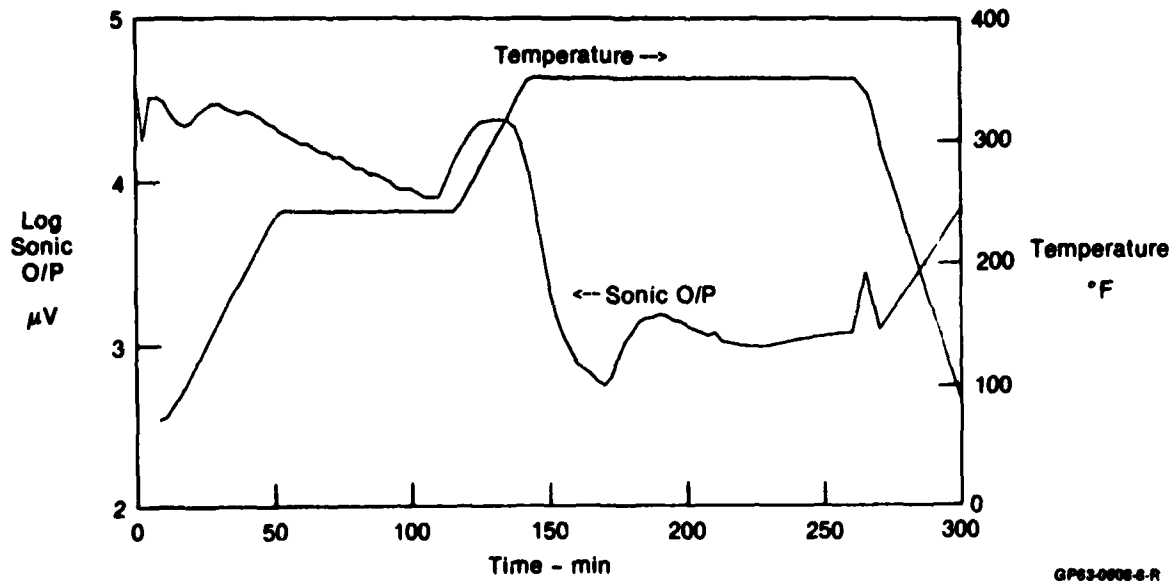

Figure 36. Typical AWG Response and Temperature Profile for AS4/3501-6 Prepreg Laminate Cure

3.4 EFFECTS OF VARIABLES

3.4.1 Waveguide Material - In order to learn about the effects of waveguide material and configuration, experiments were performed using waveguides of polyester-fiberglass, nichrome (Inconel or nickel-chromium), copper and carbon-epoxy. These materials were selected because of their low (<0.3) values of Poisson's ratio, a requirement for efficient wave transmission. They also represent a wide range of acoustic impedance: carbon/epoxy is an acoustic match with the host laminate material, and the other materials represent varying degrees of acoustic mismatch. Consequently, experiments with these different waveguide materials should yield AWG cure sensor response profiles of varying sensitivity. The metal waveguides were 0.06 inch in diameter, while the carbon-epoxy guide was 0.08 inch square, cut from a unidirectional laminate of fully cured AS4/3501-6. For comparison, data from all these experiments are displayed in Figure 37. It is clear that all the waveguides can be used to identify the start of gelation (near 130 minutes into the cure cycle) and the gelation point at the 160 to 180 minute region. In addition, the changes in wave velocity during cure can be used to identify the occurrence of gelation, Figure 38. Nichrome waveguides were used for subsequent development experiments because of their high sensitivity and ruggedness. The wire diameter was reduced to 0.02 inch to minimize any effect upon composite structural properties.

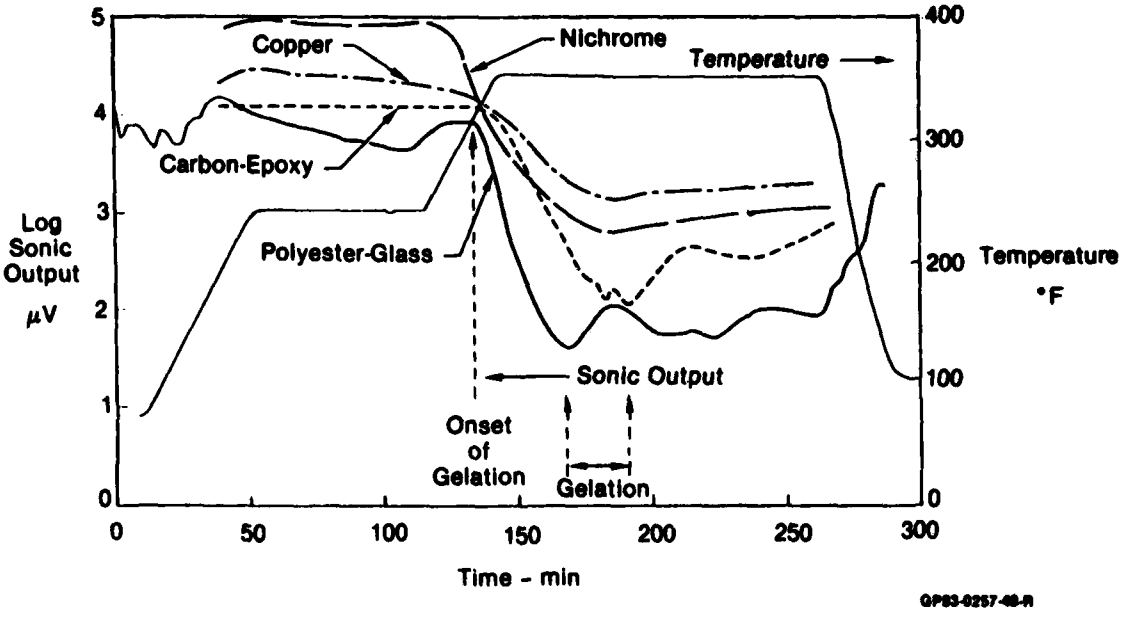

Figure 37. Effect of Waveguide Material Upon AWG Sonic Output During Cure Cycle of AS4/3501-6 Prepreg

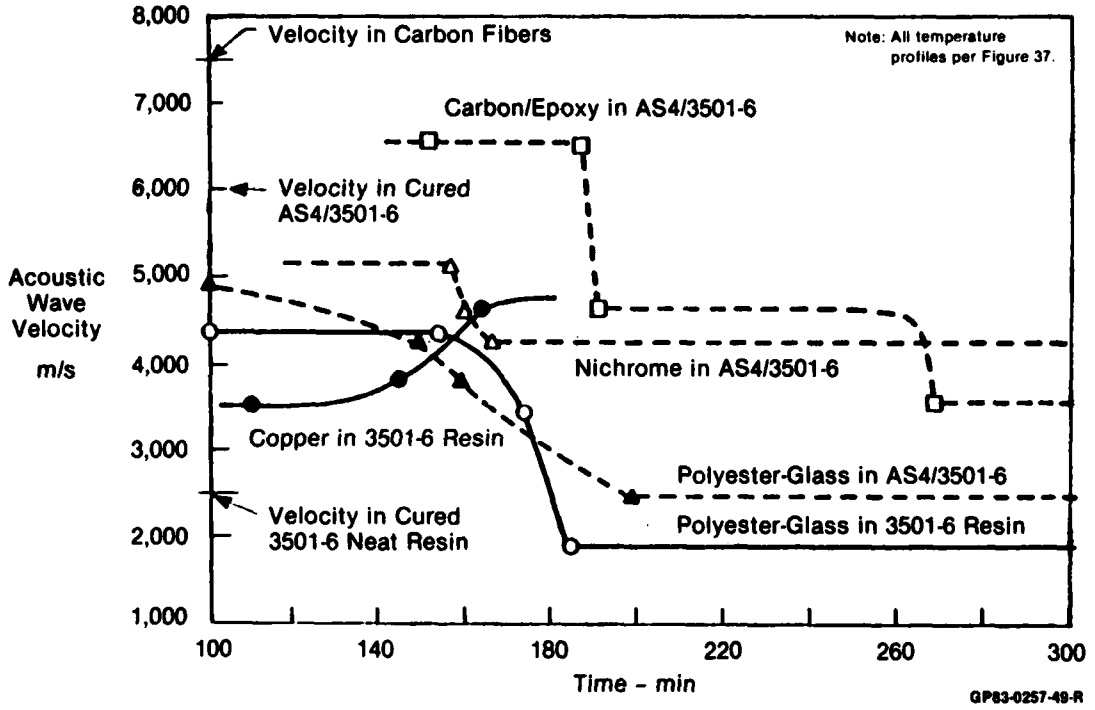

Figure 38. Effect of Waveguide Material Upon AWG Velocity Response During Cure of 3501-6 Materials

3.4.2 Length of Waveguide Embedded within the Laminate - In order to assess the effect of waveguide length embedded within the laminate, as will be experienced in monitoring parts of different sizes, three 40-ply 0-90° laminates (4 inch x 4 inch, 8 inch x 8 inch, and 12 inch x 12 inch) were cured using 0.02 inch diameter nichrome waveguides. The output curves (Figure 39) for the three laminates are similar, indicating the embedded waveguide length is not a factor in the sensor response, although the signal loss is significantly affected. An analysis of the data from experiments AWG 23 through 25 led to the hypothesis that attenuation within a waveguide is related to the length of waveguide embedded within the laminate; the loss or attenuation (α) is defined as follows:

$$\text{Attenuation, } \alpha \text{ (dB)} = 20 \log_{10} V_1/V_0$$

when V_1 = input voltage

V_0 = output voltage.

The attenuation can be considered a measure of the acoustic energy that is lost to the medium surrounding the waveguide. If the waveguide within the material is twice as long, then the attenuation should be 6 dB higher (i.e., $20 \log_{10} 2 = 6$). For a buried length which is three times as much, the attenuation should be 9.5 dB higher. If we examine the data in Figure 39 for the three laminates at the maximum attenuation, we note that the attenuation is 85 dB for the 4 inch length, 93 dB for the 8 inch length and 98 dB for the

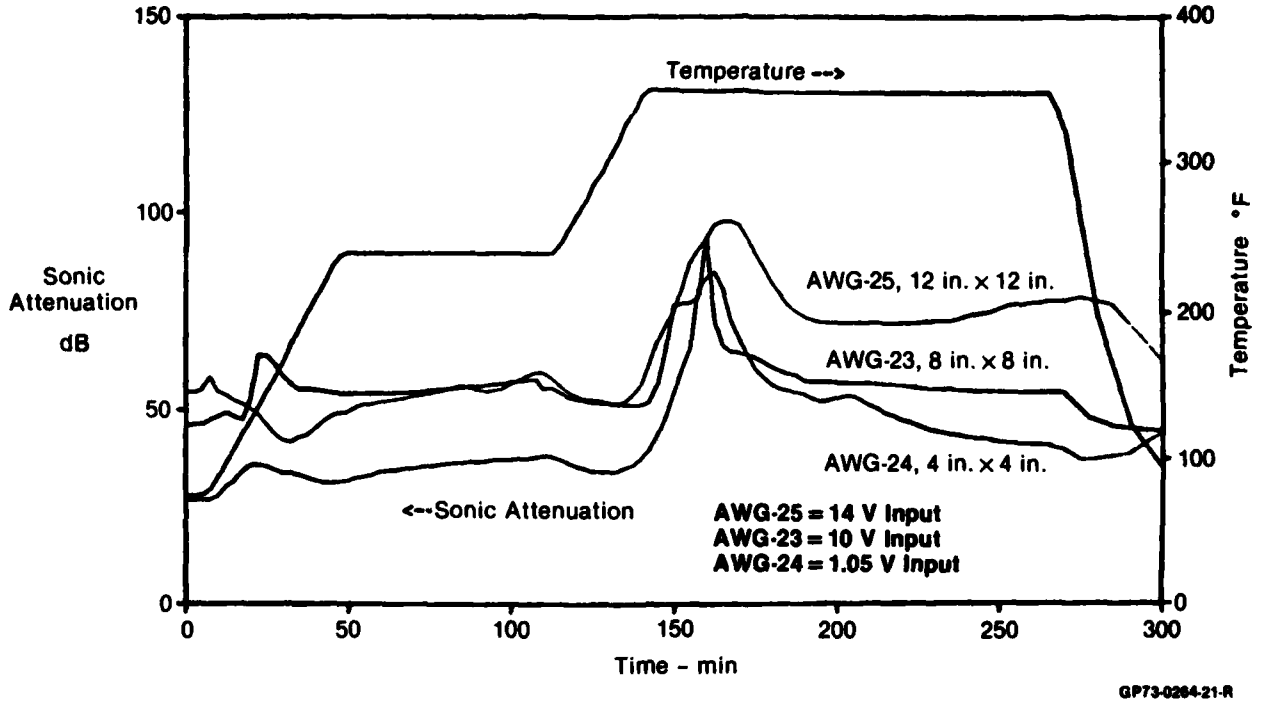

Figure 39. Effect of Buried Length Variation of 0.02 Inconel Waveguide on Response to Cure of AS4/3501-6 (40 Ply, 0° - 90°)

12 inch length. The differences are close to those predicted above for different buried lengths of waveguide. However, it should be noted that this method of analysis is not considered to be applicable to degree-of-cure estimates.

3.4.3 Laminate Configuration - To investigate the effect of laminate ply orientation three runs were made with 0.02 inch diameter nichrome waveguides and prepreg material from the same lot number that was later used in the calibration panel runs.

All panels were 12 inch x 12 inch. One cure (AWG 26) was made with a 41-ply laminate of the thick-section configuration shown in Figure 40, $[(\pm 45, 0_2)_5, 90, (0_2, \pm 45)_5]$. This laminate configuration was used for sensor calibration and demonstration cures in Task III. The waveguide was positioned in the center, parallel to the 90° ply, and the two adjacent 0° plies were cut to allow for the waveguide (Figure 41a). The second cure (AWG 27) was with a $(0\text{-}90°)_{10S}$ 40-ply laminate, similar to most of the previous AWG development runs. In this configuration, the waveguide was positioned parallel to the two center 90° plies with no cut 0° plies (Figure 41b). The third cure (AWG 29) was with a panel similar to AWG 26, except that the midpoint plies were rearranged to be identical to those in AWG 27; i.e., a second 90° ply was added and two adjacent 0° plies omitted to make a 40-ply layup (Figure 41c).

Sonic output data for runs AWG 26, 27 and 29 are shown in Figures 42, 43 and 44, respectively. The curve for the laminate configuration to be used for calibration panels (AWG 26) is significantly different than for the "standard" 0-90° laminate (AWG 27) that had previously yielded consistent

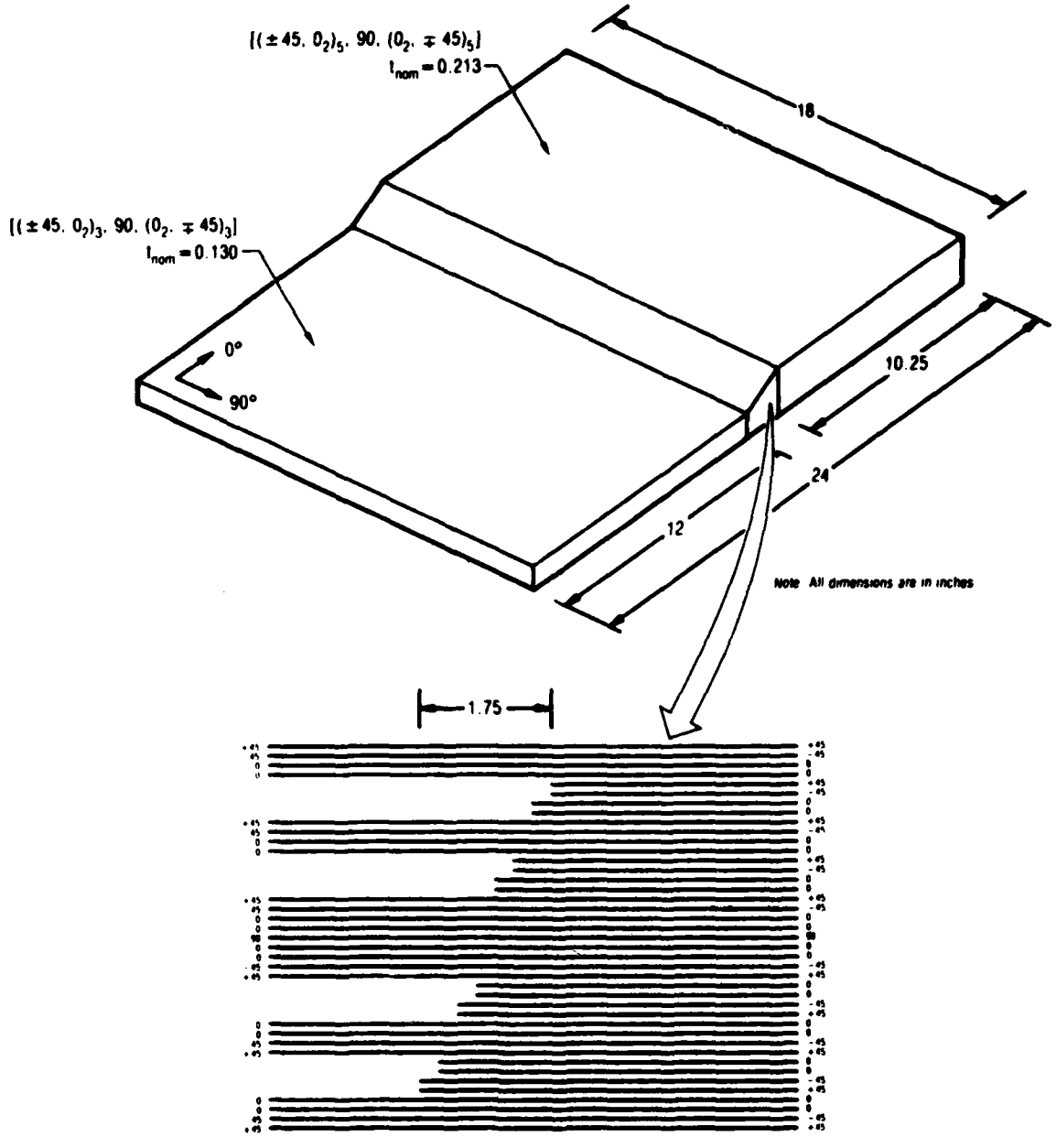

GP93-0257-2-R

Figure 40. Demonstration Test Laminate

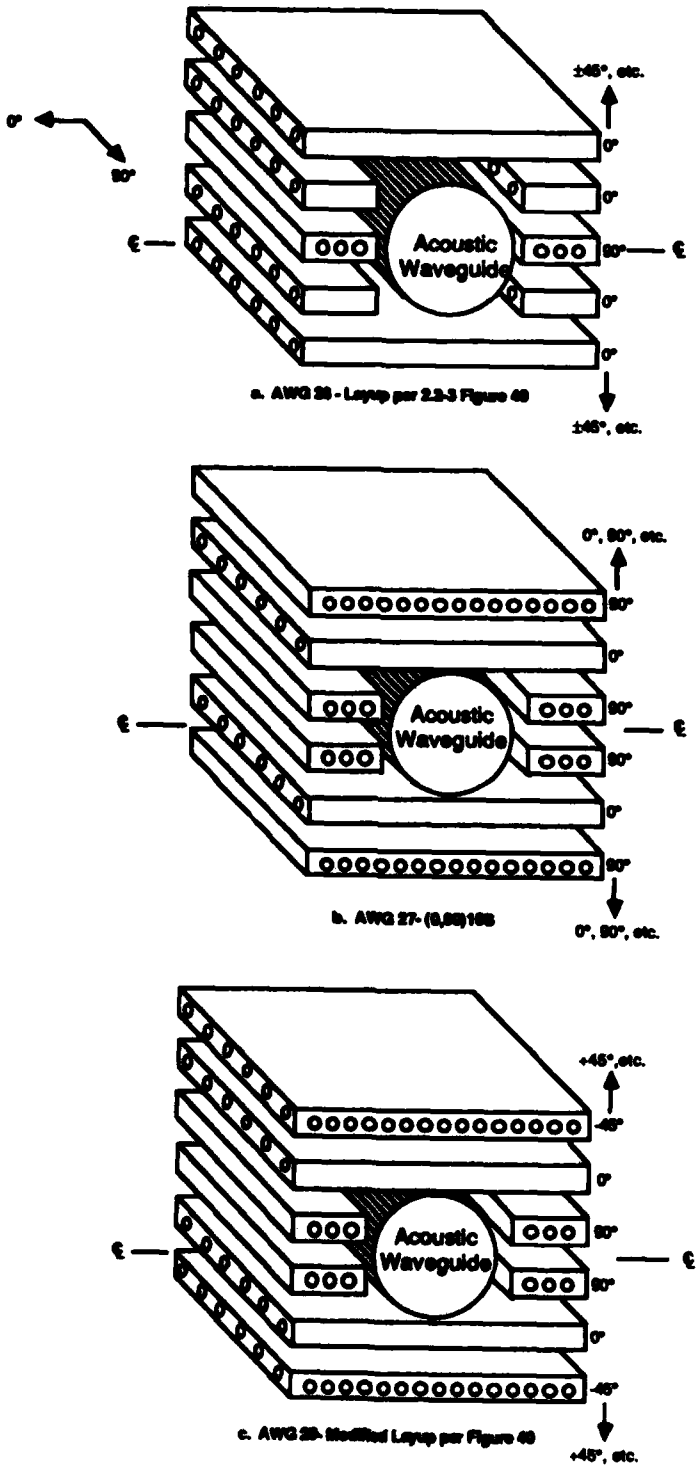

GP73-0264-18-D

Figure 41. Waveguide Locations, Ply Orientation Effects

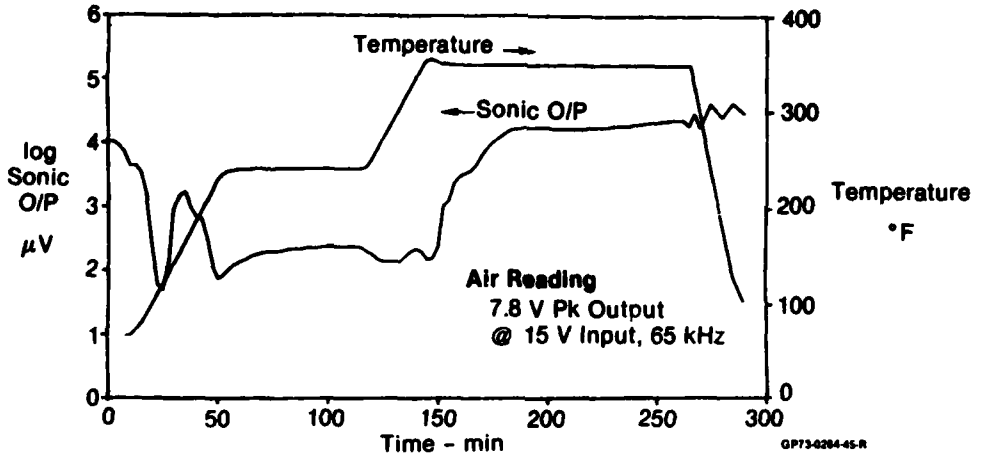

Figure 42. Ply Orientation Effect - Waveguide Location Per Figure 41(a) (AWG-26)

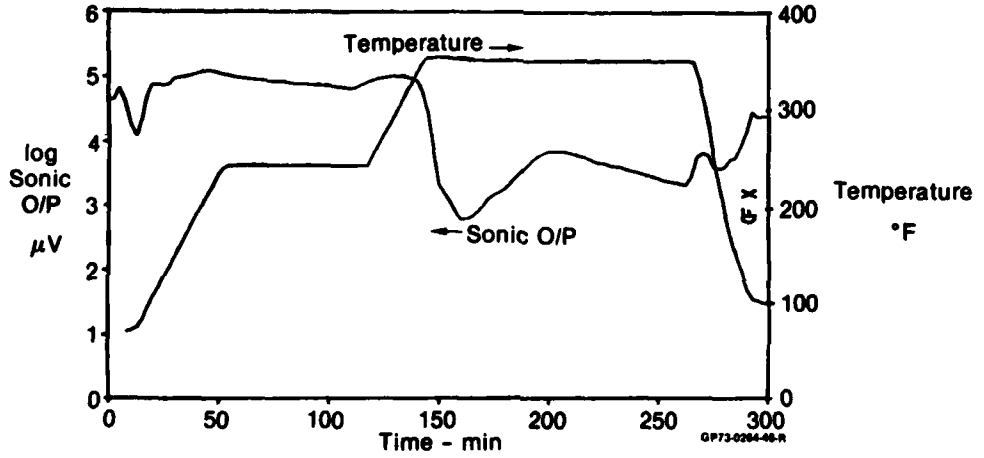

Figure 43. Ply Orientation Effect - Waveguide Location Per Figure 41(b) (AWG-27)

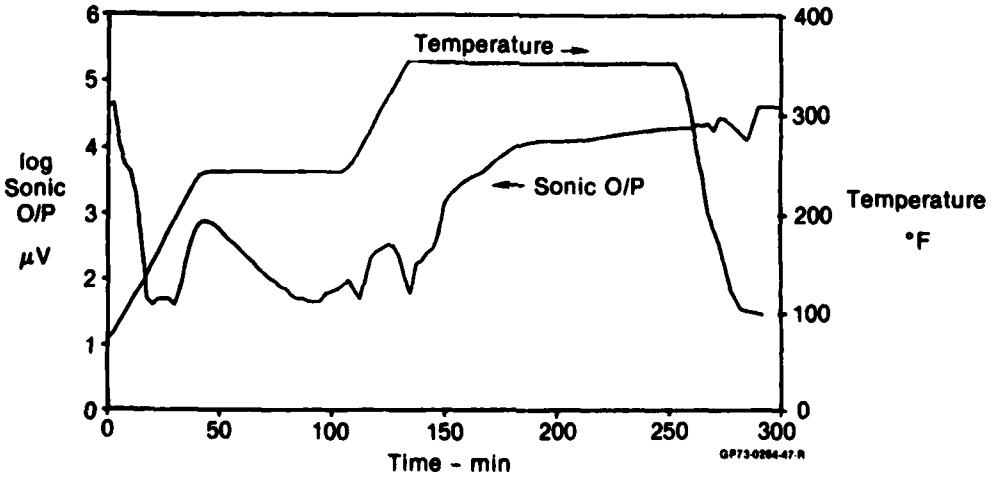

Figure 44. Ply Orientation Effect - Waveguide Location Per Figure 41(c) (AWG-29)

results. The loss in output during the early staging temperature range is clearly evident, as is the increase due to falling viscosity. However, the sharp drop to the minimum that has been typical in 0-90° layups such as in AWG 27 does not appear in AWG 26.

3.4.4 Void Content Monitoring - In devising an experiment to determine the feasibility of the acoustic waveguide cure monitoring (AWG) technique to sense void formation during cure, an experiment was first carried out on a carbon/epoxy prepreg panel in which two 0.02 inch diameter nichrome waveguides were embedded in the same layer, parallel to each other and about 4 inches apart. With acoustic sensors bonded to the waveguide terminations it was possible to obtain four sets of acoustic data during cure, i.e., the attenuation of acoustic waves transmitted along each waveguide, and also in each direction between waveguides. The results from this experiment are plotted in Figure 45, in which it is seen that the curves display a reasonable degree (±3 dB) of correlation, especially in the 100 to 200 minute time range. This indicates that the whole test panel (12 inch x 12 inch) was cured to a similar degree; more importantly, it shows that acoustic wave transmission between distant waveguides has the potential for AWG cure monitoring of large areas.

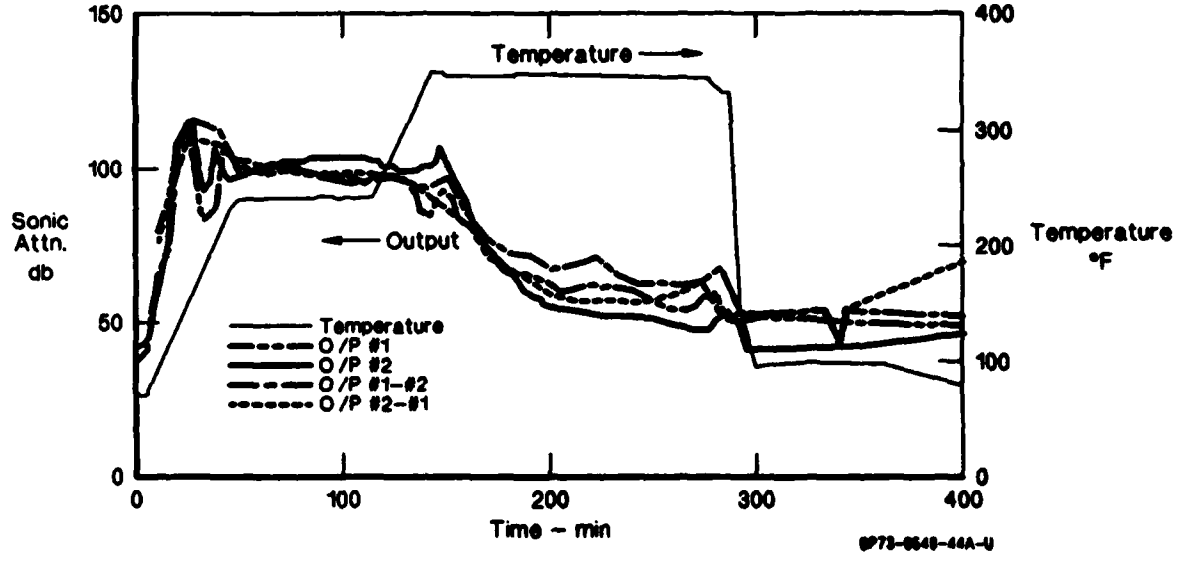

Figure 45. Response Within and Between Parallel Waveguides

Next, this experiment was repeated using a similar carbon/epoxy prepreg panel with approximately 1 percent by volume of glass voids (ceramic microballoon) distributed between the parallel waveguides. The AWG attenuation results (between waveguides) from this experiment are compared in Figure 46 with those from the previous panel. It can be seen that during cure (~120 minutes to ~250 minutes within the cycle) the curing panel with embedded voids exhibits 5 to 10 dB more attenuation. This 2-to-3 times difference in signal reduction is quite significant and suggests that AWG will be sensitive to much less than 1 percent void formation during cure.

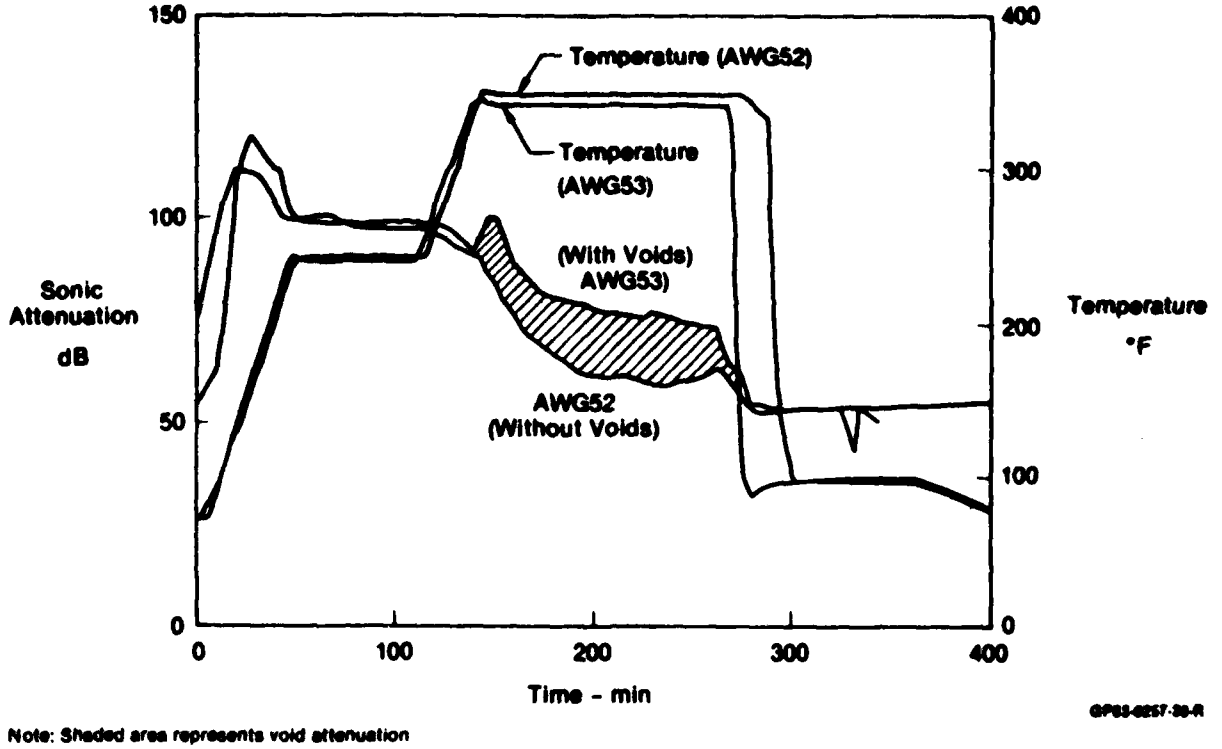

Note: Shaded area represents void attenuation

Figure 40. Effect of Voids on Attenuation Using Two Waveguides

3.5 SENSOR RESPONSE/MATERIAL PROPERTY RELATIONSHIPS

3.5.1 Monitoring of Isothermal Cures - A series of laminate cure cycles was completed for statistical analysis of sensor repeatability and for correlation with material property data obtained under the same time-temperature conditions. Four cures at 120°C (248°F) and four at 180°C (356°F) were monitored with AWGs buried in 12 inch x 12 inch, 41-ply AS4/3501-6 prepreg layups. These two temperatures correspond to the two hold temperatures of the typical step-cure cycle to be used for Task III laminates. Additional isothermal cures, one each at several temperatures [80°C (176°F), 100°C (212°F), 140°C (284°F), 160°C (320°F) and 200°C (392°F)], were also monitored to establish statistical effect of temperature upon sensor response. All laminates were of the same layup and orientation sequence to be used for Task III demonstration laminates: $[(\pm 45, 0_2)_5 \bar{9}\bar{0}]_S$. The waveguide, a 0.02 inch diameter nichrome wire, was buried in the center plies and oriented in the 90° direction as shown in Figure 41(a). All laminate cure cycles were carried out in a laboratory press with the transducers bonded to the ends of the waveguide and positioned outside the press platens.

3.5.2 Statistical Analysis of Isothermal Cure Response Data - The objectives of this task were to establish the reproducibility of the AWG system as used to follow epoxy cure reactions and to determine the degree of correlation between sensor responses and known cure parameters such as

changes in viscosity (η) and degree-of-cure (α). These parameters have been determined for the cure reactions of the 3501-6 epoxy resin system in the Computer-Aided Curing of Composites (CACC) program, in which the curing conditions of temperature, time and kinetic models are inputs, and η and α are outputs. Model tables for η and α were developed for the specific batch of 3501-6 resin in the prepreg used for these laminates; a description of these resin characterization data is given in Section 4.

Sonic attenuation response data obtained during the 6-hour isothermal cures at 120°C (248°F) and 180°C (356°F) are shown in Figure 47 and 48 respectively. Attenuation was considered to be more representative of response than the raw voltage output for purposes of run-to-run data comparison. Inspection of the data in Figures 47 and 48 discloses a considerable amount of scatter; statistically, the data from run to run are not reproducible.

Superimposed upon the attenuation-time curves are the average log viscosity and degree-of-cure versus time curves for 120°C (248°F) cure condition, and degree-of-cure (α) versus time for the 180°C (356°F) condition. These curves were computed from the actual time-temperature cure profiles using the raw data from these runs as inputs to the resin characterization models. The log viscosity and degree-of-cure curves shown in Figures 47 and 48 are average values, calculated from the four AWG isothermal time/temperature profiles, and generated for the 120°C (248°F) and 180°C (356°F) cures by the computer.

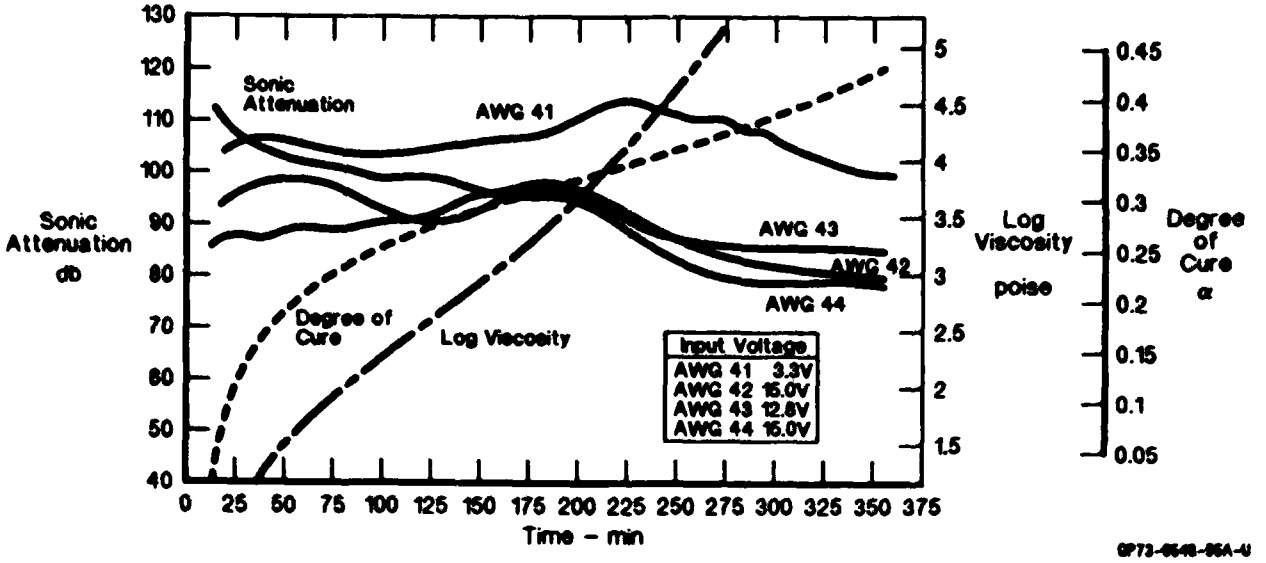

Figure 47. AWG Sensor Response for 120°C (248°F) Isothermal Cures, Viscosity (RDS) and Degree of Cure (DSC) vs Time

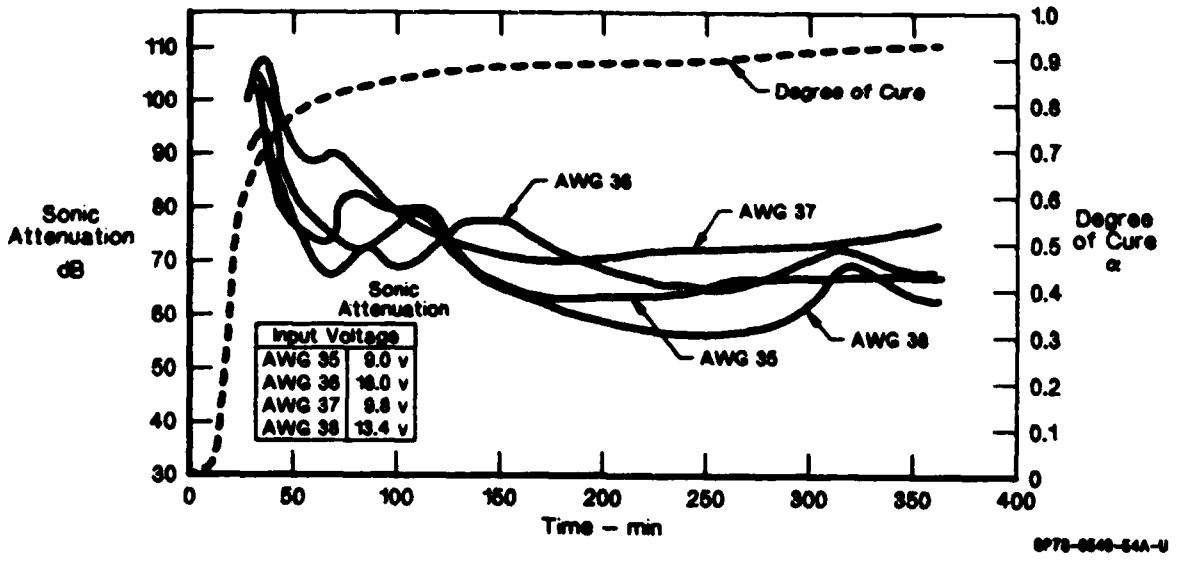

Figure 48. AWG Sensor Response for 180°C (356°F) Isothermal Cures and Degree of Cure (DSC) vs Time

The relationships between AWG responses and material properties are shown in Figures 49 through 51. For the 120°C (248°F) runs, the log η/log sonic output curves (Figure 49) show that changes in viscosity over a range of four decades were not reflected in any predictable change in sensor output. In other words, sensor response cannot be used to predict viscosity changes during the early pre-gelation cure stage. The relationship of AWG response to log α at 120°C (248°F) in Figure 50(a) showed similar results. However, there appears to be a consistent drop in sonic output at about $\alpha=0.3$. For the 180°C (356°F) isothermal cure cycles, the lack of reproducibility (Figure 50b) is also evident; there is wider data scatter for $\alpha<0.5$. There appears to be a recurring event at about $\alpha=0.7$, where attenuation abruptly increases. This phenomenon also appears to occur in the 160°C (320°F) and 200°C (392°F) isothermal cures (Figure 51).

Plots of data from the different isothermal temperature cures, from 80°C (176°F) through 200°C (392°F) (Figures 49 through 51), indicate that there are no trends due to temperature effect between AWG sensor response and viscosity (for low temperatures) and degree-of-cure (for high temperatures). Two explanations are possible: (1) Temperature may not have an effect upon the relationships, or (2) the effect of temperature may be less important than the effect that other system-related factors have on the relationships (scatter effects). Those factors would be the same conditions that contributed to the non-reproducibility in the four trials at 120°C (248°F) and 180°C (356°F).

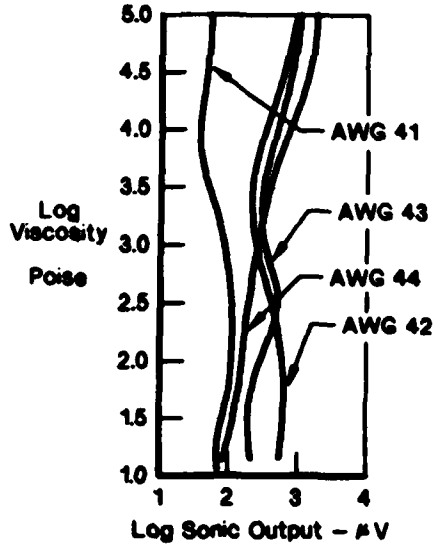

Figure 49. Correlation Between AWG Response and Viscosity for 120°C (248°F) Isothermal Cures

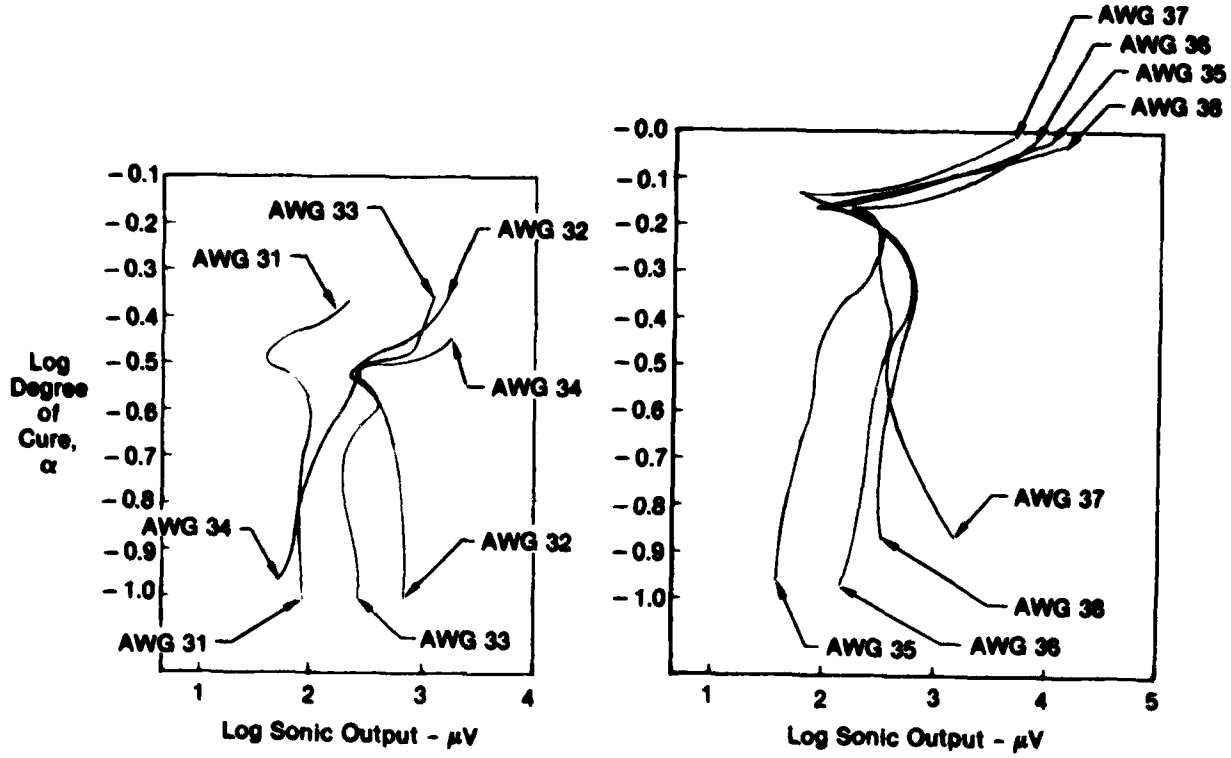

Figure 50. Correlation Between AWG Response and Degree-of-Cure for Isothermal Cures of AS4/3501-6

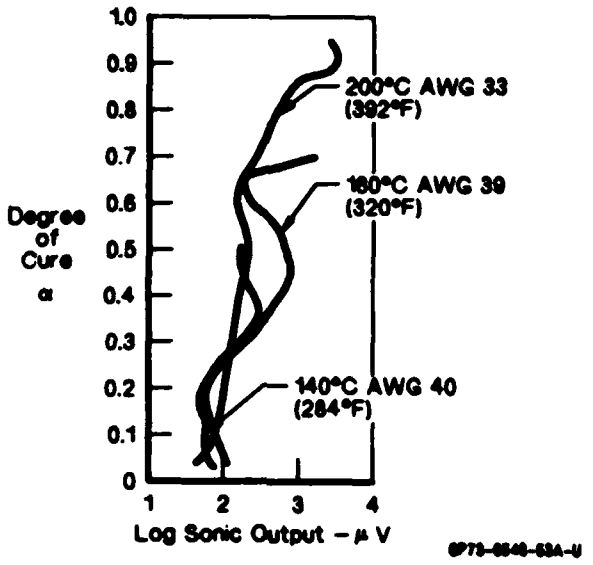

Figure 51. Effect of Cure Temperature Upon AWG Response vs Degree-of-Cure (DSC)

3.5.3 Discussion of Results

3.5.3.1 Sensor Response - Cure Parameter Relationships - The causes of non-reproducibility of isothermal cure cycle response data are not fully understood, although the loss factors resulting from variations in wave guide bonding and inherent part-to-part lay up differences are partly responsible. Tabulations of input voltage to the waveguide, taken before burying the waveguide in the laminate, are shown in Figures 47 and 48. Differences in input voltage reflect variations in transducer-to-waveguide bonding efficiency, i.e., a low input voltage indicates poor bonds and consequently higher signal loss within the sensor system itself. The unusually high attenuation of the response throughout Run AGW-41 (Figure 47) is probably attributable to this factor. It is also probable that laminate system-related variables (e.g., resin content, fiber proximity and orientation) also influence run-to-run responses, particularly in the early and late cure stages where only minor changes in acoustic response attributable to viscosity or cure state changes take place. These subtle system differences contribute to the data scatter from run to run.

However, the onset to resin gelation appears to be readily detectable in the $\alpha \cong 0.7$ range, at which a sharp minimum in the sonic output consistently occurs. This occurence is also consistent with the signal minimum and change-in-slope event that was observed in step-cure cycles in the sensor development experiments. There is no obvious explanation for the drop in sonic output that occurs at α=0.3 in the 120°C (248°F) isothermal cure cycles.

3.5.3.2 Kinetic Approach to Analysis of Sensor Response/Degree-of-Cure Relationship - Treatment of the AWG sonic response experimental data in terms of the chemical/physical changes that take place during cure yields evidence of the response to degree-of-cure relationship. The background for this approach and analysis of data are discussed in the following sections.

3.5.3.2.1 Background (Arrhenius Equation) - In the study of chemical reactions Arrhenius (Reference 20) was the first to realize that there is an equilibrium between "passive" molecules of the reacting species and "active" molecules formed by normal molecules by the absorption of energy. Arrhenius' hypothesis, that only a small fraction of the total number of molecules that are active at any instant can react and that chemical changes are not instantaneous because the distribution of energy (Maxwellian distribution of molecular velocities) requires time, has been overwhelmingly verified experimentally over the last 80+ years. It has also been applied to polymer cure by Gillham (Reference 21).

Specifically, Arrhenius stated that the rate of chemical reaction

$$(k) = \text{constant} \cdot e^{\frac{-E}{RT}} \qquad (1)$$

where E is the energy of activation, R is the gas constant, and T is the absolute temperature. The rate of chemical reaction (K) is the number of molecules undergoing chemical change per second and may also be termed the velocity coefficient. Equation (1) can be rewritten in the form of the well known Arrhenius equation, i.e.,

$$\text{Ln } K = \text{Ln } A - \frac{E}{RT} \qquad (2)$$

The confidence test (References 22 and 23) for data measured from chemical reactions is to plot Ln K versus the reciprocal of the absolute temperature which should yield a straight line of slope E/R, from which the energy of activation can be obtained. In addition, in previous AWG cure monitoring studies (Reference 16) it has been found that analysis of the transmitted acoustic signal will yield a straight line plot versus time which is indicative of a first order chemical reaction.

3.5.3.2.2 Interpretation of AWG Data - In interpreting AWG data, the data are plotted versus time using the following relationship:

$$\log K' = \log V_o + M \log V_t$$

where K' is the chemical reaction rate, V_o is the acoustic signal amplitude at the start of the reaction, V_t is the signal at the time t after initiation of the chemical reaction, and M is the slope of the response-versus-time curve at time t. Although the basic theory of this analysis needs to be further understood, it appears to be valid, as plots of Log K' versus the reciprocal of absolute temperature for cure of 3501-6 neat resin give straight lines from which credible values of activation energies can be calculated. In addition, AWG cure monitoring data does correlate well with standard dielectrometry measurements, as shown in Figures 32 and 33. In the case of neat resin cure data, initially the slope M is large and negative, and thus log K' is negative prior to gelation, but M reverses to a positive value, and log K' becomes positive. It is believed that this reversal of log K' sign from negative to positive coincides with gelation, and is well defined acoustically by both maximum wave attenuation and a sudden change in acoustic wave velocity.

The changes in signal response for cures of carbon/epoxy prepreg are less than for neat resin, but still substantial (2 to 3 orders of magnitude), although the slopes of the cure curves are not always clearly defined. This is perhaps expected, because the prepreg is only about 40 percent resin by volume, and contact of the waveguide with carbon fibers will occur in different amounts during the processing of successive specimens. In analyzing AWG data from carbon/epoxy laminate cures, it is necessary to use "best-fit" straight lines to identify major changes in signal level. When it is not practical to use the actual value of M or even an average value, such as when many oscillations appear in the signal-versus-time curve, then M can be treated as a constant with a negative sign before gelation and a positive sign after gelation. In this manner an approximate measure of the cure process is still possible.

This method of analysis was applied to the responses from AWG monitoring of AS4/3501-6 laminates cured isothermally for 4 to 6 hours at different temperatures [80°C (176°F) to 200°C (392°F)] providing different degrees of cure. Several acoustically monitored isothermal cure curves are shown in Figure 52, together with the cure of neat resin step-cured per the cycle shown in Figure 29.

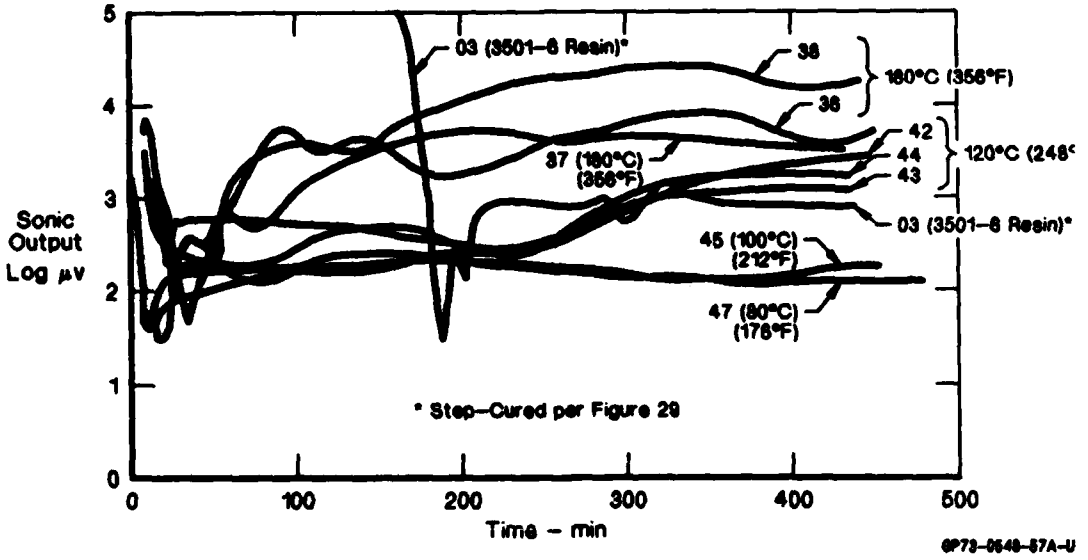

Figure 52. Comparison of AWG Monitored Isothermal Cure Cycle Curves for AS4/3501-6

In analyzing the data for measure of cure achieved using log K' = log V_o + M log V_t, it is only necessary to decide the point in time when the gelation occurs, using -M before and +M after this point. Then, drawing a straight line through the minor "wiggles" of the curve, the trend or measure of cure can be obtained. Data shown in Figure 52 treated in this manner are shown in Figure 53. As a measure of degree-of-cure, the neat resin step-cured per the profile shown in Figure 29 (Run 03) yields a final ordinate value of 8; the three 180°C (356°F) carbon/epoxy isothermal cures yield final values of 7.0 to 7.5, while the 120°C (248°F) isothermal cures have values in the 6.0 to 7.0 range. The 100°C (212°F) and 80°C (176°F)

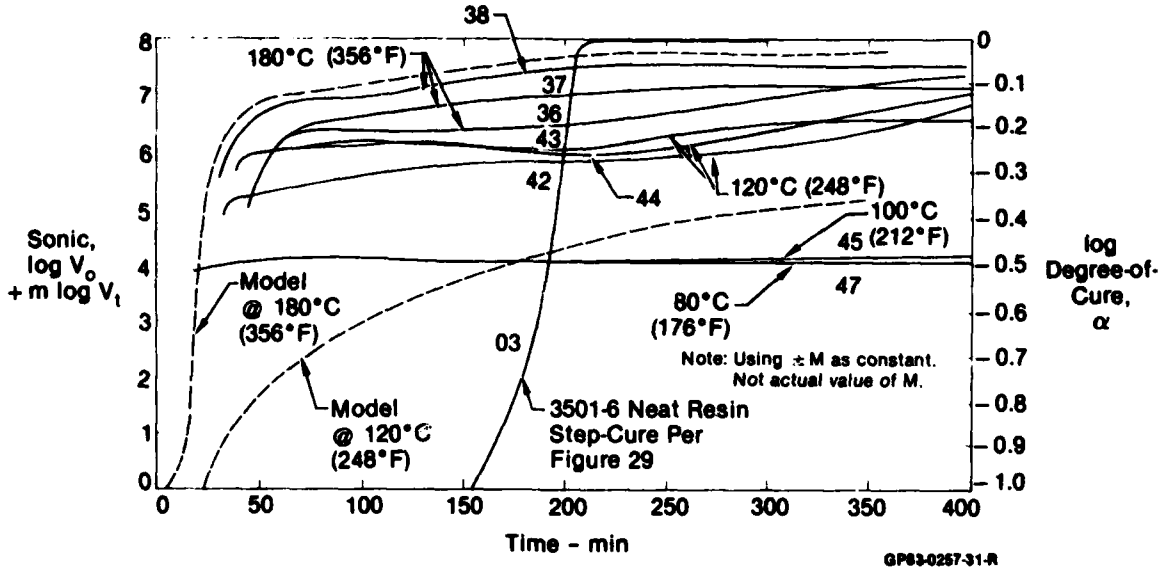

Figure 53. Comparison of Sonic Response (log K') and Degree-of-Cure Data (log α From DSC) for Isothermal Cures of AS4/3501-6

isothermal cures achieve values of only 4.0. For comparison, log α values from DSC measurements also shown in Figure 53. The similarities of the AWG response data calculated as log K' to the degree-of-cure curves from model-generated values (DSC data), both for 3501-6 cures, indicate the validity of the AWG sonic output-α relationship.

This analysis provides evidence that this method does indeed yield a measure of cure. In addition, the curves in Figure 50 (b) dramatically illustrate a rapid change in slope and attenuation just prior to α = 0.7. The consistency of this inflection indicates the reproducibility of AWG in identifying resin gelation.

3.6 SIGNAL PROCESSING AND DATA OUTPUT

The laboratory experiments at Westinghouse were performed using a signal generator (70-80 kHz) connected to the transmitting acoustic transducer bonded to one end of the embedded waveguide, and a high pass filter (>30 kHz) and oscilloscope connected to the receiver transducer at the other end of the waveguide, Figure 25. In this way, the peak value of received signal was measured together with the wave transit time, and a T.V. camera was used for a permanent record. At McDonnell, a programmable signal generation and data acquisition system was used. This system feeds digitized data to a microprocessor for storage and retrieval via a host computer. This allows interface with an operator and the examination and graphical printout of data during the cure cycle.

In contrast to the Westinghouse laboratory acoustic cure monitoring signal transmission (max. 15 volts) and reception (min. ~20 μV) system, the McDonnell factory system has a maximum signal input of 100 volts and the capability of sensing a 10 μV acoustic signal. This feature allows more than

an order of magnitude improvement in overall system response during cure. The DAS selected for use in sensor validation cure cycles provided flexibility in selecting signal output and response parameters, multichannel capability and choice of data presentation format. In addition to acoustic response data, the system processed the miniature pressure transducer and thermocouple outputs. Plotting capabilities included ability to print one-curve plots of pressure (miniature transducer or tool-mounted transducer), part temperature, waveguide response, waveform or frequency response; and two-curve plots of pressure-temperature, waveguide response-temperature or waveguide response-pressure. All parameters were plotted against cure time. Data could be monitored in real time and printed at the end of each run.

Block diagrams of the signal transmitter and receiver sections of the DAS are shown in Figures 54 and 55 respectively. Figure 56 shows the elements of the DAS microprocessor software.

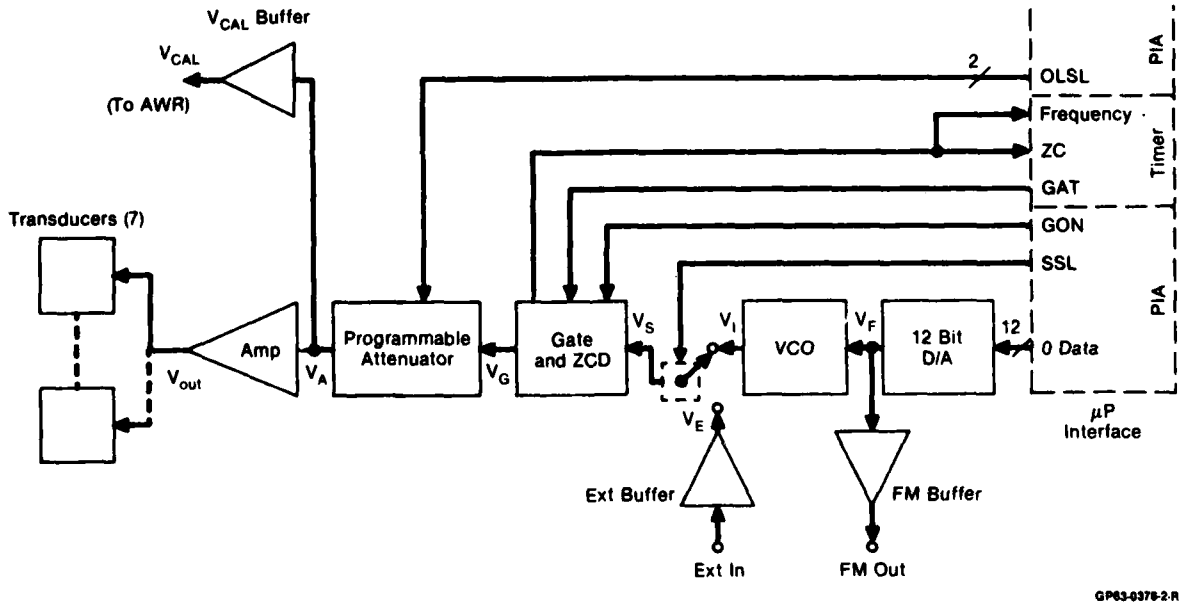

Figure 54. Acoustic Waveguide Transmitter (AWT) Block Diagram

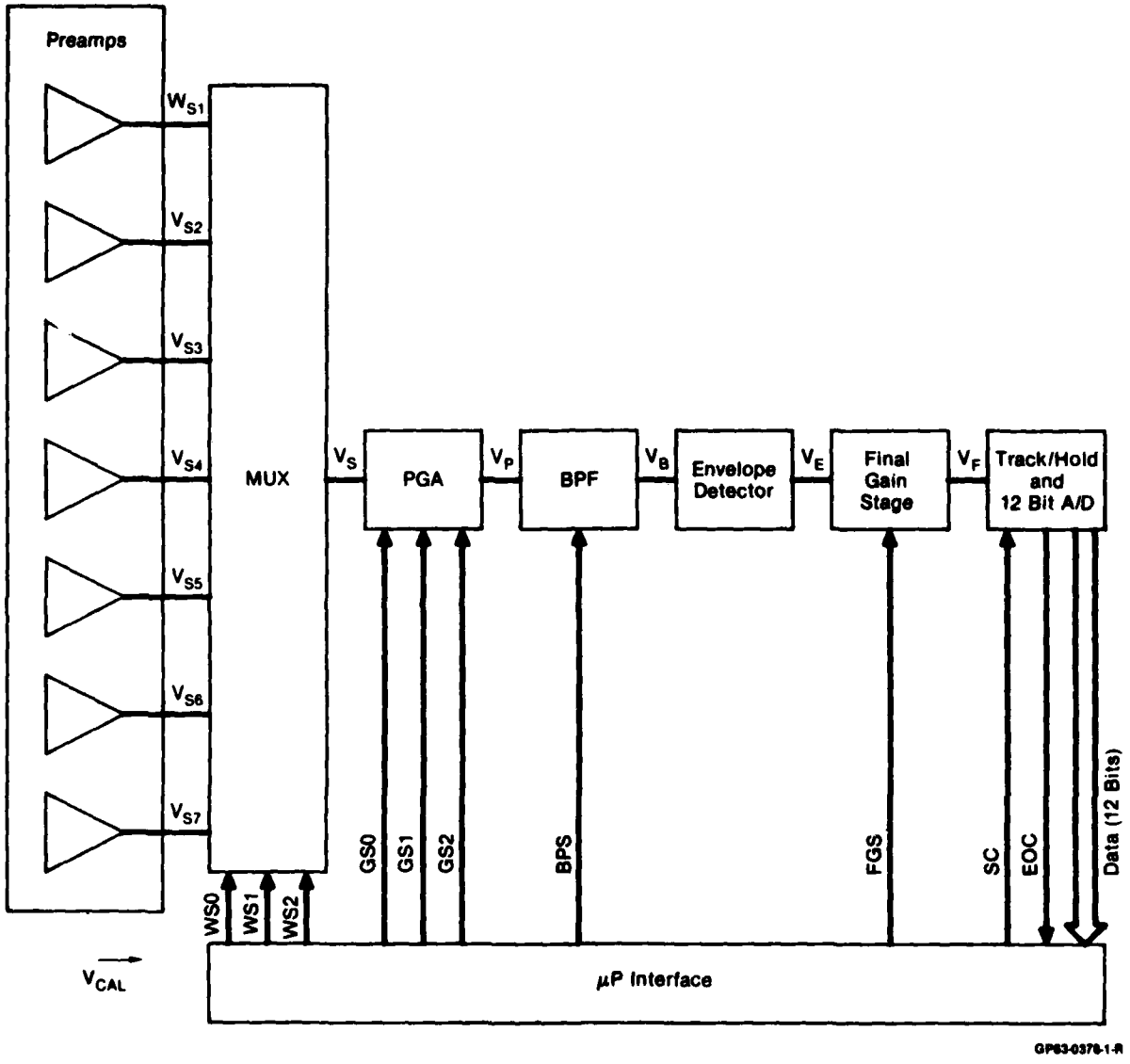

Figure 55. Acoustic Waveguide Receiver (AWR) Block Diagram

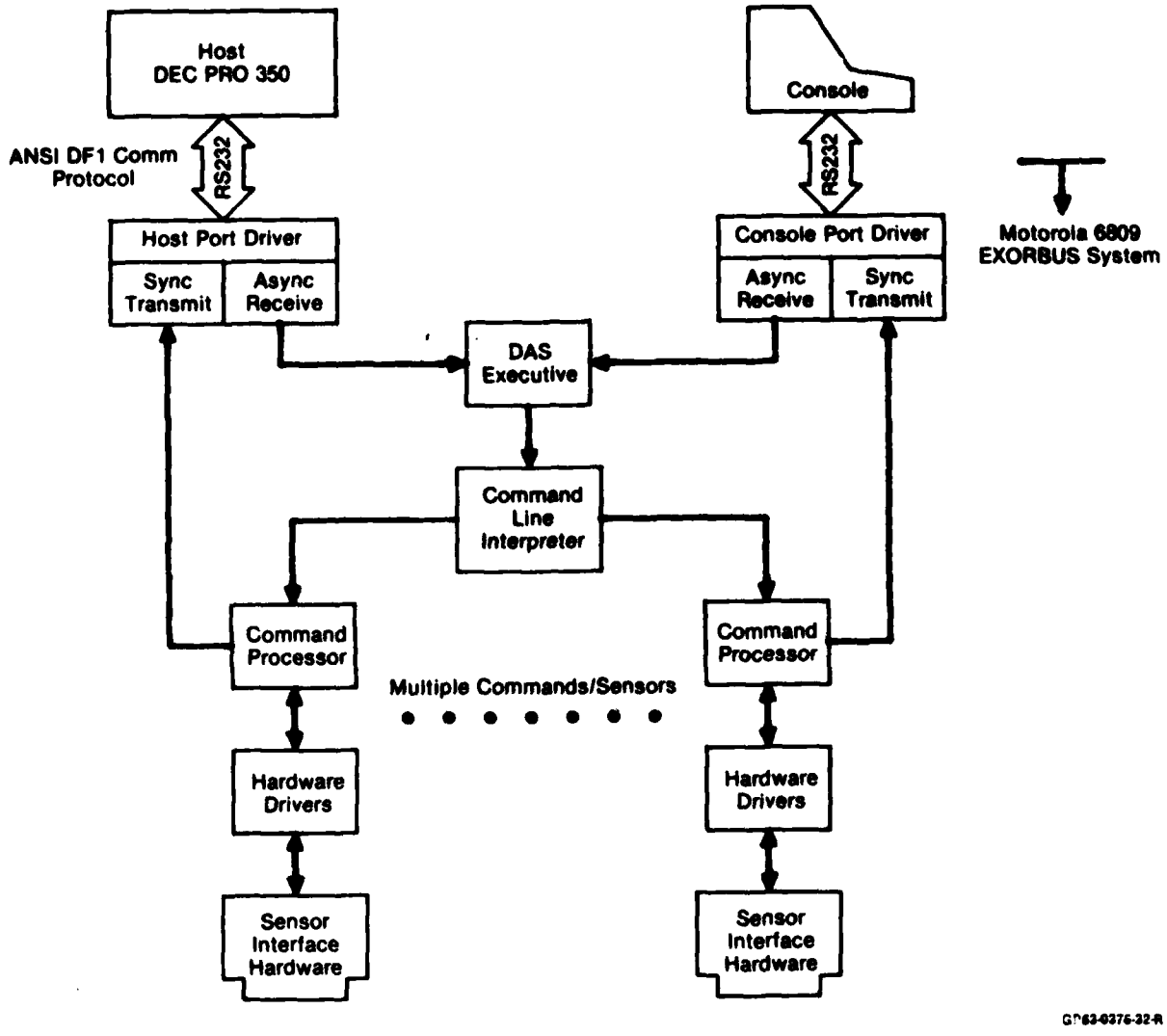

Figure 56. Data Acquisition System (DAS) Microprocessor Software Design

4.0 RESIN PROPERTY MODELING

4.1 OBJECTIVE

A principal step in the sensor development efforts described in Sections 2.0 and 3.0 was to establish a direct correlation between basic resin properties (degree-of-cure and viscosity) and the sensor signal. It was not feasible to monitor viscosity and degree-of-cure changes directly in the laboratory cure cycles for the laminates prepared in the sensor development work or for those in Task III autoclave demonstration. Instead, it was necessary to develop mathematical models for viscosity and degree-of-cure. The same proven procedures used to develop similar models for 3501-6 properties for the "Computer Aided Curing of Composites" program (Reference 1) was used, except that the models developed for this program were for a specific batch of 3501-6 resin. This batch of resin was used not only for the model development but also for all sensor development work and Task III laminates. This model development approach allowed direct correlation of viscosity and degree-of-cure with sensor output and eliminated any differences in thermal cycles and resin batch-to-batch variations.

4.2 GENERATION OF MODEL DATA

Viscosity and degree-of-cure data were determined experimentally for the 3501-6 resin as a function of processing conditions over the entire range of cure conditions normally experienced in composite fabrication. This type of data had similarly been developed for the"Computer-Aided Curing of Composites" program to predict material/process relationships.

Figure 57 shows the test matrix that was used to establish the mathematical models. The range of temperatures and cure cycle profiles encompassed those conditions that yield useful viscosity and degree-of-cure data. Degree-of-cure and rate of change values were generated from heat of reaction data measured by a Perkin Elmer Model 2C Differential Scanning Calorimeter. A Rheometrics Dynamic Spectrometer RDS-7700 was used to generate viscosity data.

The time-temperature profile of each sensor-monitored cure cycle was used for model input to generate corresponding curves for viscosity and cure state. This allowed a direct correlation between the model outputs (degree-of-cure and viscosity) and sensor output and eliminate any differences in thermal cycles. For sensor correlation runs, all data taken prior to reaching the desired isothermal test temperature were eliminated.

All sensor response/material property relationships discussed in Sections 2 and 3 utilized the material property data generated by the developed mathematical models. Temperature-time data from each sensor-monitored cure cycle produced the viscosity and degree-of-cure profiles in an off-line simulation. It would be possible to incorporate the developed models into the sensor data acquisition system software to achieve real time monitoring of these material parameters, and to use the profile data for closed-loop control of autoclave processes.

Type of Heating Cycle	Cure Parameter	
	Viscosity (RDS)	Degree-of-Cure, $\Delta H_t/\Delta H_o$ (DSC)
Temperature (Isothermal)		
80°C (176°F)	X	
100°C (212°F)	X	
120°C (248°F)	X	X
130°C (266°F)	X	X
140°C (284°F)	X	X
150°C (302°F)	X	X
160°C (320°F)	X	X
170°C (338°F)		X
180°C (356°F)		X
190°C (374°F)		X
200°C (392°F)		X
Dynamic		
1°C/min (1.8°F/min)	X	
2°C/min (3.6°F/min)	X	X
5°C/min (9°F/min)		X
10°C/min (18°F/min)		X
20°C/min (36°F/min)		X
Standard Cure Cycle Profile **(Figure 59)**	X	

GP83-0257-32-T

Figure 57. Resin Test Matrix for Characterization of AS4/3501-6

5.0 EVALUATION OF PRESSURE SENSORS

5.1 BACKGROUND

One of the critical composite cure processing parameters is the hydrostatic pressure within the resin matrix, particularly during the pre-gelation stage of cure. Studies (Reference 2) have shown that the gas pressure within the autoclave shell is not necessarily the same as the pressure within the resin. Hydrostatic resin pressure is affected by the resin flow and physical characteristics of the reinforcement and bleeder material. When the vapor pressure of volatile materials that may be trapped within the liquid resin phase exceeds the hydrostatic resin pressure, voids will form. Voids from this source, as well as those from air entrapped within the prepreg layup, will create porosity and reduce performance of the cured structure. Since the elimination of voids depends upon the application of adequate pressure to the resin during the pre-gelation stage, the ability to monitor pressures within the laminate can lead to an understanding of the formation of voids and suggest methods for their elimination.

Ideally, it would be desirable to monitor resin hydrostatic pressure throughout the entire part during cure. The sensor response could then be used to control autoclave pressure so as to ensure "adequate" resin pressure. Since this is not a realistic goal, it was the objective of this program effort to evaluate pressure sensors for use in predicting void formation, and to correlate resin pressure with void-detection capabilities of other cure-monitoring sensor systems.

In the past, tool-mounted transducers provided the only method for measuring hydrostatic resin pressure. Because of advances in the development of miniaturized pressure transducers, sensors are available that can be buried within the laminate at any location. With this capability, it is now possible to measure pressure gradients throughout the laminate. The Kulite type LQ-110-125-100A miniature transducer shown in Figure 58 was selected for resin pressure monitoring studies. The tool-mounted transducer, Kulite HEM-375-100A, was also used for tool-surface pressure monitoring.

5.2 PRESSURE SENSOR CURE MONITORING

A series of AS4/3501-6 laminates with pressure sensors incorporated was cured in accordance with a standard autoclave cure cycle (Figure 59) to monitor the effects of composite cure parameters and tool-laminate-bagging system variations upon resin pressure and void formation. A test matrix (Figure 60) was established to evaluate the following conditions: (1) horizontal pressure gradients, (2) vertical pressure gradients, and (3) pressure gradients along ply drop-offs.

5.2.1 Pressure Sensor Calibration - Prior to test laminate fabrication, four miniature pressure transducers were calibrated under autoclave cure cycle conditions (Figure 59). In each of two calibration runs, two sensors were exposed to autoclave free air and two were immersed in uncatalyzed resin. Figure 61 shows the indicated sensor output versus time for the first run, in which only temperature but no autoclave pressure was applied (0 psig); data shown in Figure 62 are from the second run, in which both temperature and pressure cycles were imposed. A temperature correction curve

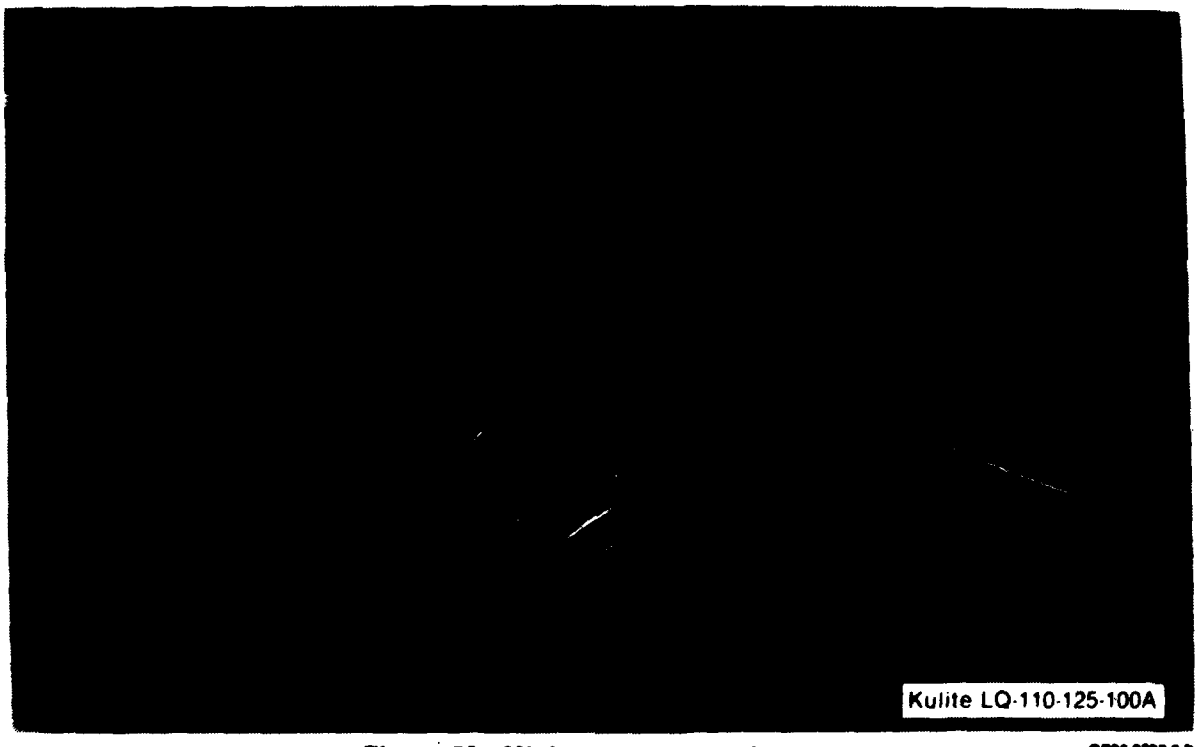

Figure 58. Miniature Pressure Sensor

GP63-0257-6-R

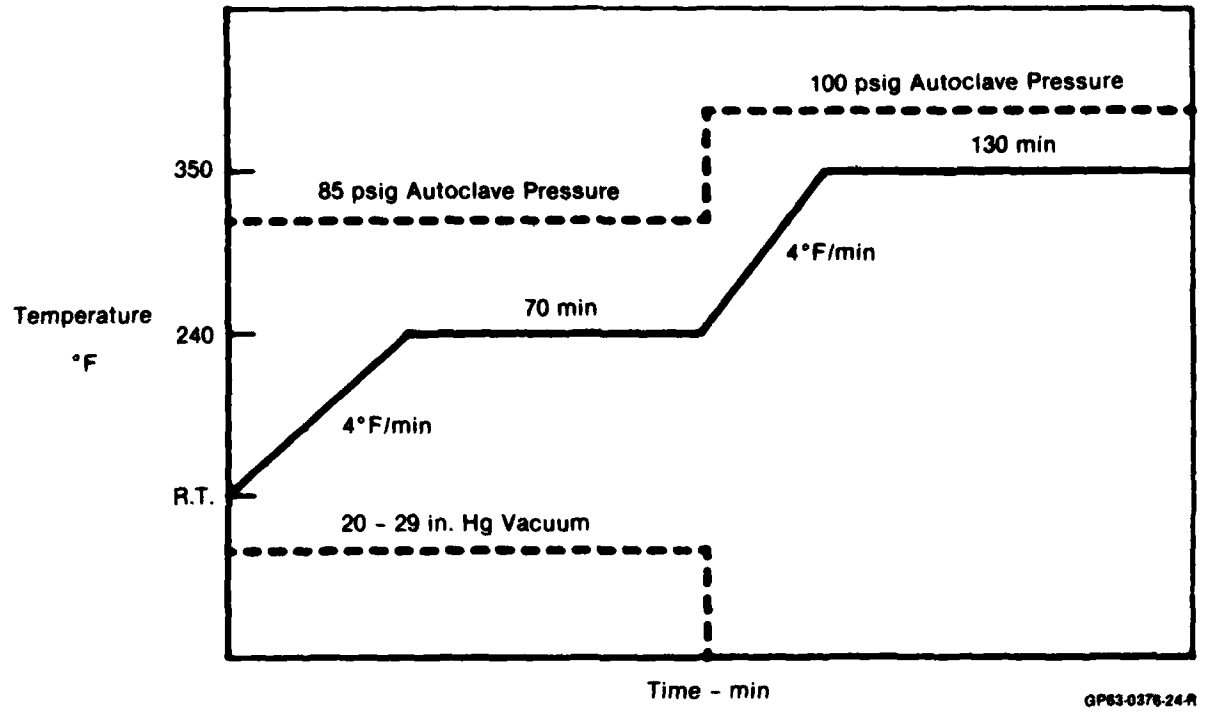

GP63-0378-24-R

Figure 59. Standard Autoclave Cure Cycle

Laminate Number	Description	Configuration	Transducers	Fabrication Procedures
1	Horizontal Flow (Large Gap Distance)	12 in. x 12 in. x 25 Plies $[\pm 45, 0_2)_3, 90, (0_2, \mp 45)_3]$	• 4 Tool Mounted(1) • 2 in Laminate(2) • 1 at Laminate Edge(2) • 1 in Bleeder(2)	Figures 64 and 65
2	Horizontal Flow (Small Gap Distance)			
3	Vertical Flow	24 in. x 24 in. x 60 Plies $[(\pm 45, 0_2)_3, \pm 45, 90_2, \mp 45 (0_2, \mp 45)_3]_s$	• 3 Tool Mounted(1) • 3 in Laminate(2) • 1 at Laminate-Bleeder Interface(2) • 2 in Bleeder(2)	Figure 66
4	Ply Drop-Off	Figure 67	• 3 Tool Mounted(1) • 3 in Laminate(2) • 2 in Bleeder(2)	Figure 67

Notes:
(1) Tool mounted transducers - Kulite HEM-375-100A
(2) Miniature transducers - LQ 110-125-100A

Figure 60. Test Matrix, Pressure Sensor Cure Monitoring

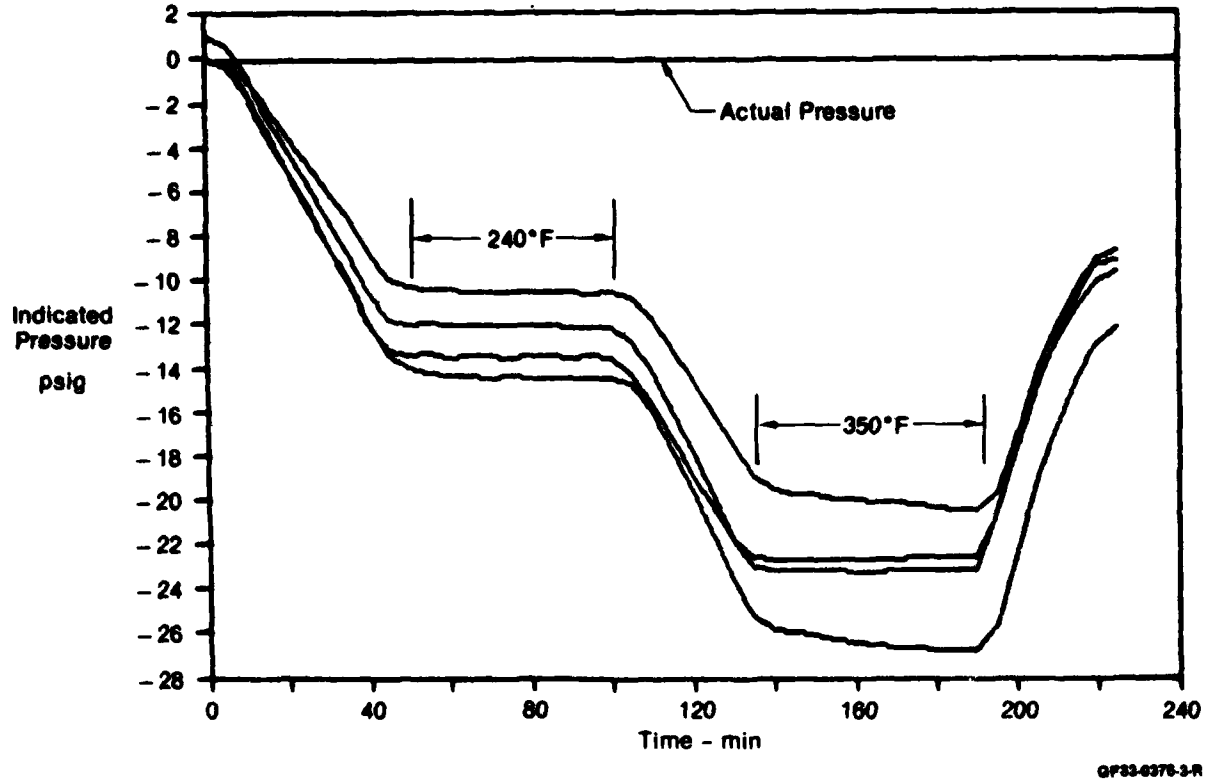

Figure 61. Miniature Pressure Sensor Calibration Results - Temperature Only

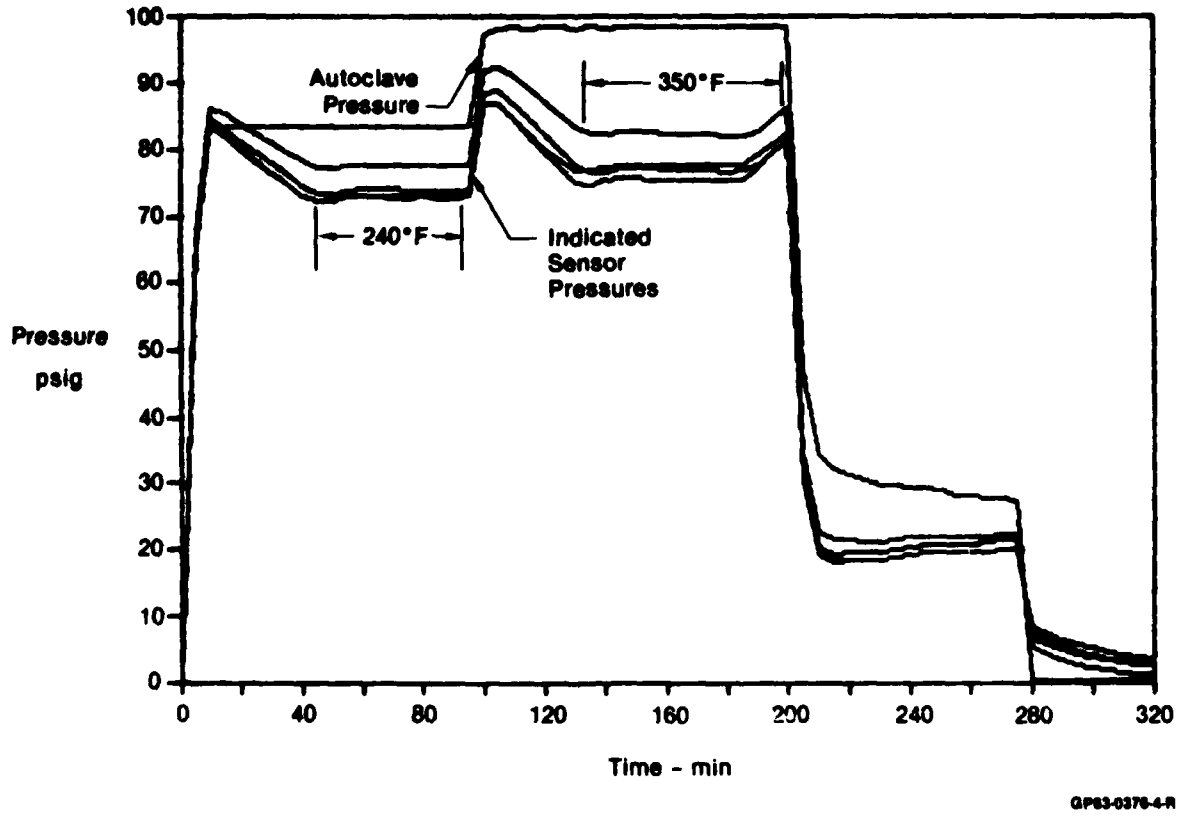

Figure 62. Miniature Pressure Sensor Calibration Results - Temperature and Pressure Application

(Figure 63) was established from these data; no additional correction for pressure was necessary. Previous work with the tool-mounted pressure transducers had indicated that no correction was required for either temperature or pressure variations within the limits of the autoclave cure conditions used in these experiments.

5.2.2 Pressure Sensor Test Setup - Pressure sensor locations for horizontal flow (laminates No. 1 and 2), vertical flow (laminate No. 3) and ply drop-off (laminate No. 4) are shown in Figures 64 through 67. Typical placement of miniature transducers between layup plies is shown in Figure 68; tool mounted transducers were at the laminate - cure plate interface. The difference between laminates No. 1 and 2 (horizontal flow tests) was in the gap between the layup edges and the resin-restraining dam. The separator layer between layup and "bleeder" was impermeable, to prevent vertical flow and bleedout, except at laminate edges. For laminate No. 3 (vertical flow), this separator layer was permeable to allow free vertical flow into the bleeder material, excessive bleeder material was used to magnify pressure drops and edges were sealed to prevent horizontal flow. Internal pressure sensors in laminate No. 4 (ply drop-off effects) were positioned at both ends and at the center of the thickness-taper area, and 12 inches from each side of the laminate; excessive bleeder was also used in this layup.

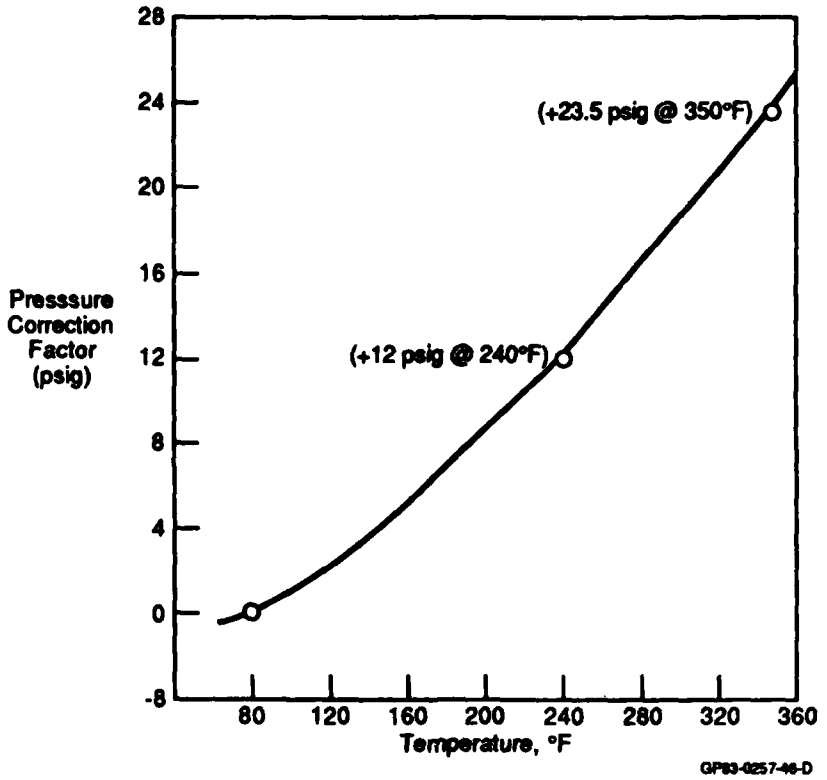

Figure 63. Pressure Correction Factor for Temperature Variations - Miniature Sensors

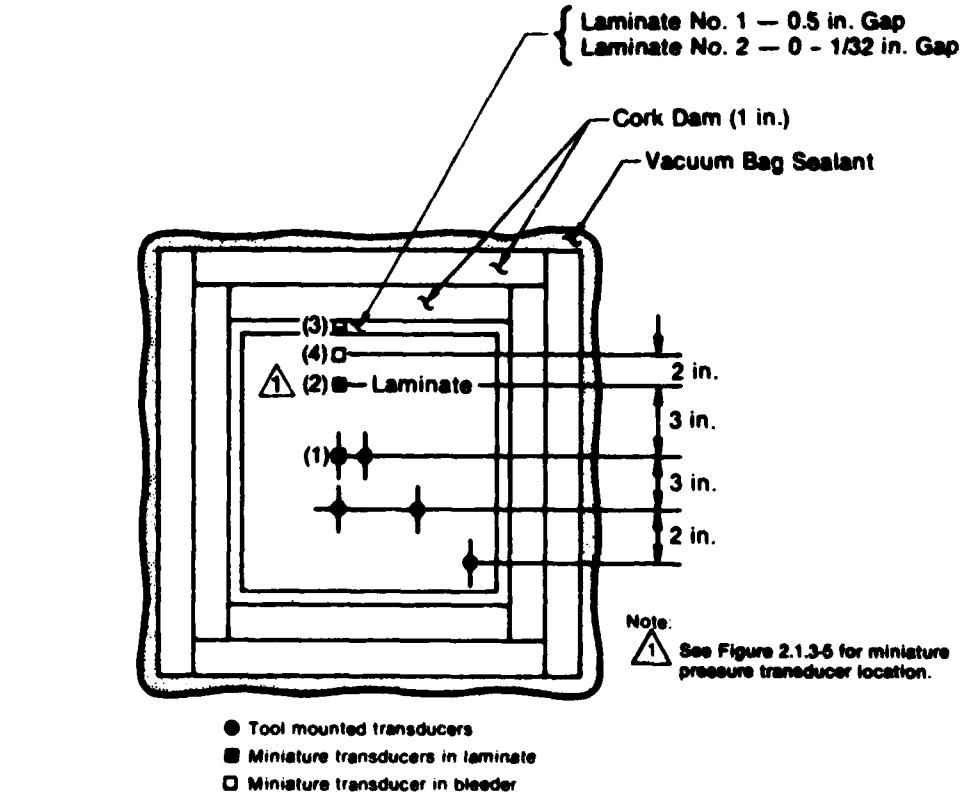

GP93-0376-17-R

Figure 64. Horizontal Flow Laminates

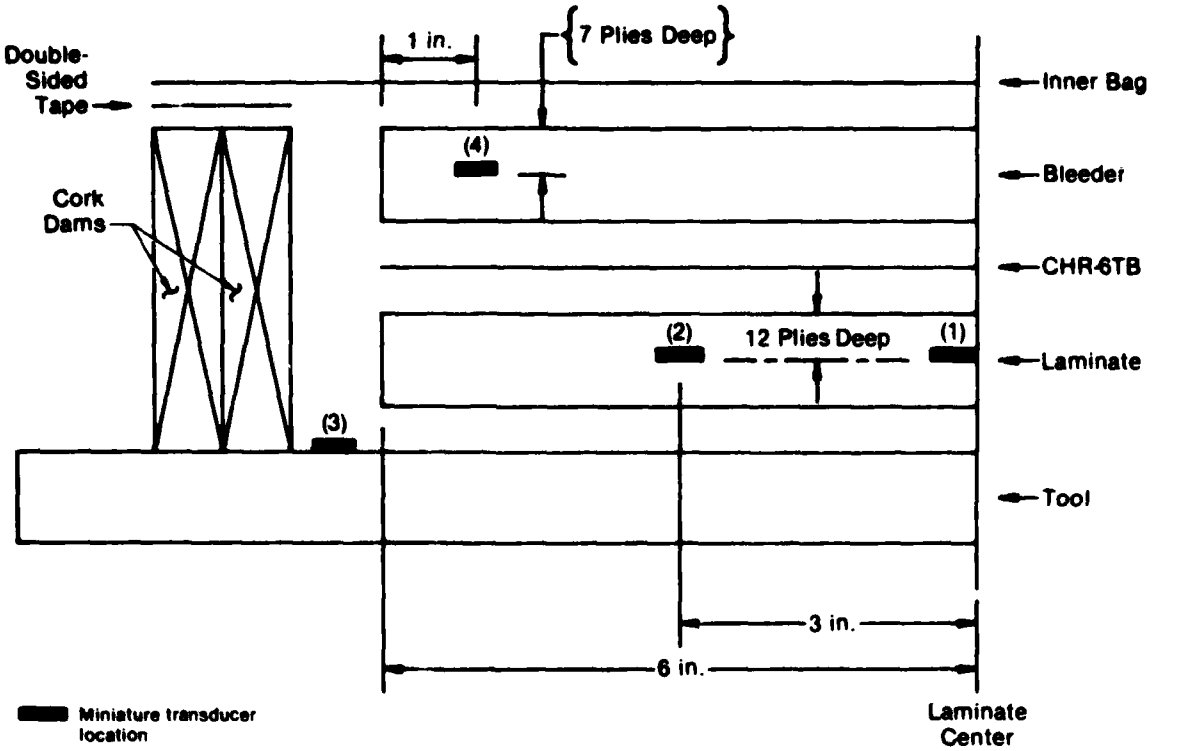

GP93-0376-18-R

Figure 65. Miniature Transducer Location for Horizontal Flow Laminates

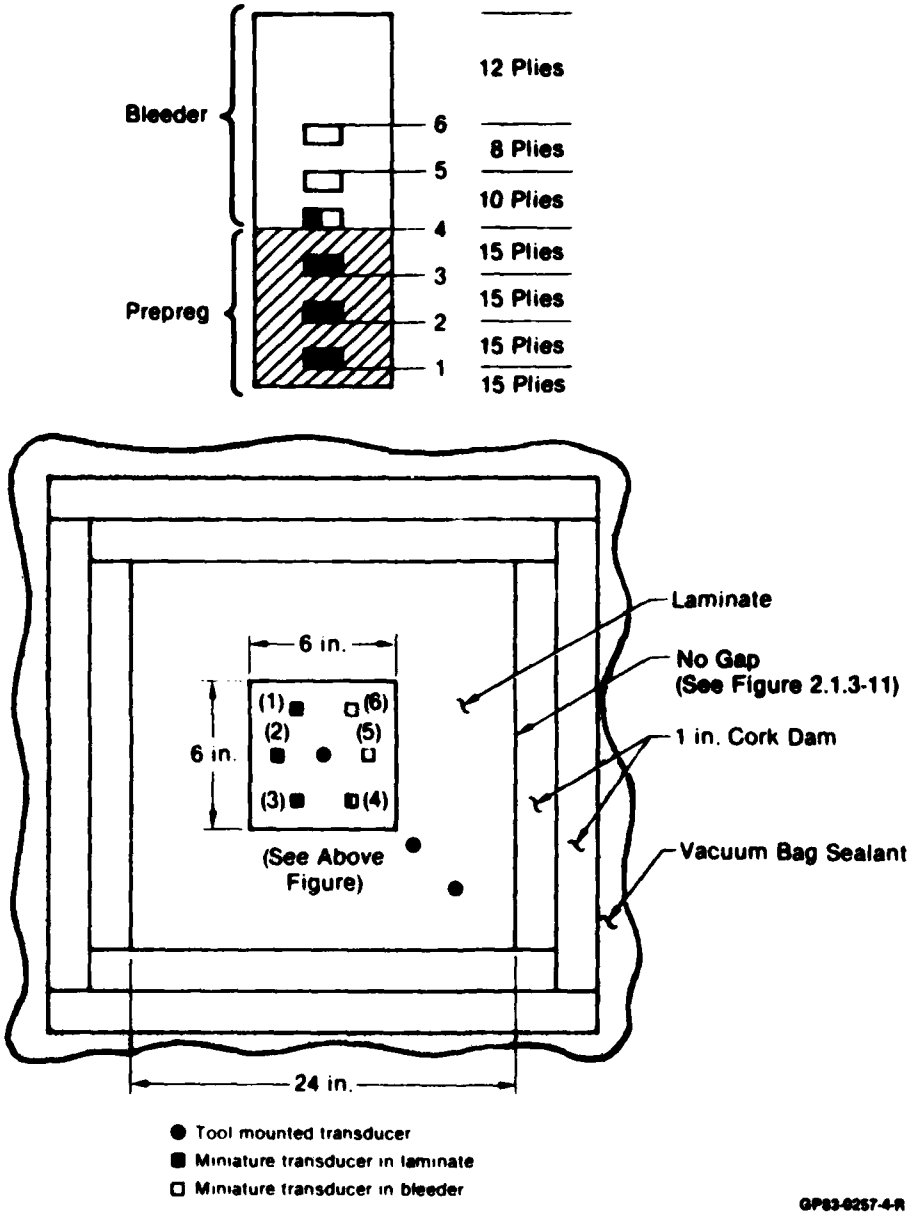

Figure 66. Vertical Flow Laminates

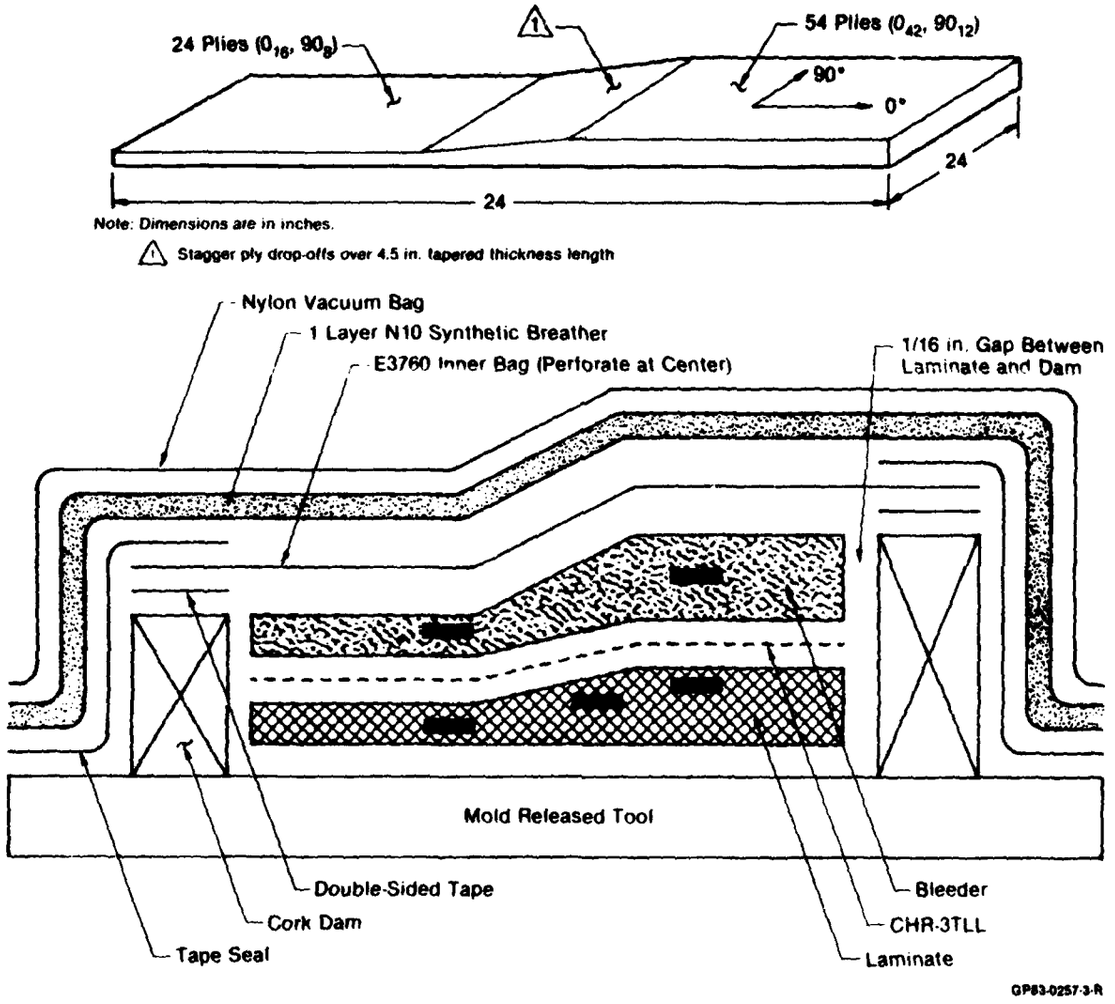

Figure 67. Ply Drop-Off Bagging Schematic
(Not to Scale)

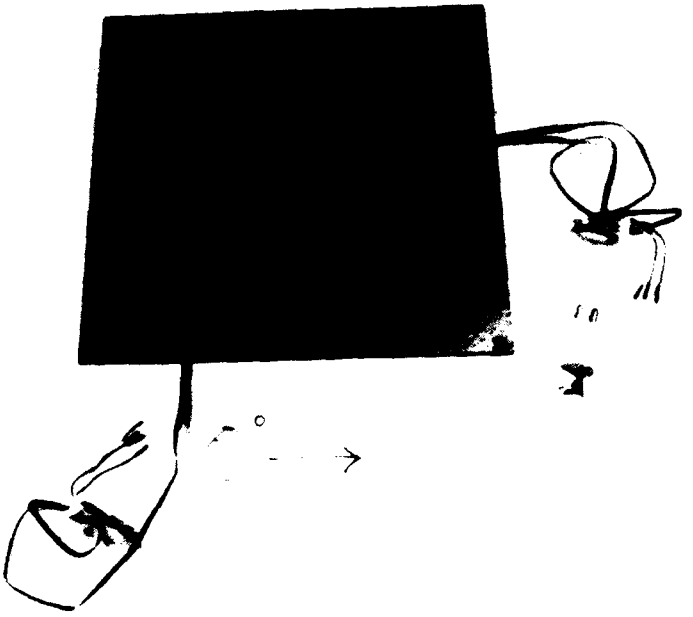

GP83-0608-32-R

Figure 68. Typical Miniature Transducer Placement

5.2.3 Test Results - Pressure data accumulated for the autoclave air and laminate-bleeder systems, during the autoclave cure cycles (Figure 59), are shown graphically in Figures 69 through 77. Operation of the miniature transducers and data acquisition system was nearly flawless; only one transducer gave erroneous readings.

Note that none of the plots of miniature pressure sensor readings was corrected for temperature changes; the factor shown in Figure 63 must be added to these readings. The rapid pressure drop of the embedded sensors that takes place after the autoclave pressure reaches 100 psi has no significance with respect to resin flow; this is the post-gelation stage of the cure cycle, in which internal laminate pressures are influenced by other factors.

- o Horizontal Flow Tests (Figures 69 through 72) - The effect of a wide edge-gap, which allowed a large amount of horizontal resin flow, is evidenced by the significant pressure loss, particularly within the laminate. Tool-mounted pressure sensor readings for the 0.5 inch gap (Figure 69), showed nearly 20 psi drop in the center of the 12 x 12 inch laminate and up to 45 psi drop near the laminate edge; for the small (0.03 inch) gap, no pressure drop was found (Figure 71) except at the laminate edge. Results for miniature pressure sensors located in the center of the laminate thickness (Figures 70 and 72) were similar to those for the tool-mounted sensors.

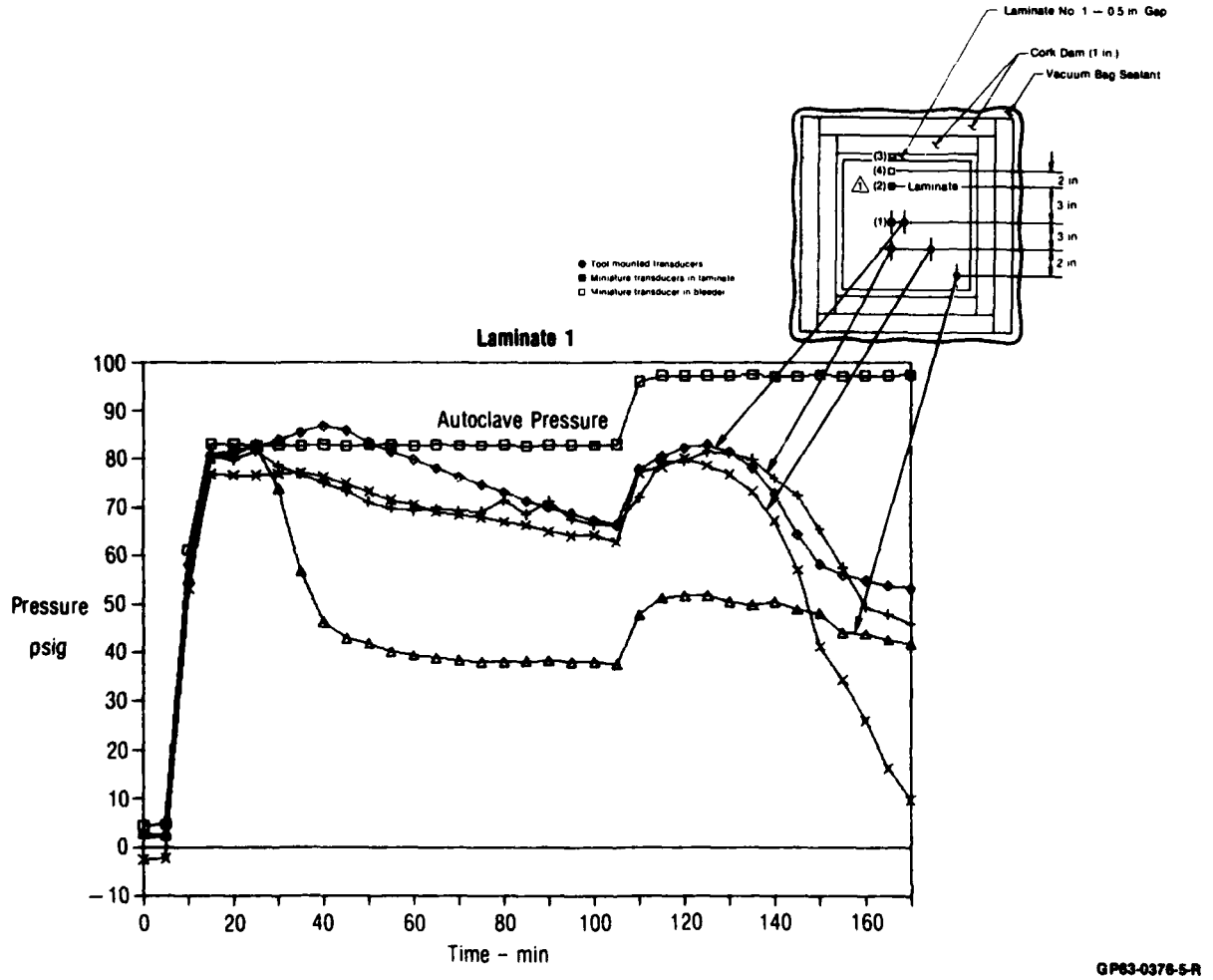

Figure 69. Horizontal Flow Laminate - Large Gap Distance
Tool Mounted Pressure Transducers

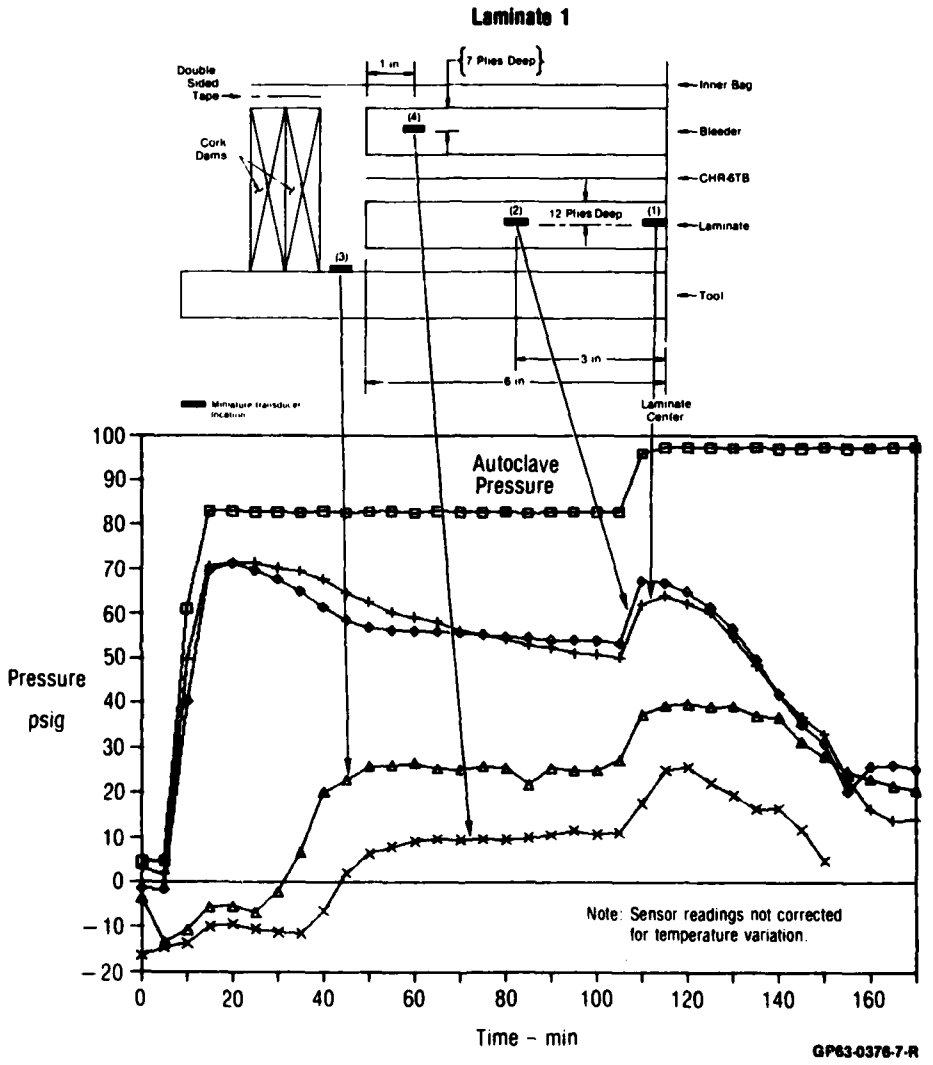

Figure 70. Horizontal Flow Laminate - Large Gap Distance
Miniature Pressure Transducers

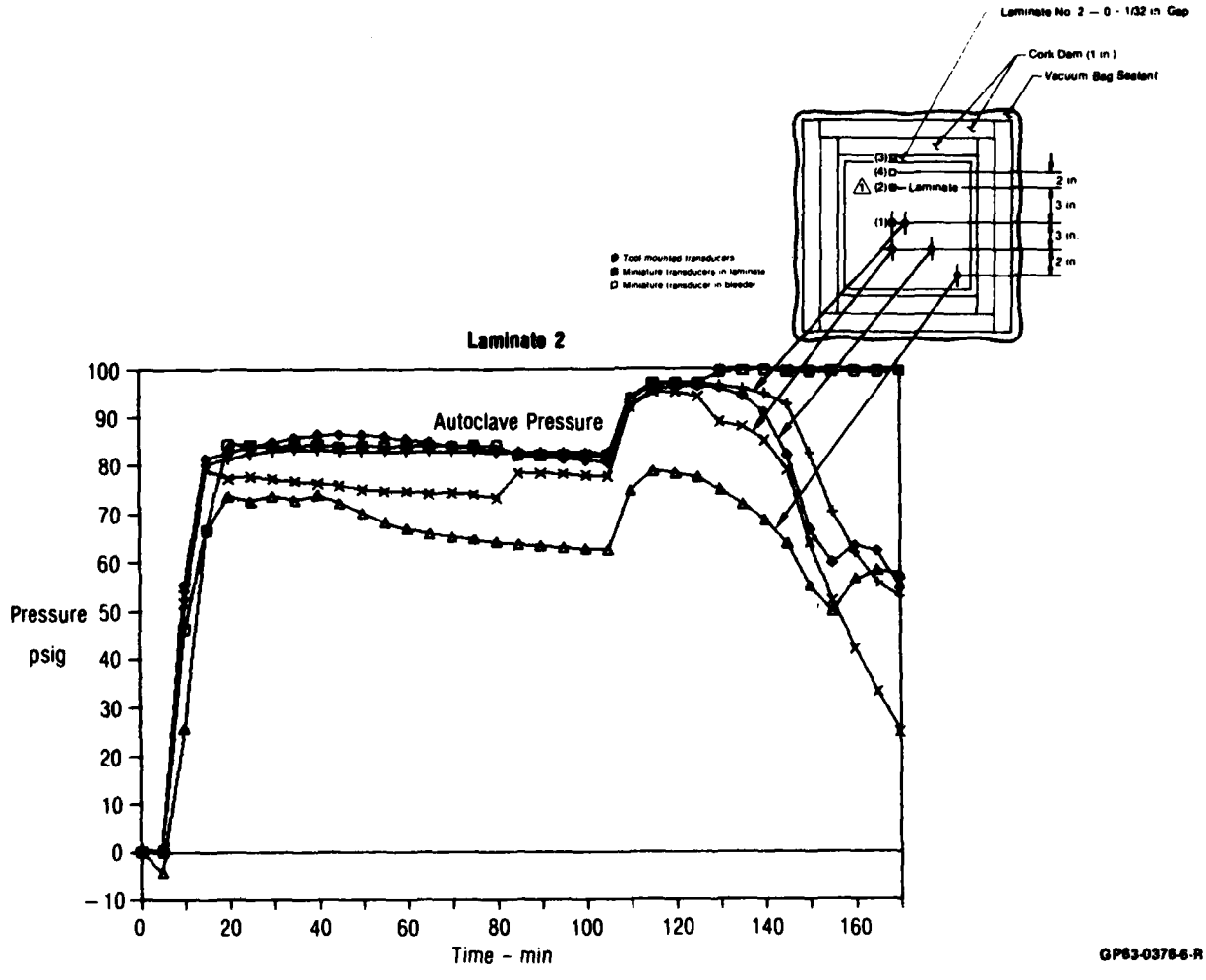

Figure 71. Horizontal Flow Laminate - Small Gap Distance
Tool Mounted Pressure Transducers

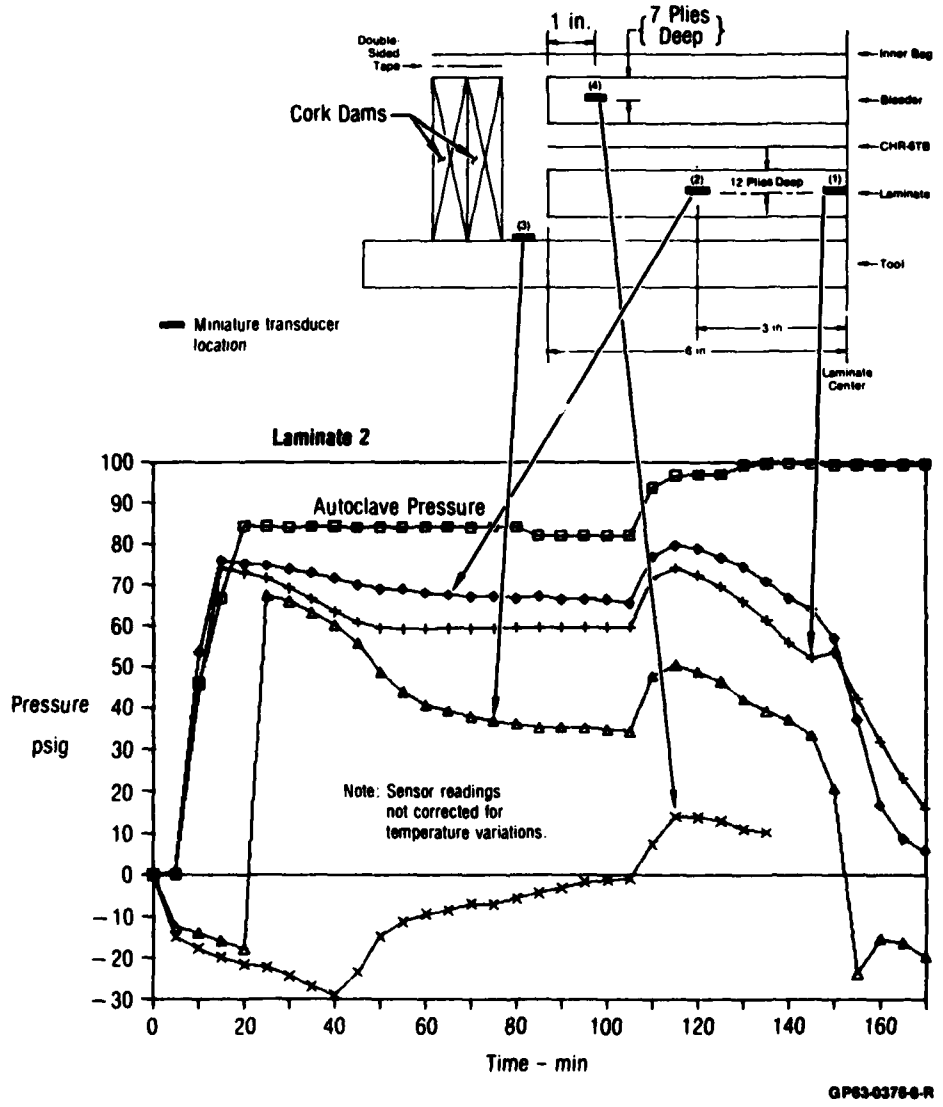

Figure 72. Horizontal Flow Laminate - Small Gap Distance Miniature Pressure Transducers

- Vertical Flow Test (Figures 73 and 74) - The miniature pressure transducers showed the large vertical pressure gradient that existed through the laminate and bleeder. Limitations of using tool mounted transducers or thick laminates were evident. The tool mounted transducers showed only a slight drop in resin pressure at the tool interface.

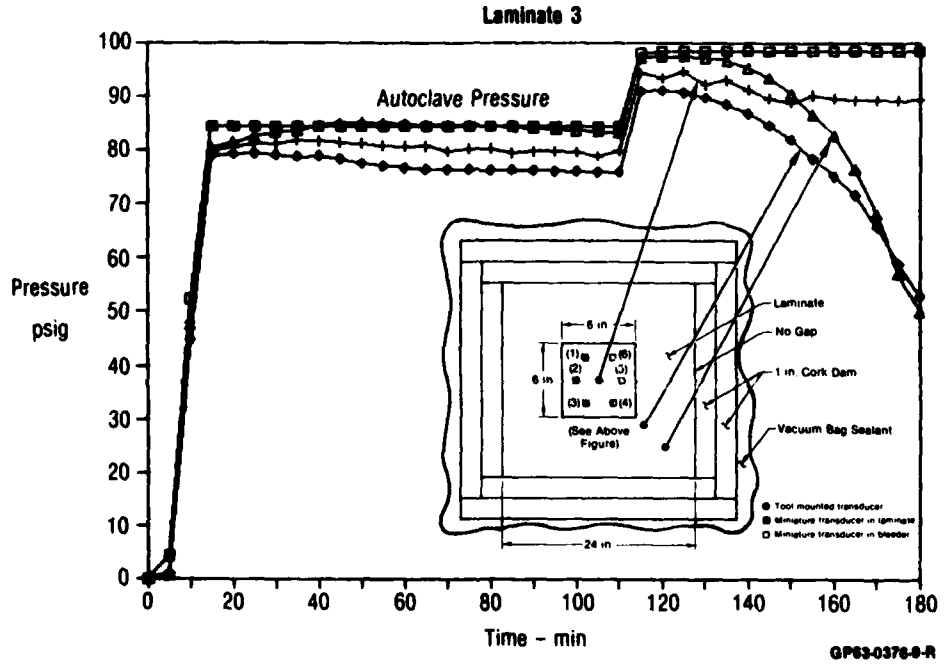

Figure 73. Vertical Flow Laminate
Tool Mounted Pressure Transducers

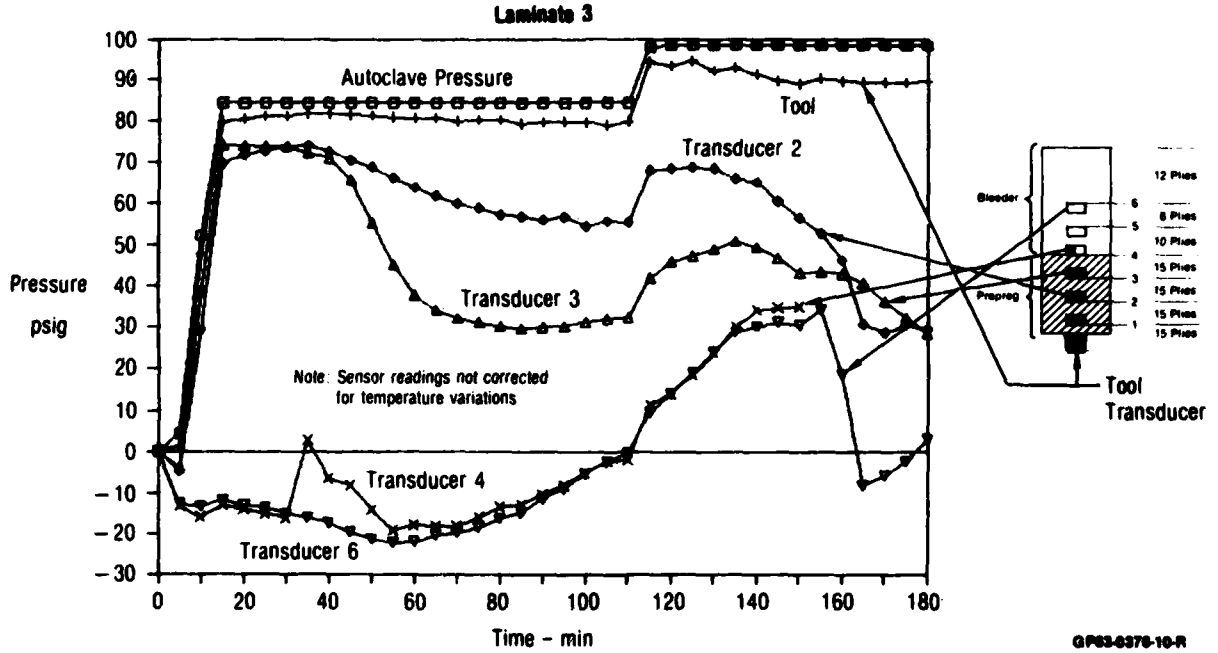

Figure 74. Vertical Flow Laminate Miniature Pressure Transducers

o Ply Drop-Off Test (Figures 75, 76 and 77) - The miniature pressure transducer responses showed that resin pressure differences in a ply drop-off region are very small. Again, the inability of tool-mounted

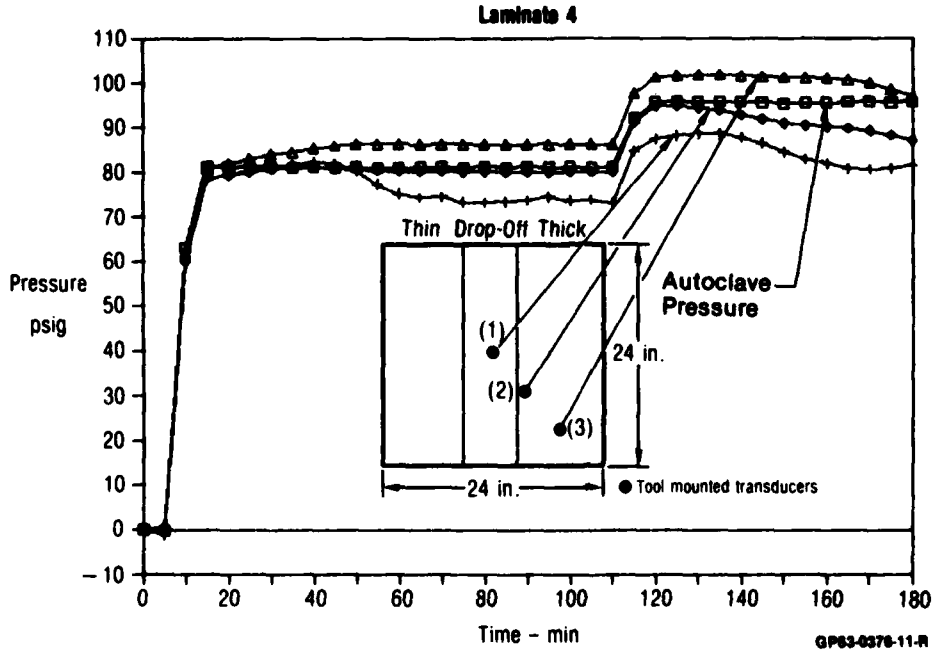

Figure 75. Ply Drop-Off Laminate Tool Mounted Pressure Transducers

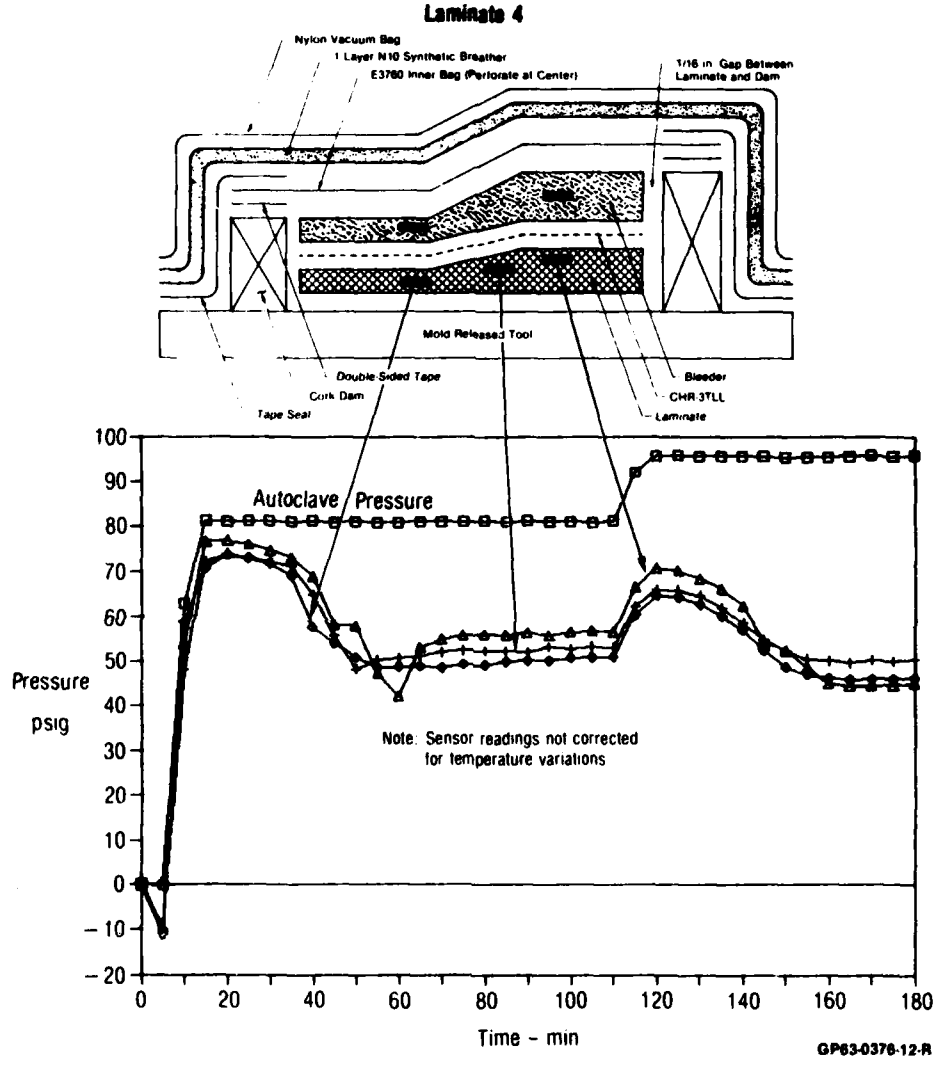

Figure 76. Ply Drop-Off Laminate
Laminate Miniature Pressure Transducers

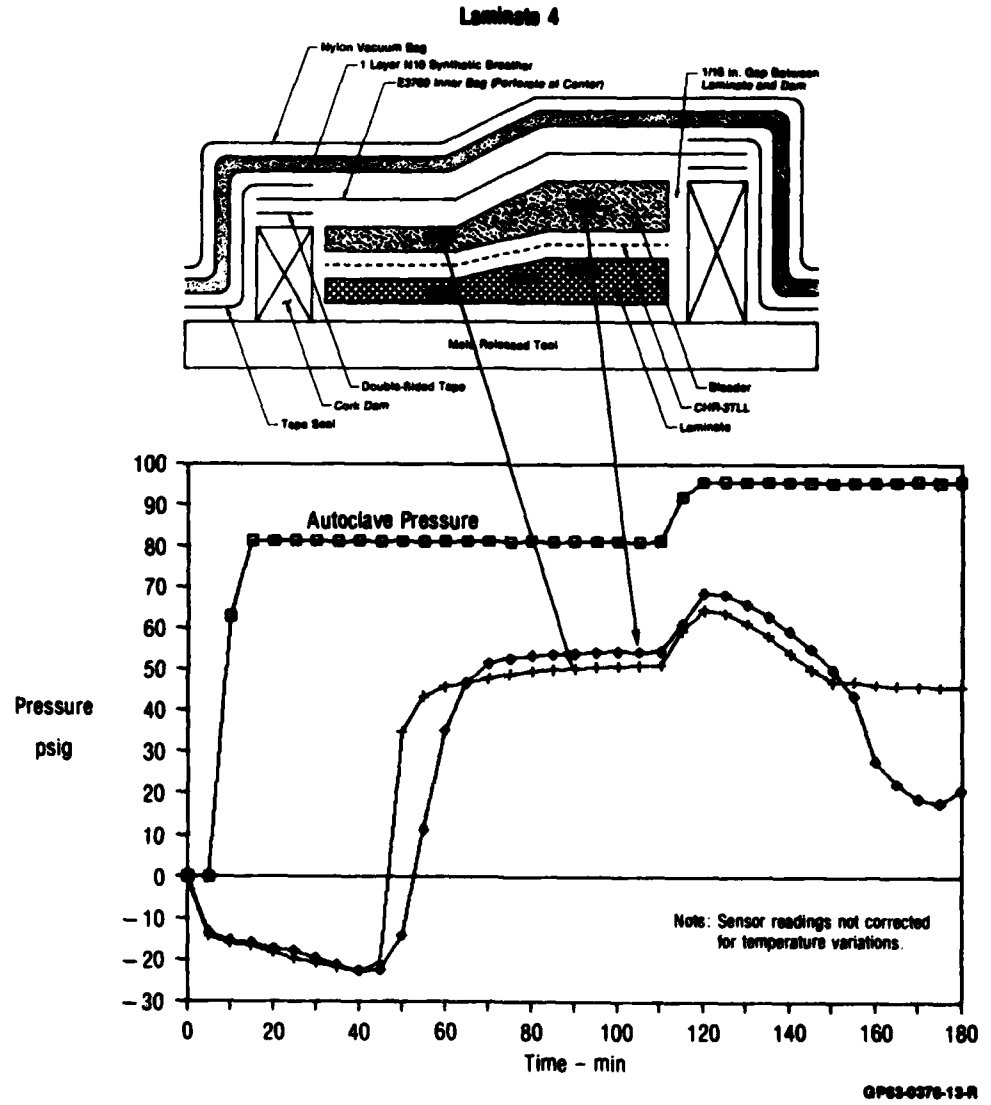

Figure 77. Ply Drop-Off Laminate Bleeder Miniature Pressure Transducers

transducers to measure pressure drops within the laminate was evident. Note that the sensors positioned in the bleeder plies (Figure 77) reflected the vacuum pressure until the bleeder became resin saturated. From that point on, the bleeder pressure was about the same as the laminate internal pressure.

5.2.4 Characterization of Cured Laminates - The four cured laminates from the pressure sensor-monitored autoclave cures were examined in order to characterize the effects of resin flow with respect to sensor responses. Thickness measurements, resin contents and photomicrographs of cross-sections were made.

Analysis of results for the horizontal-flow laminates indicated that considerably more flow occurred near the edges than at the laminate center, and that the wider edge gap resulted in more total resin flow, as had been anticipated. Since all resin bleedout was from the edges (surface bleed was prevented by the impermeable cover-ply), the laminate was thinner at the edges where the greatest pressure drop was measured.

In the vertical-flow laminate, the thickness was nearly uniform over the entire laminate area, since edge bleed was prevented and surface bleed allowed into excess bleeder fabric. Photomicrographs and resin content determinations showed that most of the flow occurred at the bleeder surface. The pressure gradient shown in Figure 74 corresponded inversely with resin flow: final resin content varied throughout the thickness of the 60-ply laminate from 26.6 percent by weight in the 20 plies nearest the bleeder to 33.0 percent in the 20 plies nearest the tool surface. Per-ply thickness varied gradually through the thickness accordingly. No voids were observed in any of the photomicrographs, despite the low hydrostatic resin pressure at the bleeder-layup interface.

The disproportionate through-the-thickness resin flow and resin content variations were also observed in the resin content measurements and photomicrographs of the tapered-thickness laminate with ply drop-offs. However, flow variations were not evident from the pressure sensor data, since all sensors were at the same laminate depth. Significantly, no voids were detected in the ply drop-off areas.

5.2.5 Application of Pressure Sensor Test Results - The pressure sensor experimental data have been used to model vertical and horizontal flow, using the Master Cure Model/Process Simulator computer code developed under the "Computer-Aided Curing of Composites" program (Reference 1). In addition, the results were used to select optimum location for the FOCS and AWG cure-monitoring sensors in the Task III demonstration laminates. The reliability of the miniature pressure transducers was demonstrated in these experiments. Positioning of sensors for cure pressure monitoring of production or pre-production development parts can be determined from these results: the most critical areas, such as edges or the outer plies of very thick sections, can be monitored to assure proper assembly practices for bleeders, edge dam gaps or the efficiency of resin containment methods.

6.0 DEMONSTRATION OF PROCESS MONITORING

6.1 EXPERIMENTAL PLAN

The objective of Task III was to provide a demonstration of the capabilities of the FOCS and AWG sensors to monitor the progress of selected cure parameters (i.e., viscosity and degree of resin cure) through a series of typical composite cure cycles. In order to provide realistic conditions that simulate a production situation, laminates were designed with size and thickness dimensions typical of aircraft composite parts, and cured in an autoclave using standard production processes. Sensor response data, as well as autoclave and vacuum bag pressure and temperature conditions, were monitored and displayed either in real time or immediately after completion of cure.

Analysis of the sensor signal profile data included comparison with the predicted viscosity and degree-of-cure profiles and with measured properties of the cured laminates. A graphic outline of Task III efforts is shown in Figure 2.

6.2 SETUP FOR AUTOCLAVE CURE MONITORING

6.2.1 Demonstration Cures - Autoclave Setup - A laboratory autoclave was equipped with ceramic fittings on both sides of the chamber wall for pass-through of the sensor leads. The acoustic waveguide, a 0.02 inch diameter nichrome wire, passed through both walls, with the transducers bonded to the ends on the outside of the autoclave. Transducers were mounted in silicone rubber pads as shown in Figure 78. The miniature pressure transducer leads and fluorescence optrode fiber also passed through one of these ports, but through separate holes in the ceramic tube. These leads can

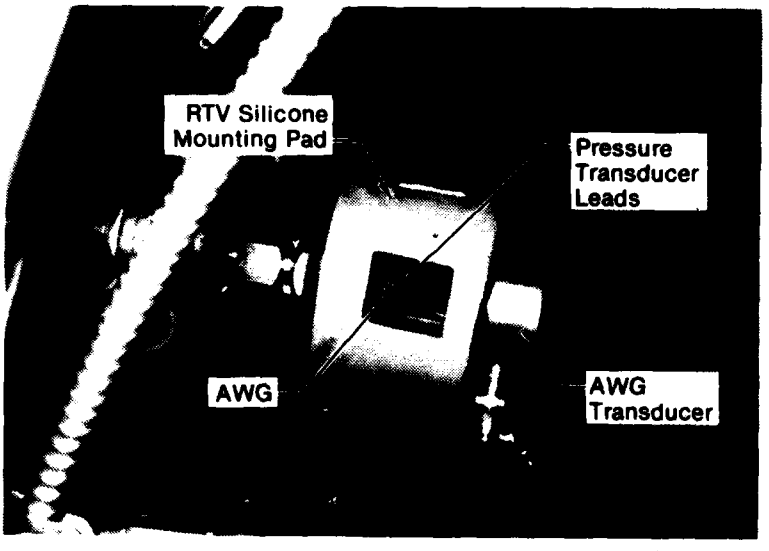

Figure 78. AWG Sensor Transducer Mounting Outside Autoclave

also be seen in Figure 78. The ceramic pass-through fittings were sealed within the autoclave wall with a teflon sleeve. The sensor leads were sealed with RTV silicone rubber on the inside of the autoclave wall to prevent gas leakage.

Figure 79 shows the 1-inch thick, 24-inch x 32-inch aluminum cure plate with thermocouples and acoustic waveguide (AWG) in position. The AWG was positioned across the chamber and through the fittings shown at both sides of the inner wall. The fluorescence optrode fiber optic sensor was mounted to the underside of the cure plate. This tool-mounted sensor FOCS was located in the center of the thick laminate section. Figures 80 and 81 show the equipment for sensor response signal processing, data acquisition, monitoring and plotting for the FOCS, AWG and miniature pressure sensor systems, which were located adjacent to the autoclave. Figure 82 is a schematic of the FOCS system interface with the autoclave. The data acquisition system (DAS) schematic is shown in Figure 56.

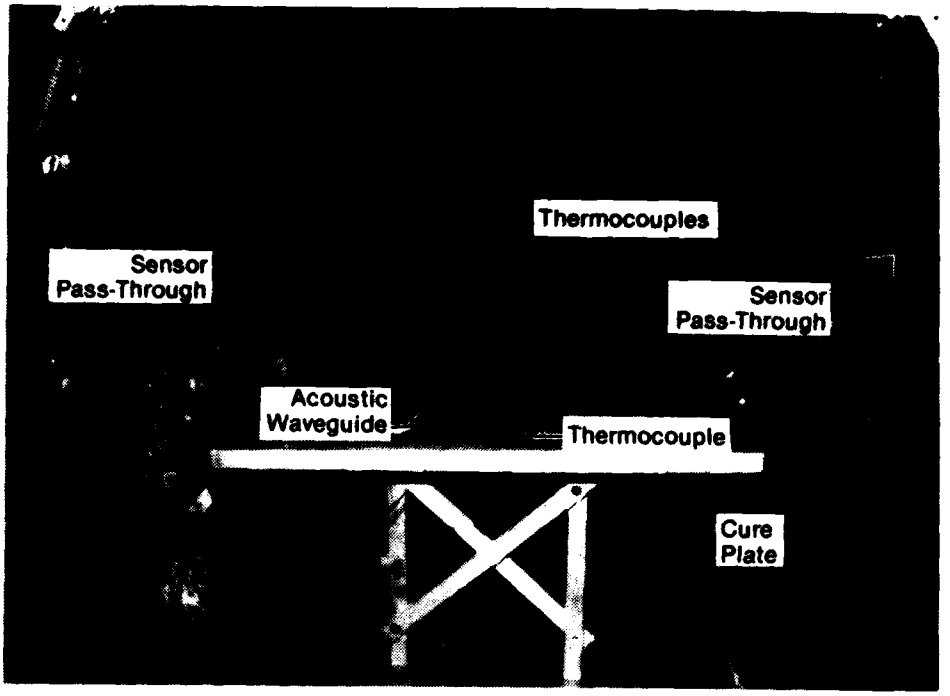

Figure 79. Autoclave Setup for Cure Plate and Sensors

GP83-0257-6-R

Figure 80. FOCS Sensor Equipment for Autoclave Cure Monitoring

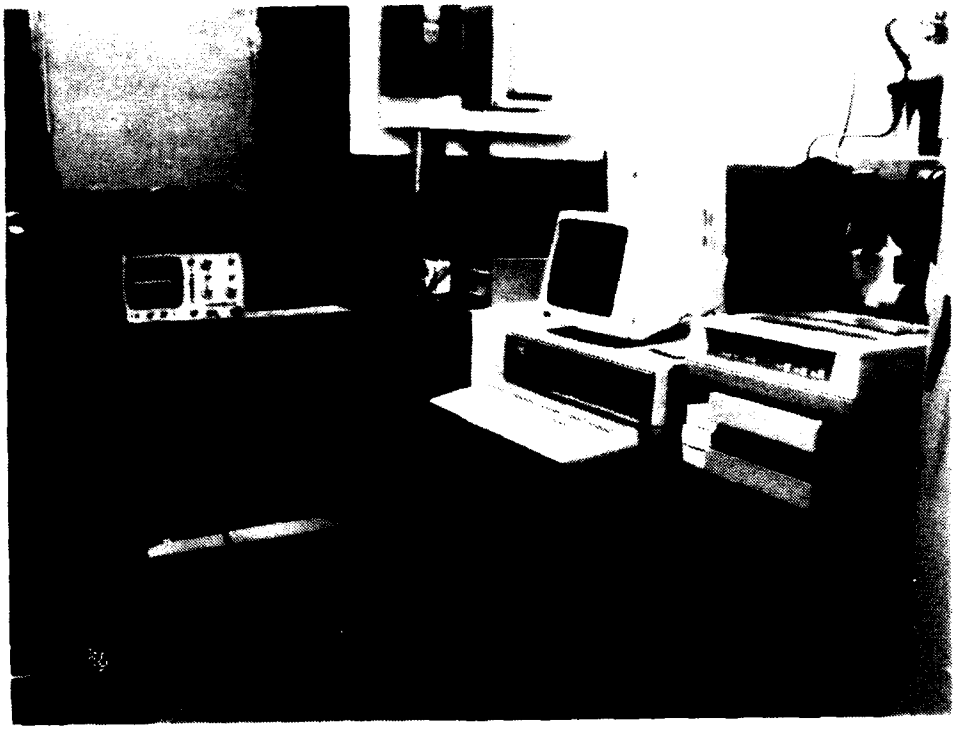

Figure 81. AWG and Pressure Sensor Equipment for Autoclave Cure Monitoring

GP83-0257-7-R

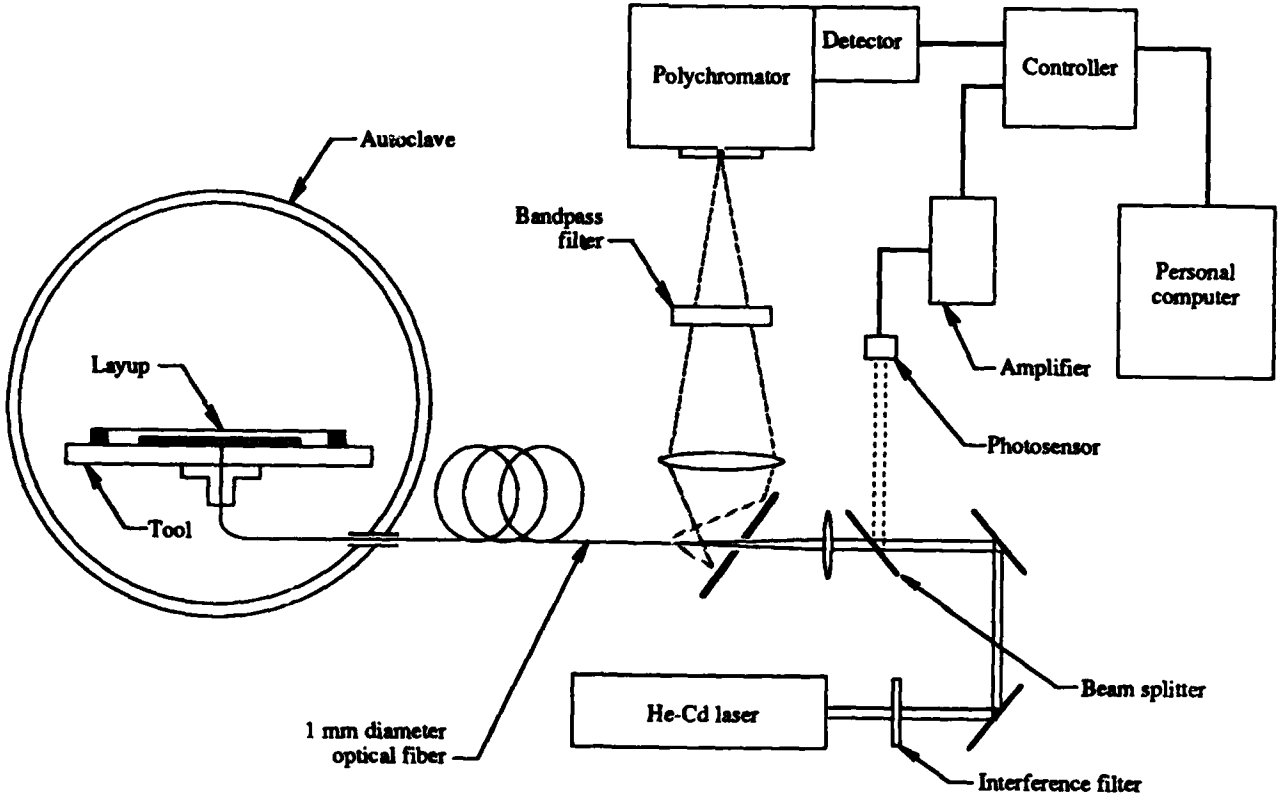

Figure 82. Schematic of Second-Generation FOCS Breadboard Interfaced to an Autoclave

6.2.2 Laminate Description and Cure Cycles - Seven AS4/3501-6 cure cycles were monitored with FOCS, AWG and pressure sensors as described in Figure 83. The baseline layup configuration for demonstration laminates was as shown in Figure 84; however, some of the laminates were as shown in Figure 85, with 41 plies throughout. All sensors were positioned in the 41-ply section for all cures, as shown. A slot was cut in the three center plies of each laminate, as shown in the sketch, Figure 41(a), to accommodate the 0.02 inch diameter nichrome wire waveguide sensors (Figure 84 shows the slots for two AWG's installed in layups for Runs No. 6 and 7).

Cure	Cure Cycle Description	Prepreg Condition	Bleeder Amount	Sensors Monitored			Response Parameters			
				FOCS	AWG	Pressure (Internal)	Viscosity	Resin Pressure	Void Formation	Degree of Cure
1	Baseline "Standard" Cycle	Normal	Normal	1	1		✓			✓
2	Optimized Cure, Interrupted at $\alpha = 0.95$	Normal	Normal	1	1		✓			✓
3	Multi-Step Cure, Internally Pressurized Bag (IPB), Interrupted at $\alpha = 0.85$	Normal	Normal	1	1		✓			✓
4	One-Step Ramp, Delayed Pressure (Applied at Minimum Viscosity)	Normal	Normal	1	1	1	✓	✓	✓	✓
5	Optimized IPB Cure	Moisturized	Excess	1	1	1	✓	✓	✓	✓
6	Optimized IPB Cure, Two AWGs for Void Detection	Moisturized	Excess	1	2	1	✓	✓	✓	✓
7	Optimized IPB Cure, Delayed Pressure Application, Two AWGs for Void Detection	Moisturized	Excess	1	2	1	✓	✓	✓	✓

GP83-0257-6-R

Figure 83. Sensor Demonstration Autoclave Cure Cycles

AD-A197 034 COMPOSITE CURING PROCESS NONDESTRUCTIVE EVALUATION(U) 2/2
MCDONNELL AIRCRAFT CO ST LOUIS MO P W HARRUFF ET AL.
JUN 88 AFWAL-TR-88-4005 F33615-85-C-5024

UNCLASSIFIED F/G 11/4 NL

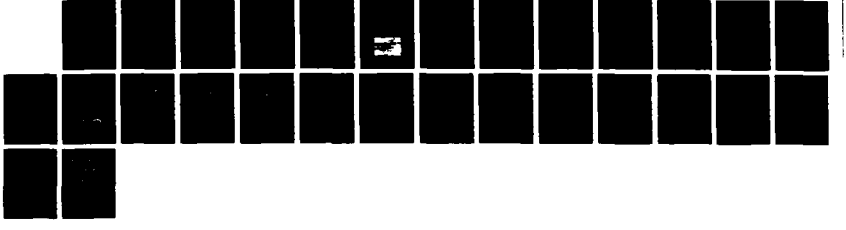

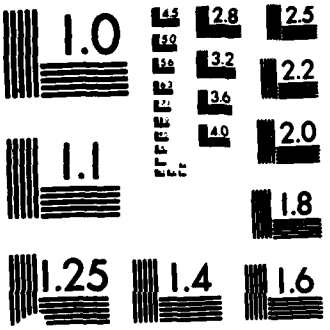

UTION TEST CHART

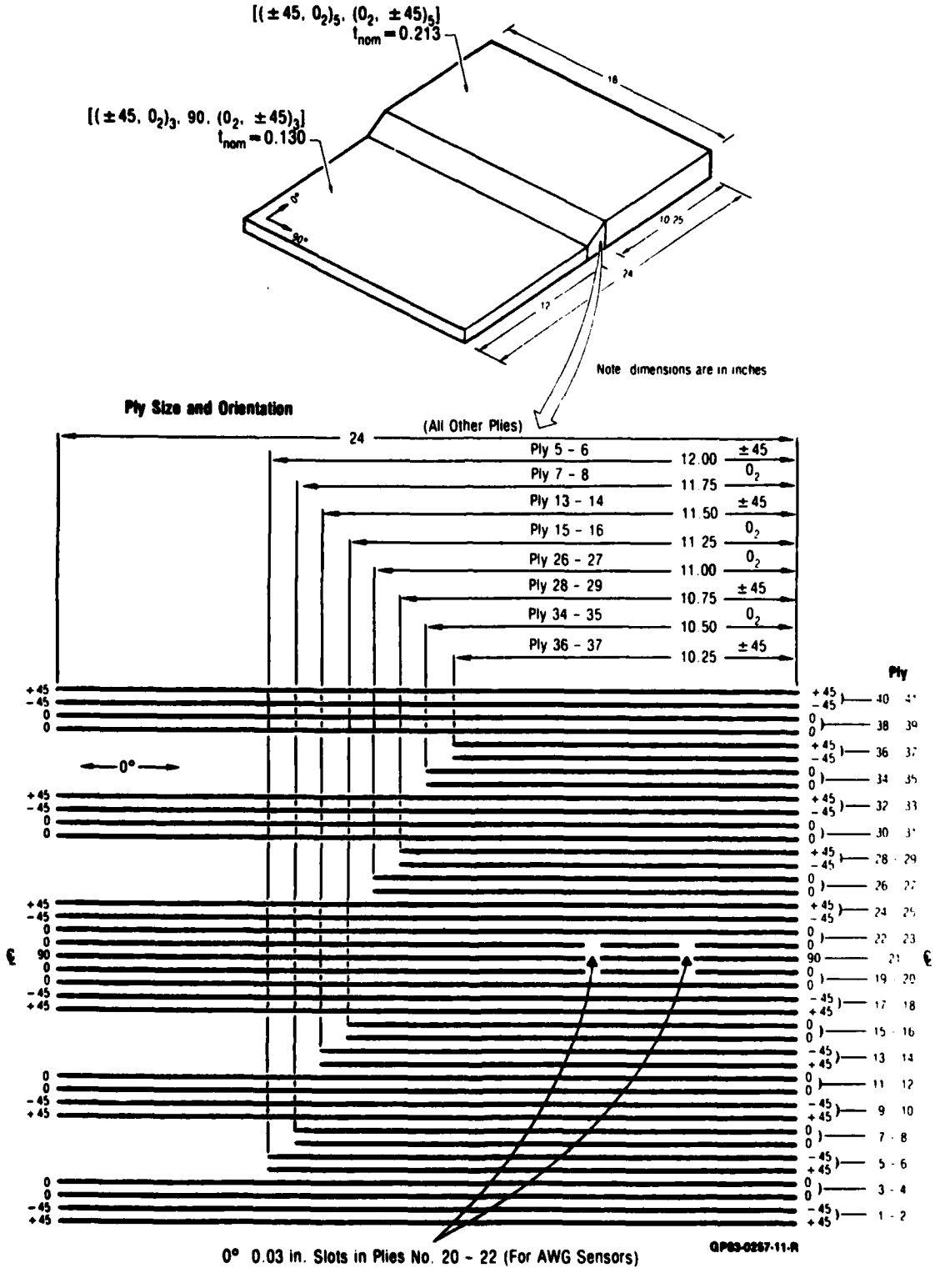

Figure 84. Baseline Sensor Demonstration Laminate Configuration

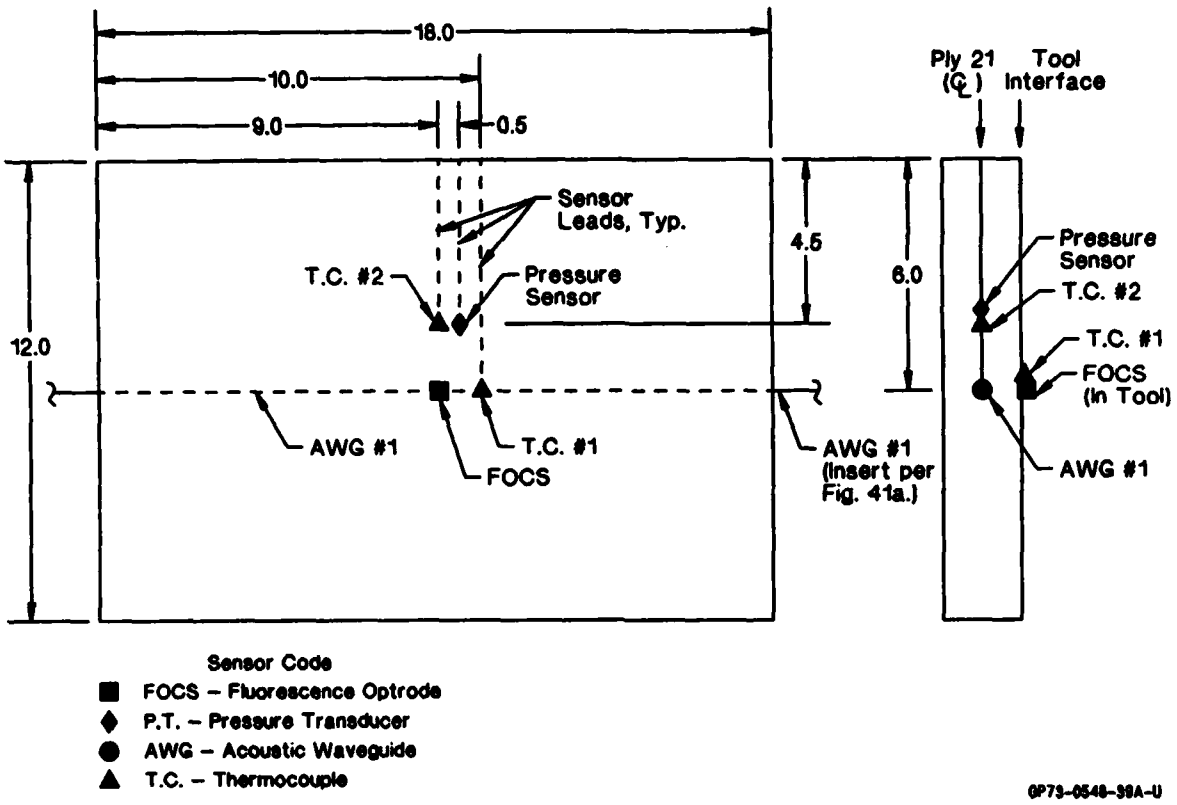

Figure 85. Sensor Locations – 41-ply Laminate With One AWG

Details of the bagging are shown in Figure 86. Locations of sensors are not shown, for clarity. Note particularly the excess bleeder material used for Runs No. 5-7. For those laminates with 41 plies of prepreg, the bleeder amount shown over the thick section in Figure 86 was used.

Figure 83 is a description of the processing and monitoring parameters for the seven cures and the response parameters that were identified as potentially significant. The cure cycles were selected to represent either production cures of AS4/3501-6 composite parts, cures that were optimized in the CACC program (Reference 1), or cures that demonstrate the effect of special conditions (e.g., moisturized prepreg, excess bleeder and improper pressure application) that are known to contribute to the evolution of voids within the laminate. For cure cycles that could result in void formation, the miniature pressure sensor shown in Figure 58 was used to monitor internal laminate pressure.

Cure cycles (i.e., temperature and pressure profiles as a function of time) were selected to produce a wide range of resin material properties that would exercise the sensors:

- o resin viscosity changes prior to gelation
- o hydrostatic resin pressure variations prior to gelation
- o formation of voids prior to gelation
- o degree of resin cure state after gelation

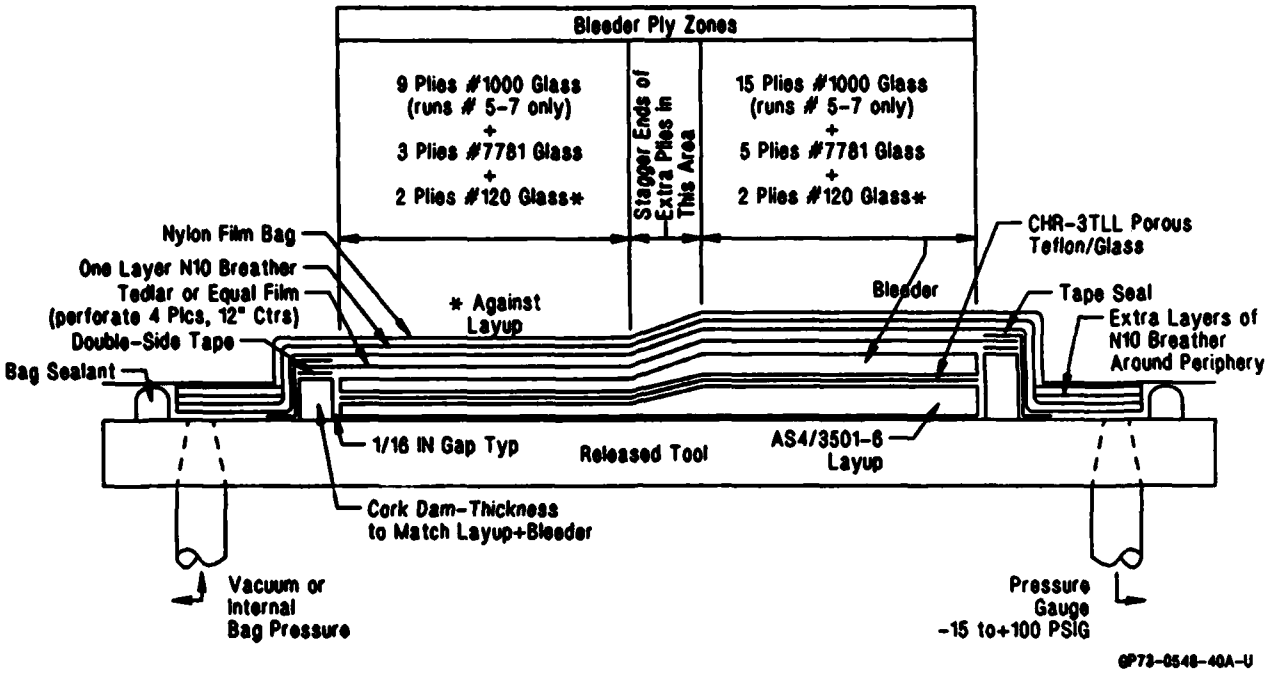

Figure 88. Bagging System for Demonstration Laminates

Actual temperature and applied pressure profiles for the Task III laminate cure cycles are shown in Figure 87.

6.3 LAMINATE PROPERTIES

After cure, the seven sensor demonstration laminates were subjected to nondestructive and destructive testing to assess the quality of the composite and to correlate the predicted and experimentally determined properties with cure-monitor sensor outputs. Results of laminate property testing are shown in Figure 88. Only minor variations in physical properties were found, despite the range of cure conditions and prepreg properties described in Figure 83. This verifies the forgiving nature of the 3501-6 resin system, and the ability of process optimization to accommodate variations in prepreg (e.g., moisture content) and processing "errors" [e.g., excess bleeder and delayed internal pressurized bag (IPB) pressure application]. For example, Laminate No. 7 process and material conditions (Figure 83) were selected to encourage void formation; however, the effectiveness of the selected time/temperature/pressure conditions overcame the process defects to produce a low void panel.

All seven laminates yielded clear ultrasonic C-scans and radiographs, verifying the low void content values shown in Figure 88. A typical photomicrograph, Figure 89, shows the appearance of one of the few small voids detected.

The primary objective of the evaluation of cured laminates was to obtain degree-of-cure (α) data for comparison with sensor-predicted data. Figure 88 shows three columns of values, determined experimentally or predicted from model data. The data for Laminates No. 1-4 correlate fairly well. Residual

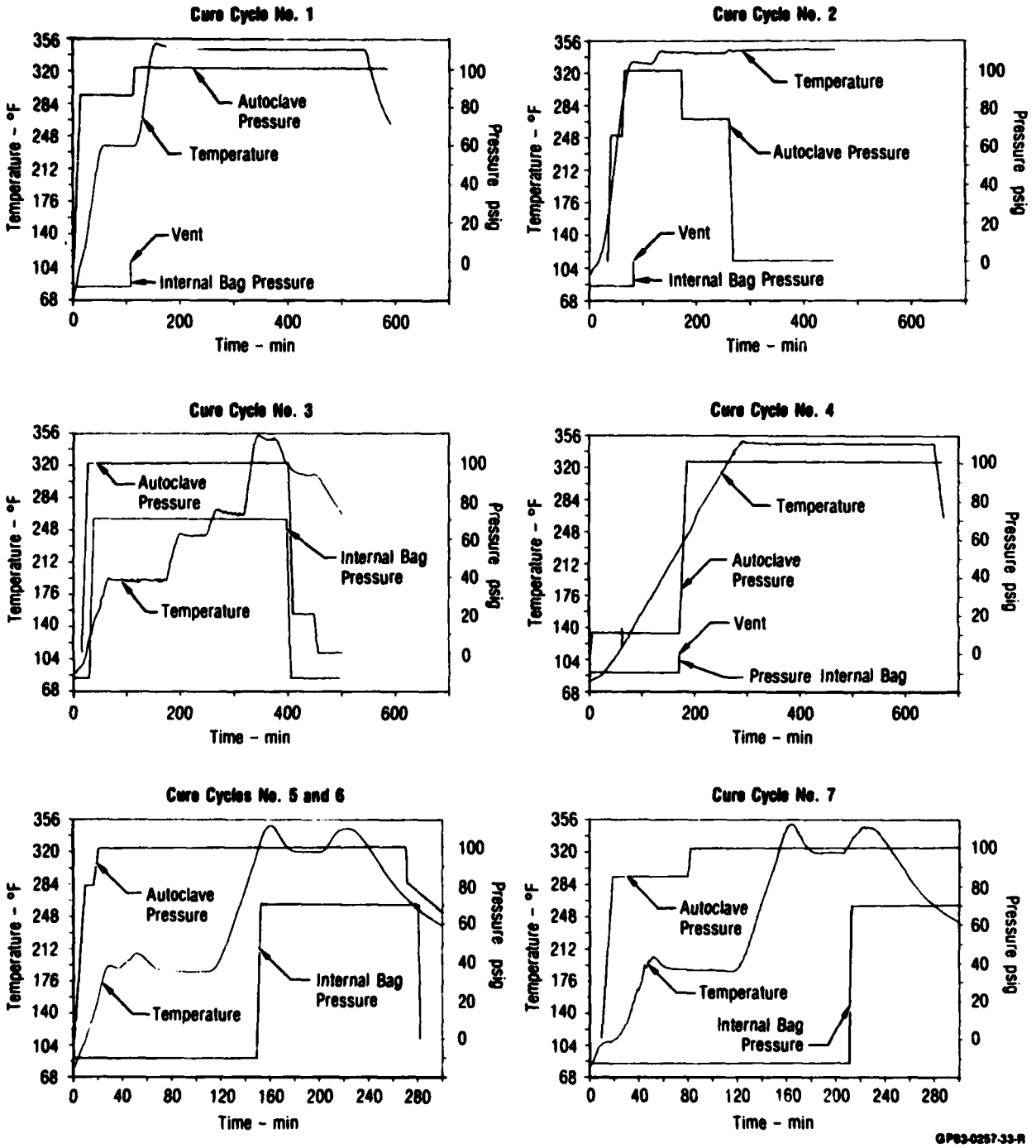

Figure 87. Sensor Demonstration Laminate Cure Cycles

Laminate Number	Thickness (in./Ply)	Resin Content (wt%)	Void Content (vol%)	Tg by DSC (°C (°F)) [Dry], Onset	Degree-of-Cure, α		
					Experimental		Predicted[3]
					$\Delta H_f/\Delta H_o$[1]	Tg Basis[2]	
1	0.0058	33	1.5	196 (385)	0.99	0.95	0.97
2	0.0062	35	1.2	203 (397)	0.98	0.97	0.97
3	0.0060	36	< 1	159 (318)	0.95	—	0.91
4	0.0060	34	1.0	201 (394)	0.99	0.97	0.97
5	0.0056	34	1.6	146 (295)	(4)	—	0.88
6	0.0057	33	1.4	153 (307)	(4)	—	0.88
7	0.0056	33	< 1	153 (307)	(4)	—	0.88

Notes:

1. Based upon residual heat of reaction (ΔH_f) from DSC curve, compared with value for uncured 3501-6 (ΔH_o).
2. Based upon previous Tg vs α data (Reference 1); no data below Tg = 175°C was obtained.
3. From model data for cure temperature/time profiles.
4. DSC curve could not be analyzed for ΔH_f.

GP83-0257-34-T

Figure 88. Properties of Cured Laminates
Task III - Sensor Demonstration

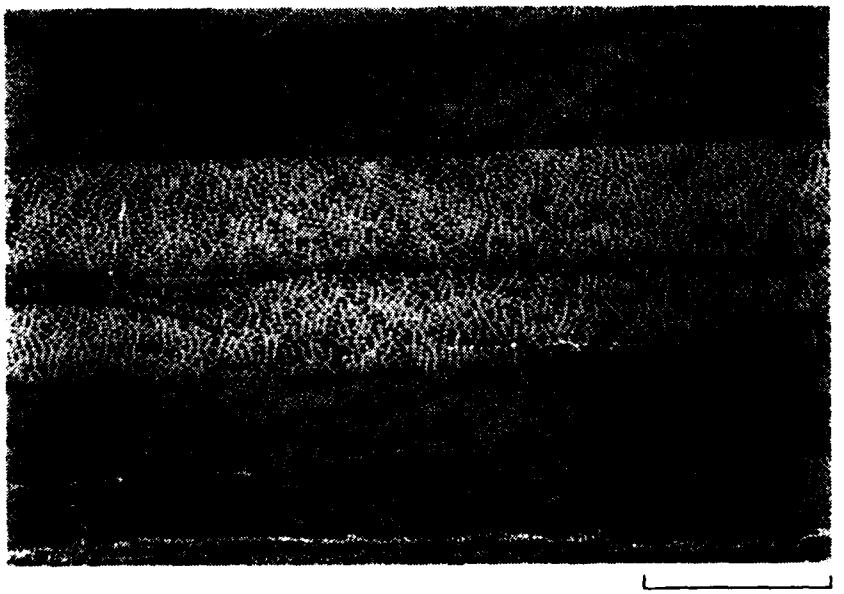

GP83-0257-35-R

Figure 89. Photomicrograph (100 x) of Laminate No. 5, With Microvoid

heat of reaction values (ΔH_f) could not be determined experimentally from the DSC curves for Laminates No. 5-7, all of which were made from moisturized prepreg. Therefore, no independent verification of the "Predicted" (model-generated) α values could be made. Since the models were based upon cures of dry, not moisturized, prepreg, these data may not be accurate. The measured Tg values are plotted against model-predicted α in Figure 90 for the seven laminates.

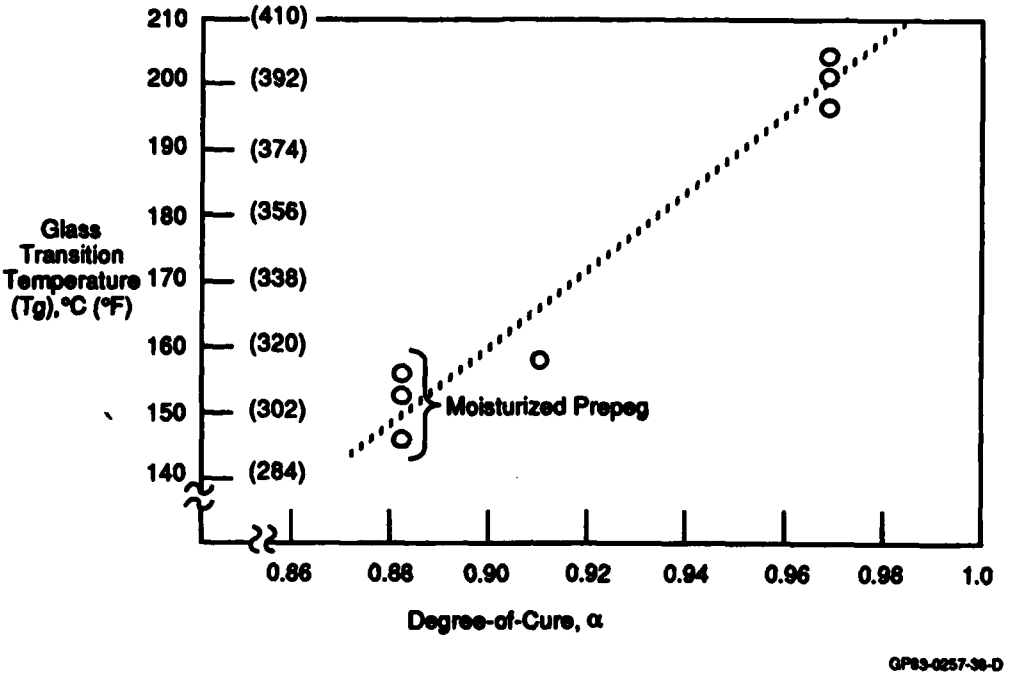

Figure 90. Relationship of Tg (DSC) of Task III Laminates and Predicted α from Model Data

6.4 RESULTS AND ANALYSIS OF FOCS PROCESS MONITORING

The autoclave curing of seven test laminates under Task III (seven different cure cycle temperature profiles) were monitored with the FOCS using the "process" version of the resin cavity optrode-laminate interface. General observations on the FOCS signal profiles and information on the interface or computer problems encountered during each run are as follows:

Run 1 - Normal (as expected) FOCS intensity signal profile with good signal levels up to 175 minutes cure when a software problem (computer clock going beyond midnight and thus resetting time to zero) caused loss of signal for 55 minutes. Signal was restored after 30 minutes cure. The wavelength signal (except for the lost 55 minutes) was good.

Run 2 - FOCS intensity signal was lower but followed the normal profile. The wavelength signal pattern followed the expected profile but had some spurious data points during the late stages of cure.

Run 3 - This cure cycle was characterized by stepwise increase of the temperature. The FOCS intensity and wavelength signals for this run are shown in Figures 91 and 92. Intensity levels were normal. The intensity signal profile followed the stepwise pattern of the temperature by dipping to lower values every time the temperature was increased. The wavelength signal also followed the kind of profile that can be expected from the stepwise temperature changes and the resulting advancement of resin cure.

Run 4 - During this run, the FOCS failed to function due to folding of the teflon release film and absence of resin in the cavity.

Run 5 - FOCS signal levels were normal, signal profiles followed the cure uninterrupted. The wavelength signal followed the expected pattern but the signal became noisy toward the end of the cure.

Run 6 - Resin flow into the cavity did not occur until the second step in the heatup cycle. After filling of the cavity during the temperature ramp to 177°C (350°F), the profiles were good and were similar to those of Run 5.

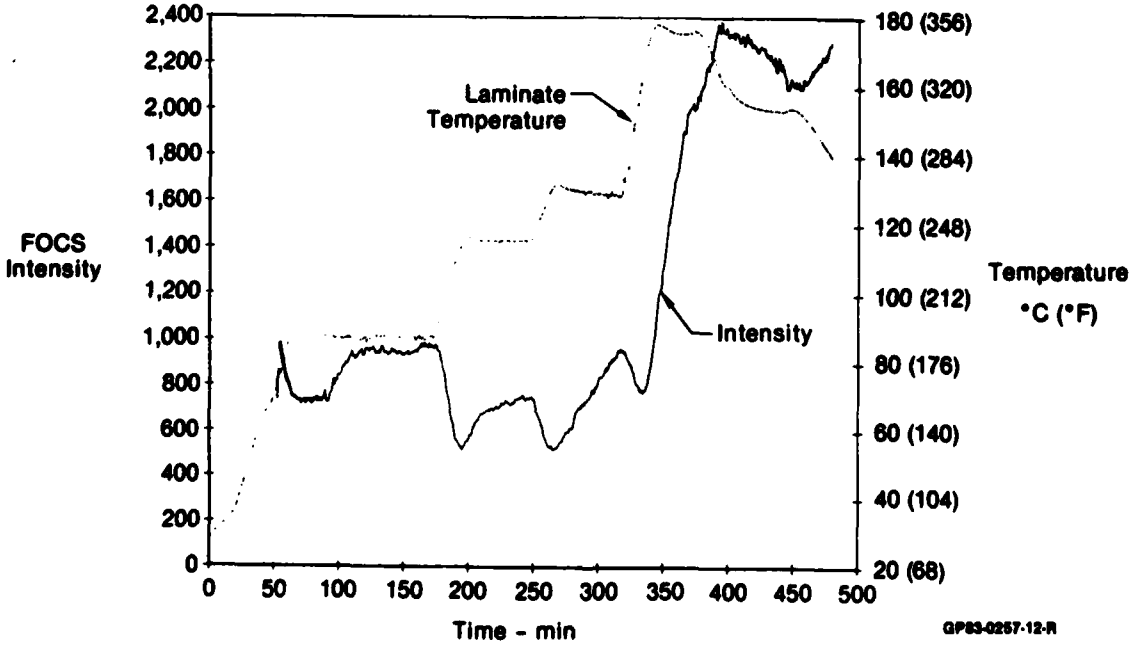

Figure 91. Cure Cycle No. 3 - FOCS Intensity Signal and Temperature-Time Profiles Autoclave Cure

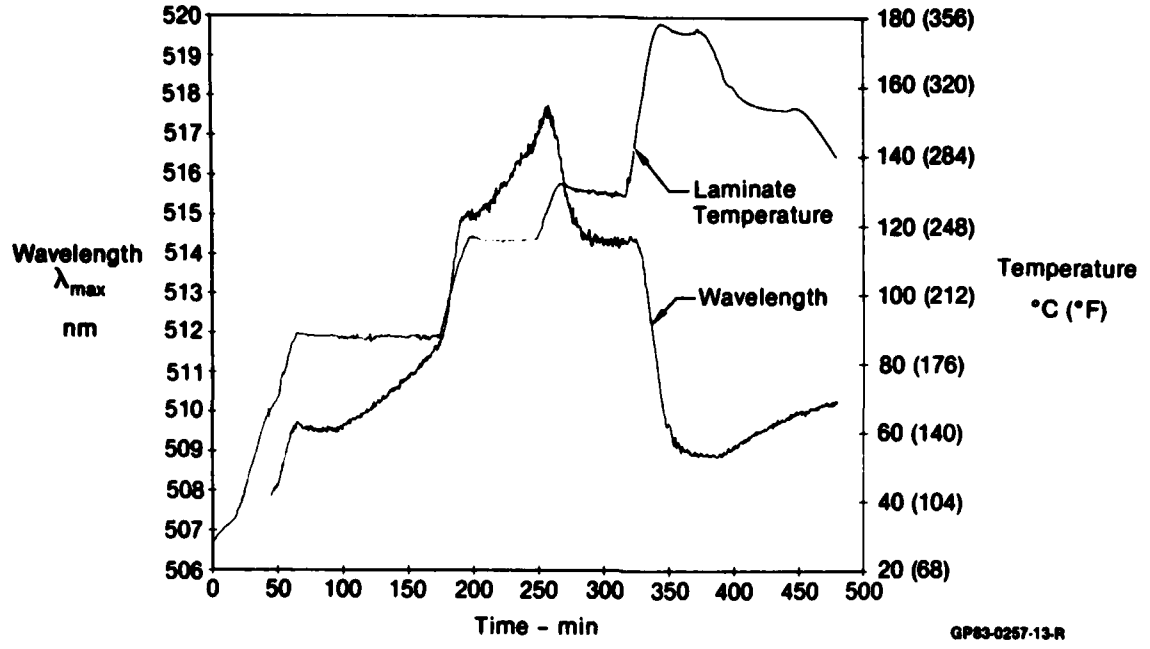

Figure 92. Cure Cycle No. 3 - FOCS Wavelength Signal and Temperature-Time Profiles
Autoclave Cure

Run 7 - After the initial resin flow and partial filling of the resin cavity the FOCS intensity signal suddenly dropped to very low values. Examination of the resin cavity after completion of the cure indicated that an air bubble had formed in the region "viewed" by the optrode thus preventing proper acquisition of fluorescence data.

6.4.1 Analysis of FOCS Process Monitoring - The point in the cure cycle at which the resin viscosity reaches a minimum is one of the main chemorheological events of interest during cure. Therefore, in order to evaluate the ability of the FOCS to determine the points of minimum viscosity, comparisons with viscosity data derived from the viscosity model were made. Figures 93 through 96 show the FOCS intensity signal obtained in real-time during cure and the logarithm of the viscosity predicted by the viscosity model provided with the temperature-time curve after the cure as functions of cure time. For each of the test laminates shown, the profiles are qualitatively similar indicating that the FOCS does follow the trends in resin viscosity. However, there are some subtle differences in cure times for minimum viscosities as shown in Figure 97, which provides a comparison of the predicted point of minimum viscosity generated by the computer model with the observed point of minimum intensity determined by the FOCS. The fact that these values are slightly different in several instances underscores the rationale for real-time cure monitoring. Although, at this time in the FOCS evolution, we cannot directly relate the signal to an absolute viscosity, we can unambiguously conclude that when the fluorescence intensity reaches a minimum, the resin viscosity has reached a minimum. Therefore, as indicated by the data in Figure 97, the FOCS is probably more accurate in detecting

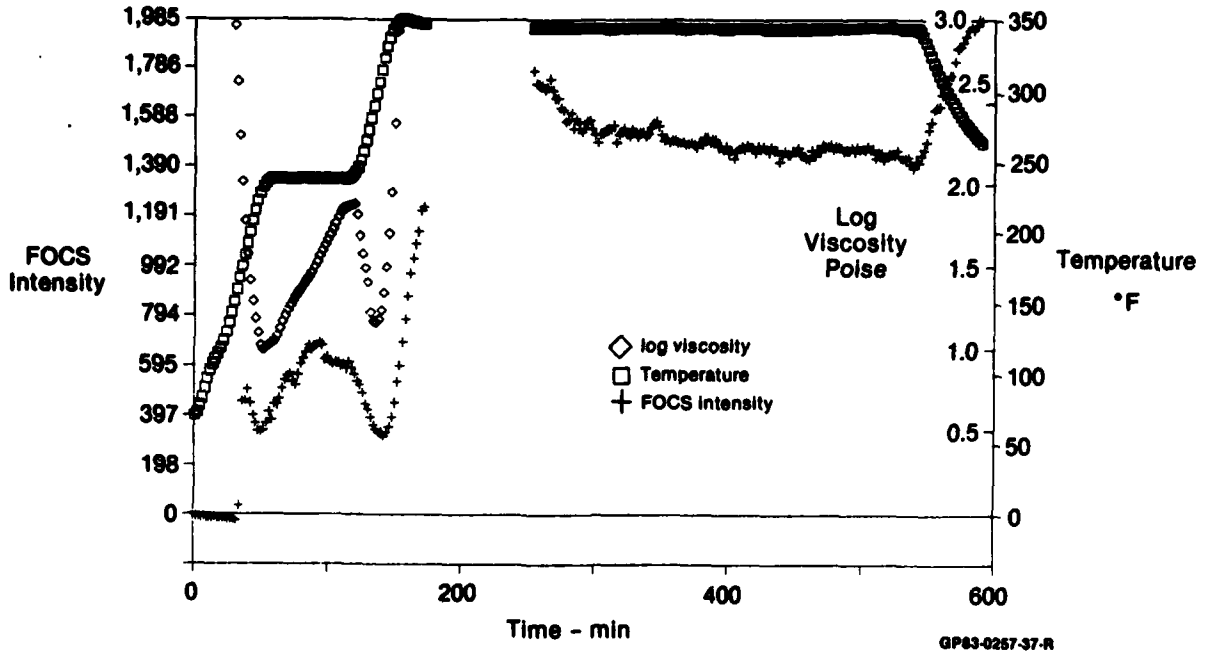

Figure 93. Cure Cycle No. 1 - FOCS Intensity - log η Relationship

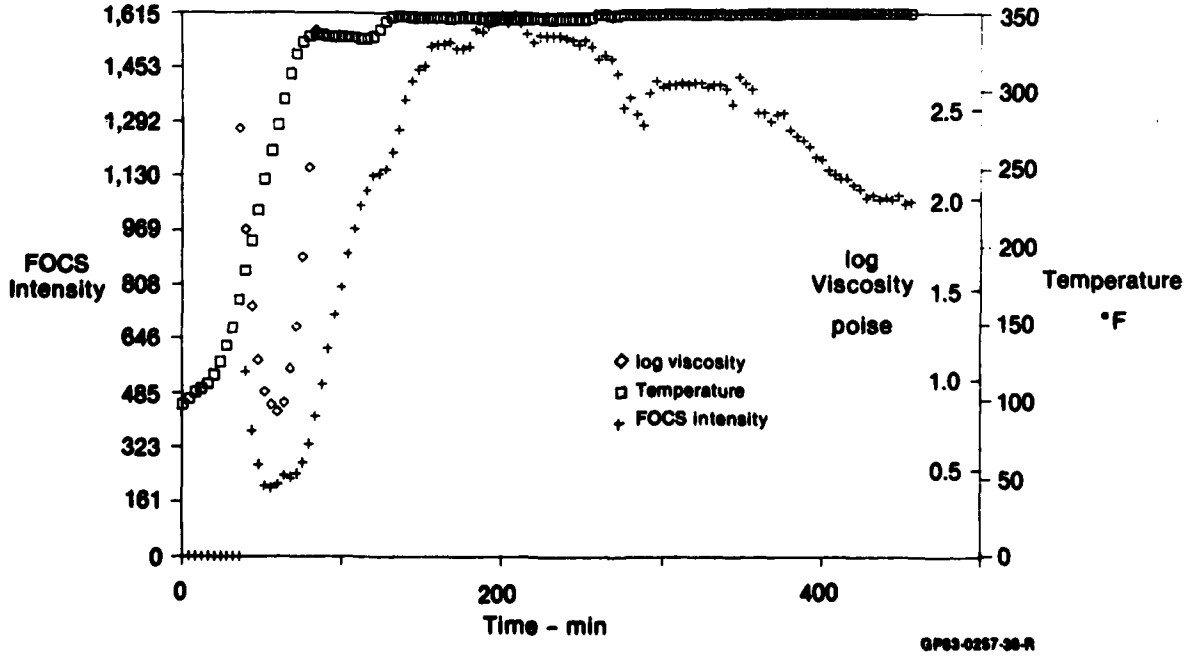

Figure 94. Cure Cycle No. 2 - FOCS Intensity - log η Relationship

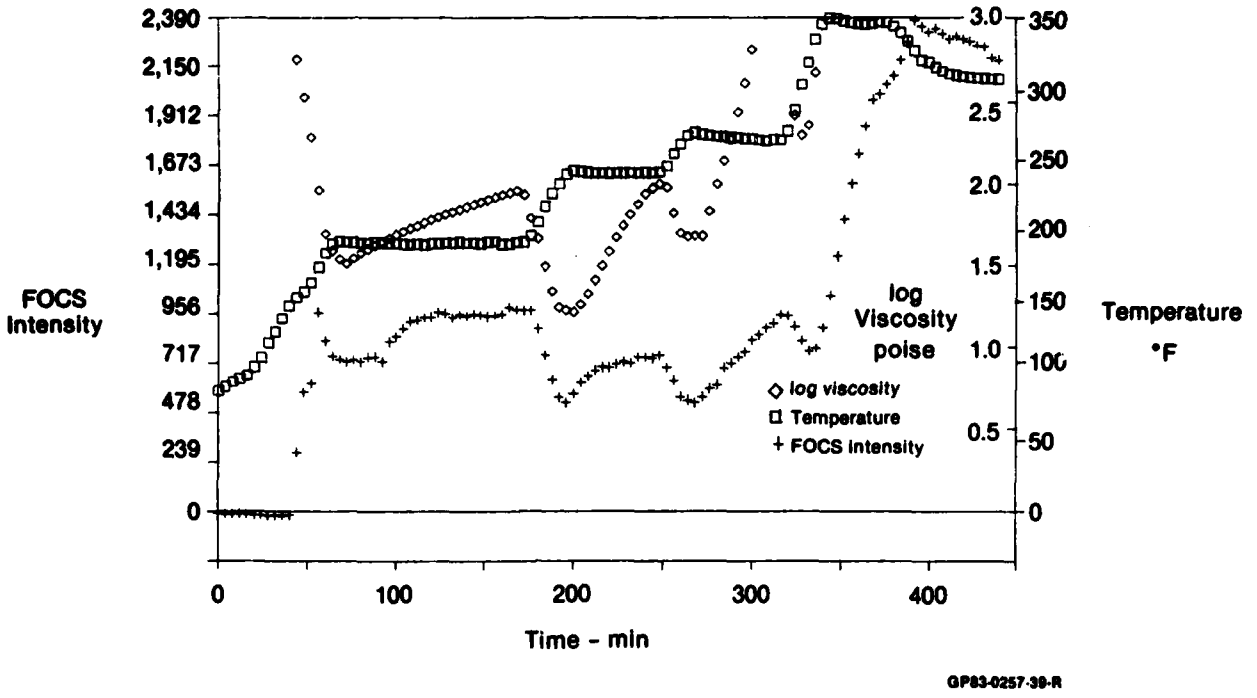

Figure 95. Cure Cycle No. 3 - FOCS Intensity - log η Relationship

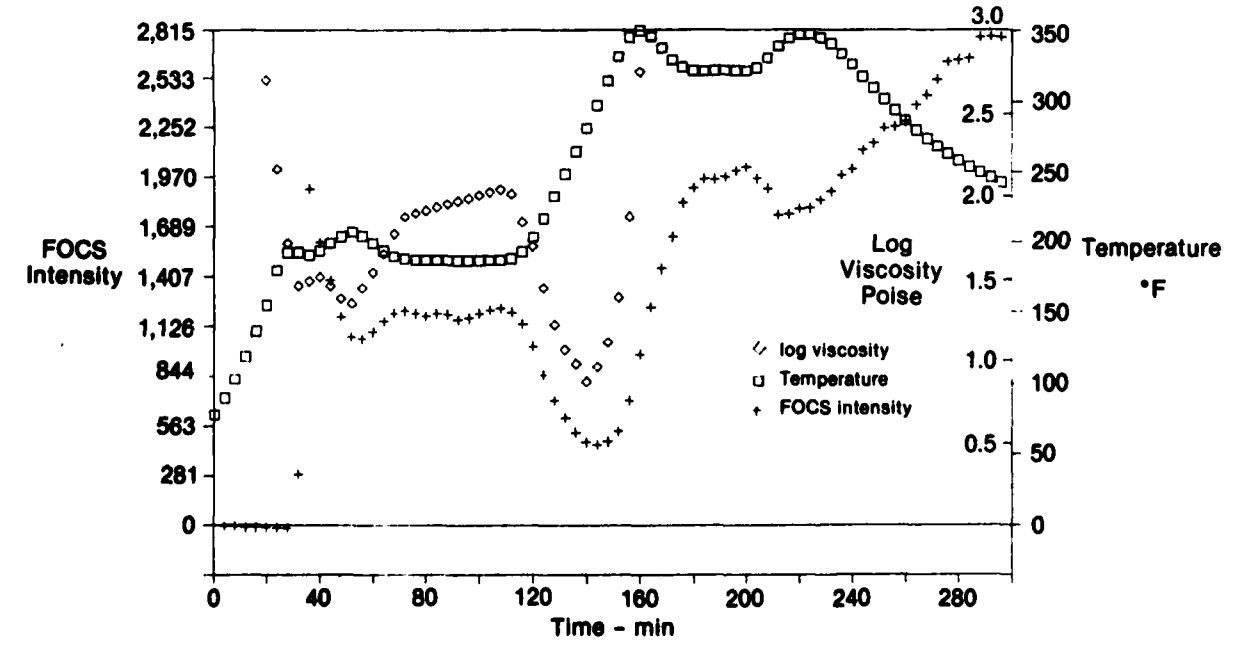

Figure 96. Cure Cycle No. 5 - FOCS Intensity - log η Relationship

Run Number	Predicted Time of Minimum Viscosity (Computer Model)	Actual Time of FOCS Minimum Intensity (Corrected for Temperature)
1	52 min	49.5 min
1	136 min	141.0 min
2	62 min	54.5 min
3	72 min	72.0 min
3	200 min	195.5 min
3	270 min	265.0 min
3	328 min	332.0 min
5	50 min	55.0 min
5	140 min	143.0 min

GP83-0257-41-T

Figure 97. Variations Between Viscosity Minimum Times (η_{min}) Observed and Predicted
Task III Cure Cycles

actual, real-time changes in viscosity because the computer model cannot account for several factors which may affect the viscosity profile. These include differences in resin history, local epoxy/curing agent/catalyst mixture variations and thermocouple malfunctions.

6.4.2 Problems with the Process Version of the Resin Cavity Interface - Runs 4, 6, and 7 of Task III failed to produce the desired sensor response data because, in all three cases, the normal flow of resin into the cavity was impeded. Consequently, the FOCS sensor data obtained was not useful. Based on inspection of the optrode-laminate interface for each of these runs after curing was completed, the most probable explanation for this problem is that the layup completely sealed the surface of the tool around the interface. This prevented entrapped air, water vapors and volatile organic compounds (evolved from the resin) from being pumped out early in the heatup cycle. If the cavity is not evacuated initially, the subsequent increase in temperature during cure causes the pressure within the cavity to increase, preventing resin flow. It will be recalled that the prepreg for Laminate Cures No. 5-7 were moisture-saturated. Alternatively, if a vacuum is drawn initially but the cavity is later sealed off by the laminate, the volatile components of the resin mixture could cause bubble formation within the cavity during cure. Any bubble formation that occurs in the volume "viewed" by the optrode would interfere with the FOCS signal. Problems of this type were not encountered during the small scale isothermal runs in the micro-autoclave because there existed a "path" from the resin cavity to the vacuum port within the bag. In any case, none of the difficulties encountered were directly attributable to the FOCS itself. There is little doubt that in cases where an inspection after curing revealed that the resin flowed into, and completely filled, the cavity, the sensor followed the trends in resin viscosity.

Given that the interface, not the sensor, was the source of the observed errors, the solution is a fairly simple one. A small vacuum line connected to the recessed area below the flow plate in the tool would assure that the cavity is initially evacuated and that the volatile components evolved during cure are removed.

6.5 RESULTS AND ANALYSIS OF AWG PROCESS MONITORING

6.5.1 Results and Sensor Responses (One Waveguide) - Data from the demonstration cure cycles are presented in Figures 98 through 109. Autoclave air and internal bag pressure data taken from autoclave strip charts have been added to these figures. Monitoring of the AWG signal response, as well as those of the embedded thermocouple and the embedded pressure sensor, was generally satisfactory. Intermittent signal distortion and interruption of the pressure sensor response was experienced which led to the inability to monitor internal laminate pressure in all runs as planned.

In all cure cycle runs, the AWG response was highly attenuated, as shown by the extremely low response levels. Preliminary calibration cycles run in the autoclave, with and without autoclave pressure of 100 psig applied, indicated that as much as 40 dB (100 to 1) signal loss was experienced with the 0.02 inch nichrome wire free-standing in the autoclave chamber. This loss was associated with the fittings through the autoclave shell. An additional 60 dB (1000 to 1) loss was measured when the wire was buried in a 41-ply layup of the carbon/epoxy prepreg, with 18 inches of the total 77 inches of waveguide length buried. As a consequence of these combined losses inherent in the system, the responses due to cure changes within the laminates were not identifiable.

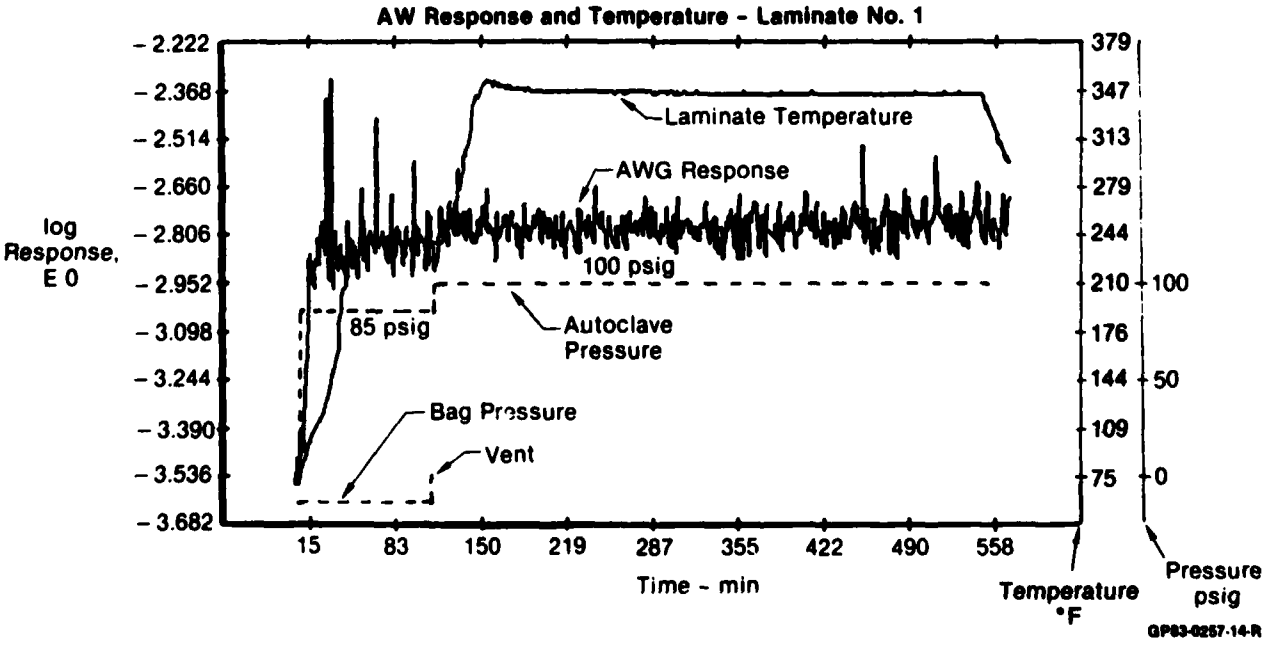

Figure 98. Cure Cycle No. 1 - AWG Response, Temperature and Pressure vs Time

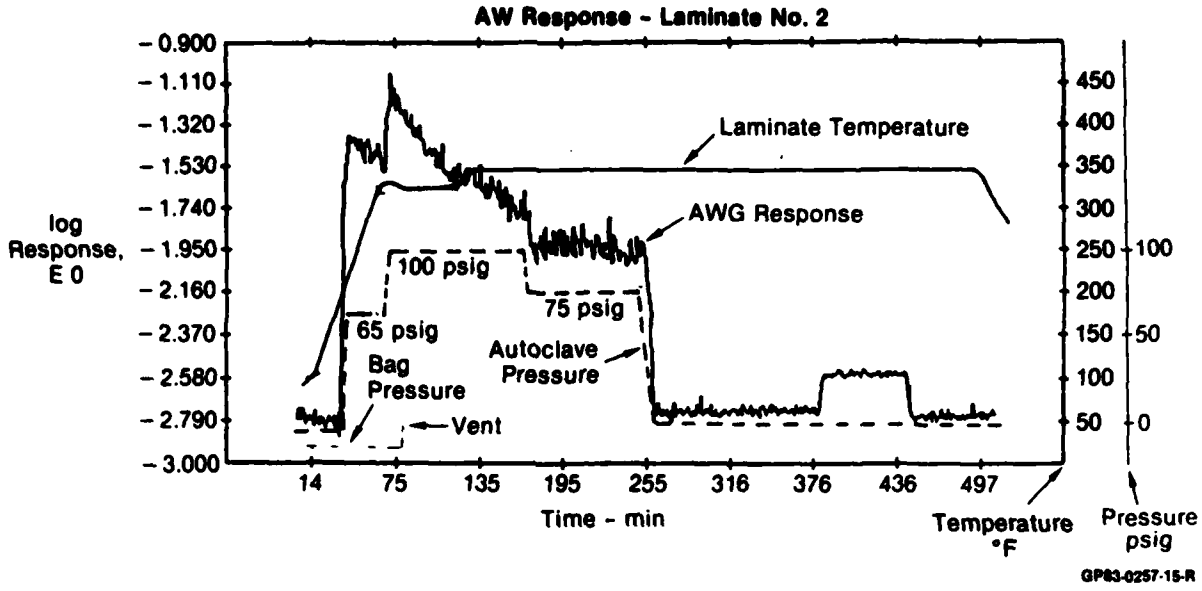

Figure 99. Cure Cycle No. 2 - AWG Response, Temperature and Pressure vs Time

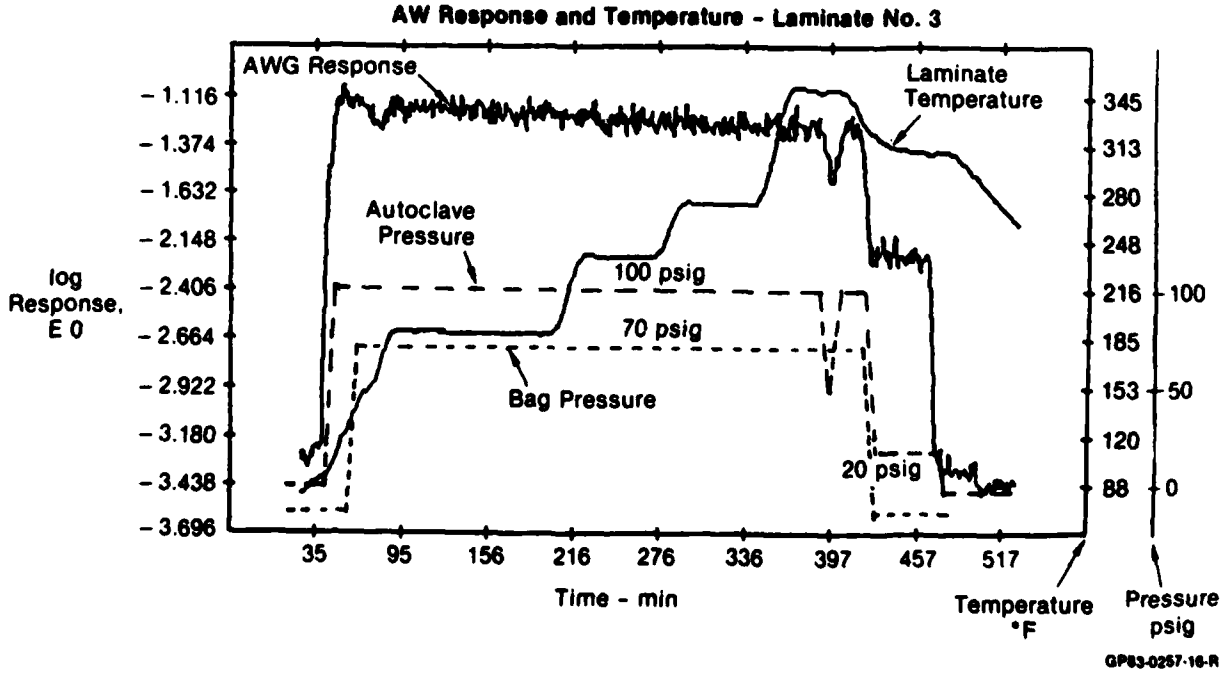

Figure 100. Cure Cycle No. 3 - AWG Response, Temperature and Pressure vs Time

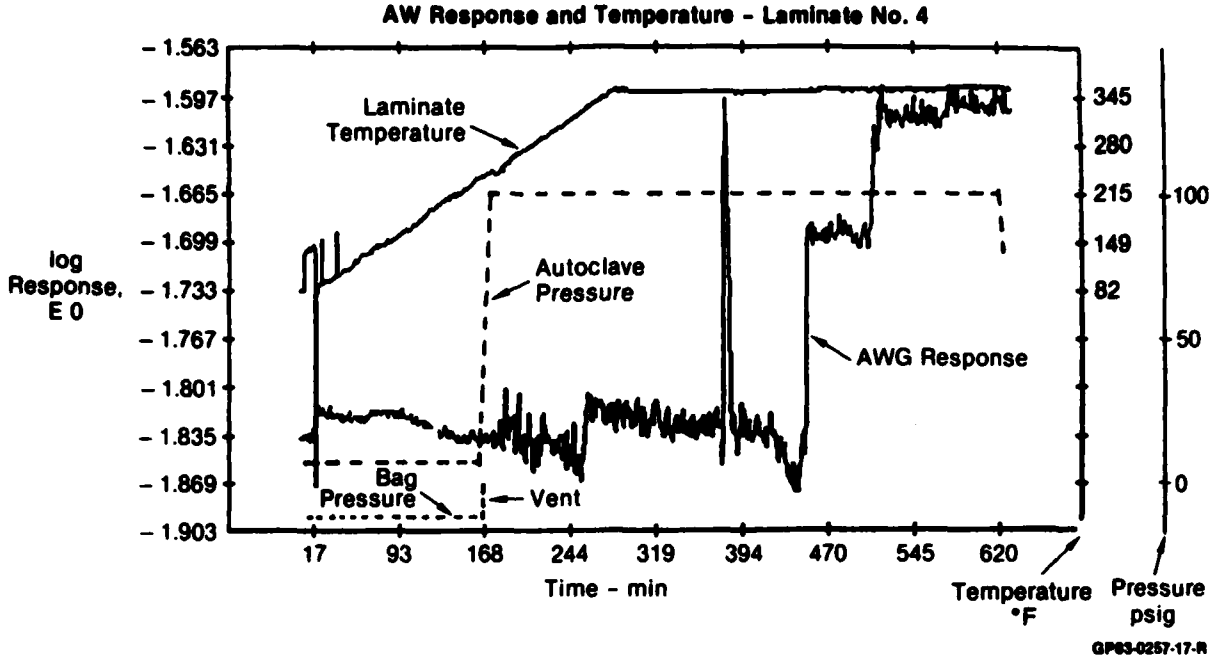

Figure 101. Cure Cycle No. 4 - AWG Response, Temperature and Pressure vs Time

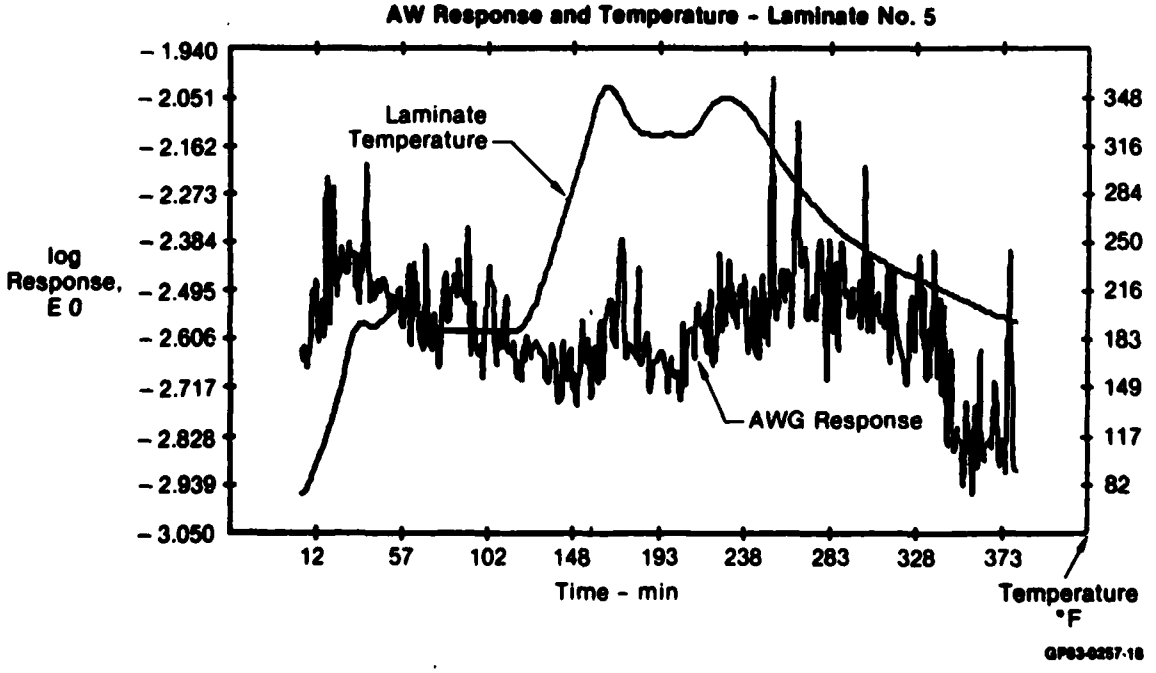

Figure 102. Cure Cycle No. 5 - AWG Response and Temperature vs Time

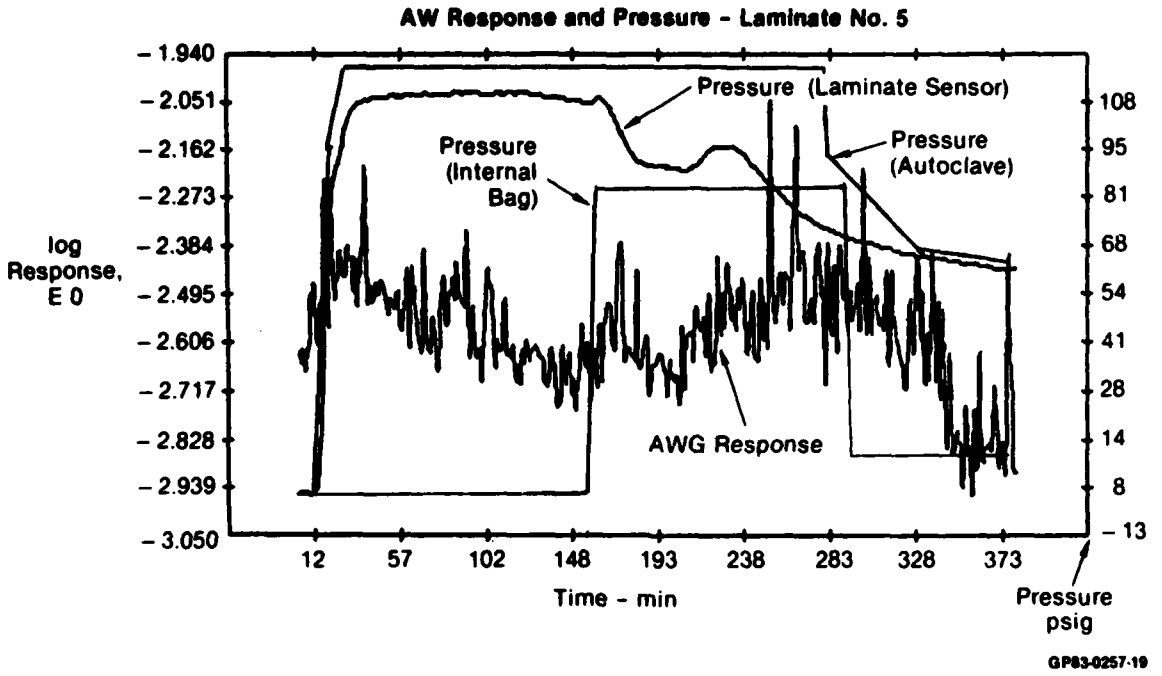

Figure 103. Cure Cycle No. 5 - AWG Response and Pressure vs Time

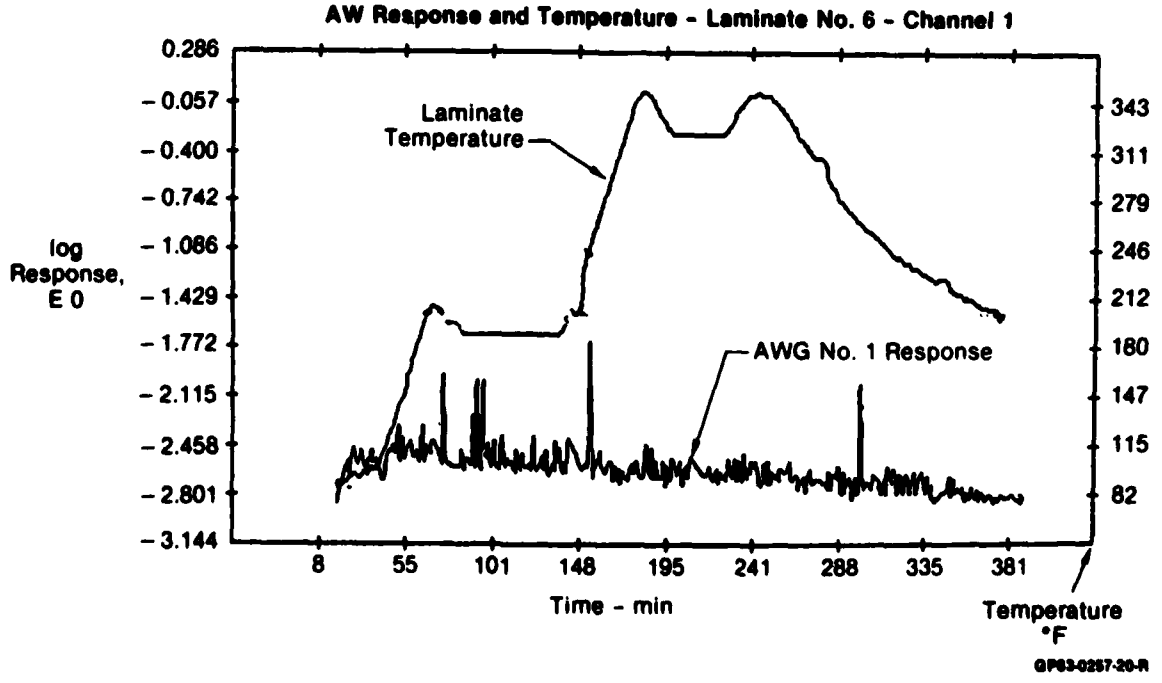

Figure 104. Cure Cycle No. 6 - AWG No. 1 Response and Temperature vs Time

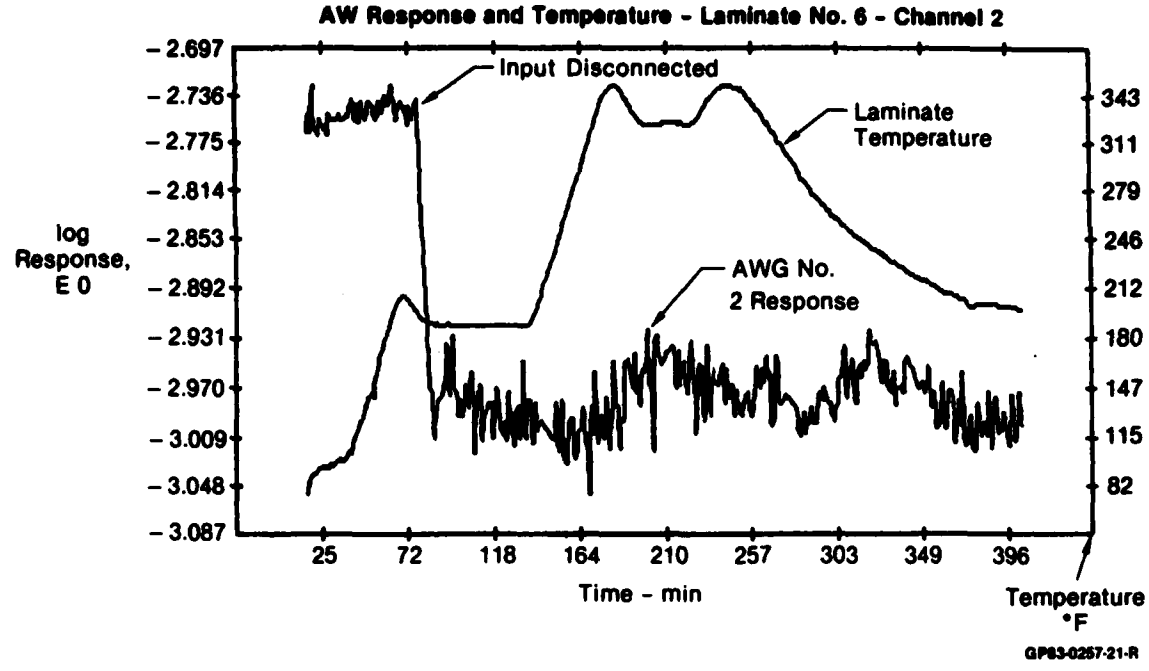

Figure 105. Cure Cycle No. 6 - AWG No. 2 Response and Temperature vs Time

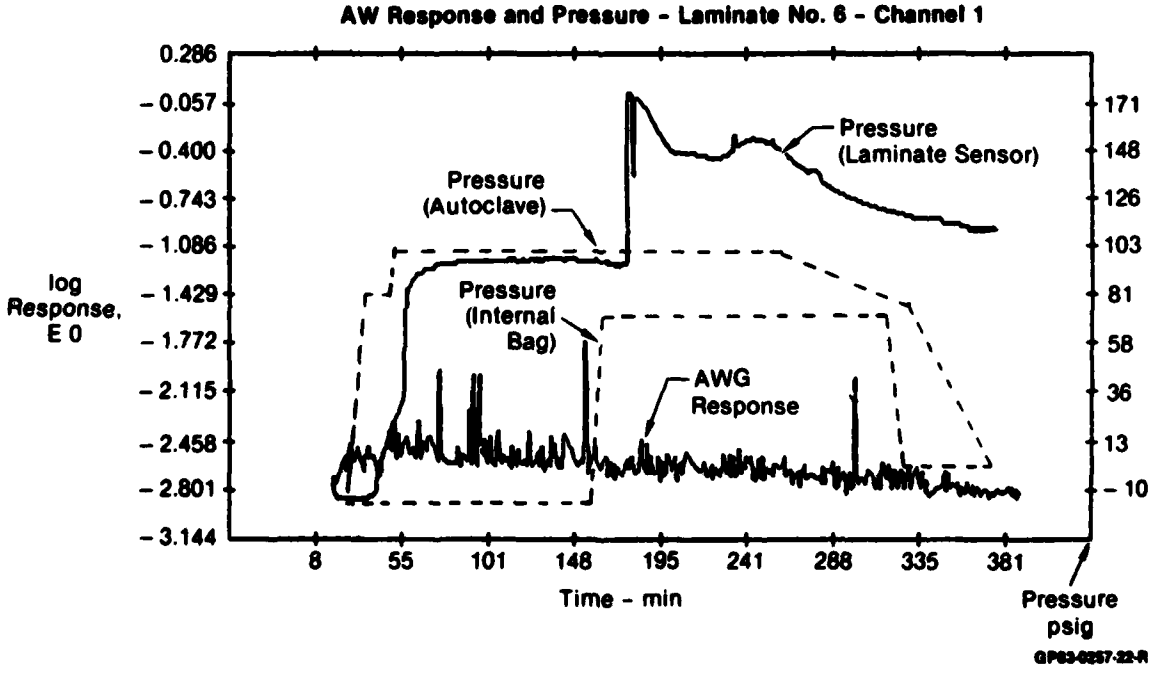

Figure 106. Cure Cycle No. 6 - AWG No. 1 Response and Pressure vs Time

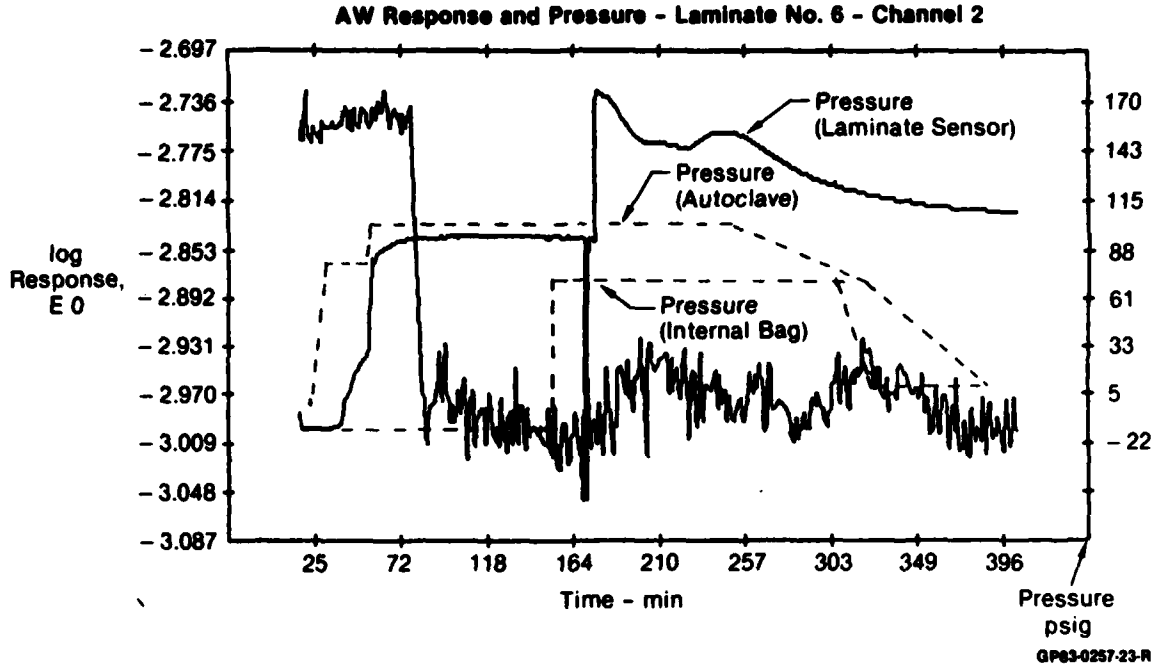

Figure 107. Cure Cycle No. 6 - AWG No. 2 Response and Pressure vs Time

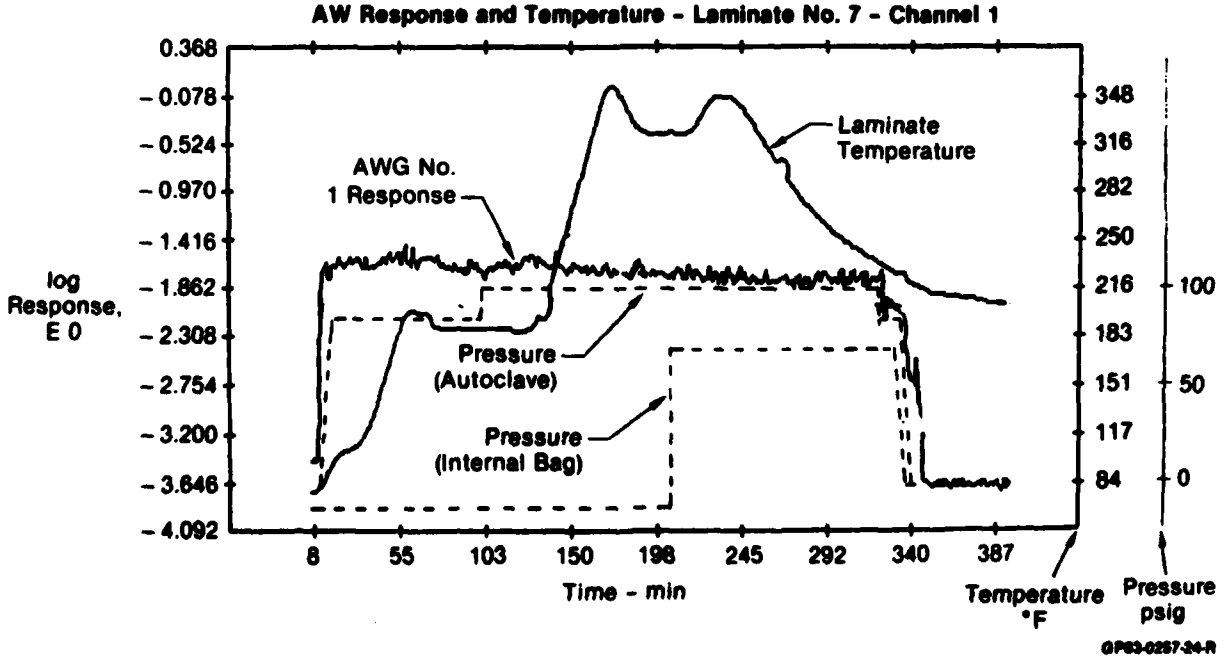

Figure 108. Cure Cycle No. 7 - AWG No. 1 Response, Temperature and Pressure vs Time

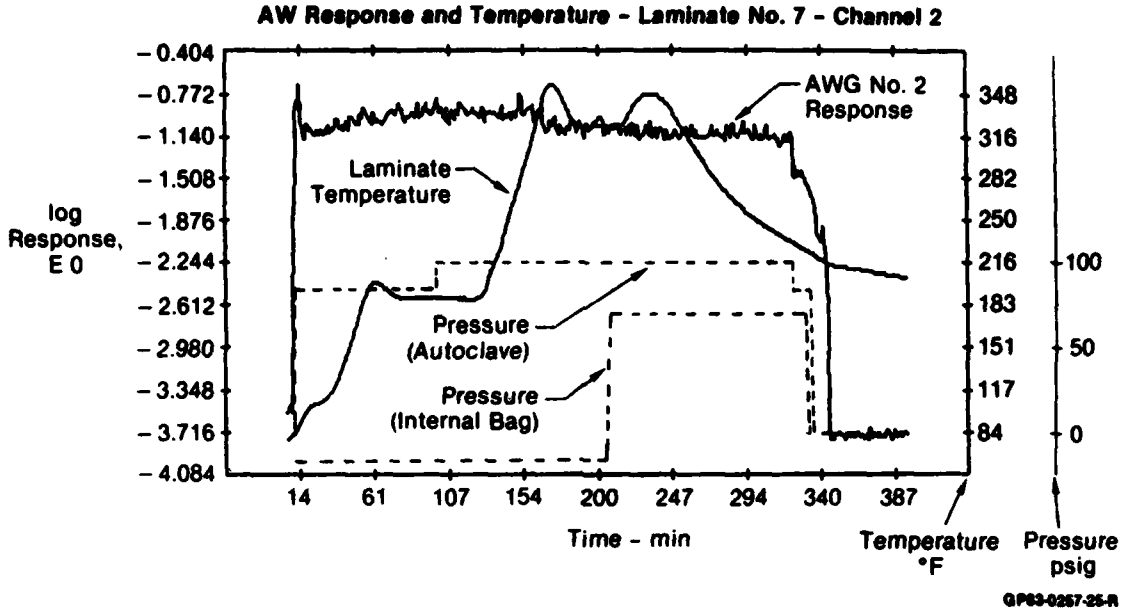

Figure 109. Cure Cycle No. 7 - AWG No. 2 Response, Temperature and Pressure vs Time

Some comments regarding the AWG responses can be made based upon the data shown in the figures, however. In some cases, e.g., cure cycle No. 2 (Figure 99), the response appeared to be influenced by pressure changes. In cure cycles No. 1, 2, 3 and 7, the response level increased (loss decreased) significantly when autoclave pressure was applied; this was not evident in the other runs, however.

6.5.2 Results and Sensor Response (Two Waveguides) - Results of the two-waveguide cure monitoring experiments were of interest. In this setup, a signal is transmitted into one waveguide and received by the other. This system was developed by Westinghouse as a technique to detect attenuation within a laminate caused by voids (Figure 46).

Parallel waveguide wires were positioned in laminates for Cure Numbers 6 and 7, which were the most likely to incur porosity due to high prepreg moisture content, excessive bleeder and (Cure No. 7) late application of internal bag pressure. The AWG's were 4 inches apart within the same ply layer, as shown in Figure 84. Signal response from both waveguides (Channels 1 and 2) are shown for cure Cycle No. 6 in Figures 104 and 105. At the beginning of the run, voltage input was applied to both waveguides, but was disconnected from Channel 2 AWG at the point indicated in Figure 105. This waveguide continued to show a signal response, although at a lower level, throughout the remainder of the cure cycle. The waveform of the signal for Channel 2 waveguide toward the end of the cure cycle (Figure 111) was also very similar to that at the beginning of the run taken while a 50 V input was being applied (Figure 110). It can be concluded that the concept of measuring attenuation between two waveguides is valid, although the absolute losses due to the resin/void sources in this experiment could not be assessed because of the high overall system losses.

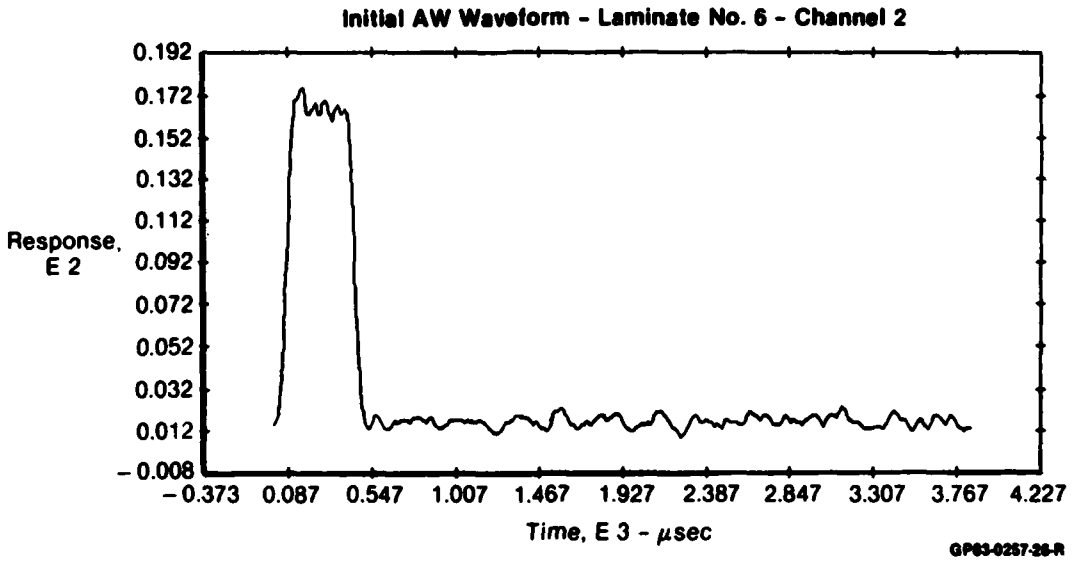

Figure 110. Cure Cycle No. 6 - AWG No. 2 Waveform at Start of Cure 50 V Input

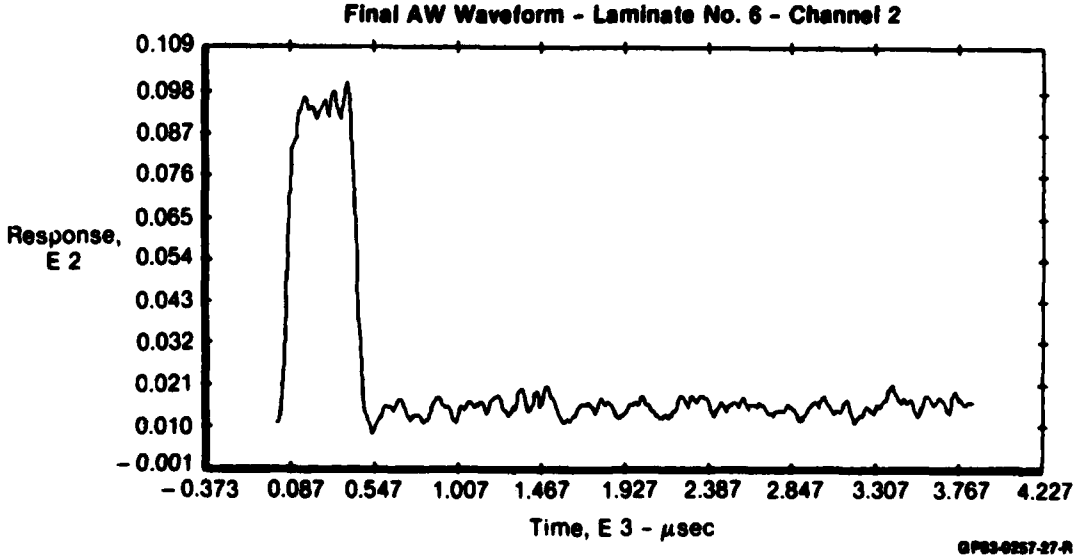

Figure 111. Cure Cycle No. 6 - AWG No. 2 Waveform at End of Cure (No Direct Input)

7.0 STATUS OF SENSOR SYSTEMS FOR CURE MONITORING AND CONTROL OF COMPOSITE FABRICATION

7.1 FLUORESCENCE OPTRODE CURE SENSOR (FOCS)

The FOCS signal profiles obtained during monitoring of approximately 100 separate cure cycles conducted during this program clearly indicate the capability of this new sensor to monitor the chemorheological changes taking place during cure and detect the minor changes taking place during the late stages of cure. The fact that the FOCS produces two high quality signal profiles (intensity and wavelength) simultaneously for each cure cycle doubles the amount of information generated and increases the probability for better control of the process.

Because the FOCS is based on a relatively new concept for cure monitoring, and because the level of effort in its development in comparison to dielectrometric and acoustic cure monitors has been small, basic knowledge of the underlying viscosity-dependent fluorescence (VDF) phenomenon is still lacking. The configuration of the optrode-laminate (OL) interface was found to be of critical importance for the reproducibility and the quality of the FOCS signal profiles. The resin cavity OL interface configuration produced good results in many laboratory tests but caused failure in three out of seven runs in the autoclave process monitoring trials. Additional development work on the OL interface is, therefore, required to realize the full potential of the FOCS.

The results obtained during the process monitoring trials are not representative of the FOCS capability. Considerable potential for improved run to run reproducibility exists. Improved reproducibility can be achieved by correcting the raw signal levels for the inner filter effects.

The usefulness of FOCS concept goes beyond cure monitoring. In work outside the scope of this program, the potential of an embedded FOCS waveguide to monitor the cure during fabrication of a laminate, and subsequently monitor the sorbed water content of the cured laminate, was demonstrated.

In the course of this work our understanding of the factors affecting the performance of the FOCS has increased dramatically and brought the technology considerably closer to the point at which the sensor will be ready for the demanding trials on the manufacturing floor.

7.2 ACOUSTIC WAVEGUIDE (AWG) CURE SENSOR

Based on the results of this program the feasibility of using embedded acoustic waveguides to monitor the cure of carbon-epoxy composites has been established, at least in laboratory-scale cure runs. It has been shown that the technique is theoretically sound, gives a reasonable qualitative measure of cure, and has the capability to pinpoint gelation by both maximum acoustic signal attenuation and a change in acoustic wave velocity. In addition, rugged 0.020 inch diameter Inconel wires that are suitable for factory use can be used for the waveguide material. A technique using two or more embedded waveguides has been shown to have the potential of scanning large areas of composites for void content.

In order to realize the full potential of AWG for real time monitoring and control of composite curing processes in a factory autoclave, additional development efforts are required in which the engineering issues associated with feeding acoustic waveguides through the autoclave walls and composite bagging with minimum signal loss are addressed. This program would also include tasks directed toward refining, improving and optimizing acoustic waveguide cure-monitoring (AWG). Specifically, these tasks would include investigations of the use of the carbon fibers within the prepreg as acoustic waveguides, and of Inconel waveguides coated with epoxy. The effects of variables within the composite laminate, such as fiber orientations and packing, and resin hydrostatic pressures before and after gelation, upon sensor response patterns should be evaluated.

8.0 ENVIRONMENTAL IMPACT

Utilization of the sensor technology developed and demonstrated in this program will have no environmental consequences with respect to either health or safety considerations. The electronic equipment required to be used in conjunction with the sensors is commercially packaged to meet applicable safety requirements. The FOCS laser light generator is enclosed, even in the experimental equipment mode, to protect personnel from potentially damaging light intensities; this will also be the case for any production-type light source. All of the electrical or light sources are shielded during transmission to the curing medium, and are of sufficiently low power to pose no safety hazard.

9. CONCLUSIONS AND RECOMMENDATIONS

9.1 CONCLUSIONS

9.1.1 Fluorescence Optrode Cure Sensor (FOCS)

- Cure-monitoring of epoxy composites, using a tool-mounted sensor interface, has been successfully demonstrated under actual autoclave environments. FOCS sensor output signal profiles closely track viscosity profiles, and show correlation with degree-of-cure progress during the final cure stage.

- The lack of good reproducibility and data scatter, from run-to-run, result in an inability to predict absolute levels of viscosity or degree-of-cure with accuracy. Sources of these sensor response variations have been postulated, and should be controllable.

- The tool-mounted optrode interface, although shown to be adequate for standard cure-monitoring conditions, requires minor modifications to be fool-proof for all autoclave conditions. This element in the FOCS system is essentially applicable as-is for production cure-monitoring.

- Real-time monitoring and display of FOCS output data and cure temperature profiles have been proved in many actual trials. The system can readily be integrated into a production environment; real-time control of cure parameters could be implemented.

9.1.2 Acoustic Waveguide Cure Sensor (AWG)

- Acoustic waveguide cure monitoring for epoxy composites has been demonstrated, under laboratory conditions, to provide a reasonable measurement of the degree-of-cure. The gelation event can be pinpointed by the response signal.

- Rugged waveguide materials, suitable for factory use in composite materials, have sufficient sensitivity for cure-monitoring.

- Use of multiple embedded waveguides has the potential for monitoring large areas of composites for attenuating conditions such as porosity.

- Current level of understanding of the sources of signal attenuation is inadequate. The effect of these losses is to reduce the signal to noise ratio, reduce run-to-run reproducibility and mask the response characteristics that are solely attributable to cure parameters. Some sources, such as autoclave pass-throughs, are identifiable; others, such as fiber orientation effects, are more subtle.

9.1.3 Pressure Sensors

- The ability of miniature pressure sensors, embedded into a composite material, to provide real-time measurement of resin hydrostatic pressure changes during cure has been demonstrated. The effects of laminate preparation procedures and cure conditions upon the internal pressure changes were shown to be significant; practices that can lead to void formation were identified.

- The utilization of miniature sensors for routine cure monitoring in production would not be realistic, because of the cost of sensors and potential degradation of material properties. However, the use of sensors buried at critical locations, as identified in this program, would be useful in prototype parts to establish optimum conditions of lay up, bagging, tooling and autoclave pressurization cycles.

9.1.4 Cost Considerations

The cure-monitoring sensor systems developed and evaluated in this program have the potential for relatively low cost impact upon overall production cost for composite structures.

In its current configuration, the fluorescence optrode cure sensor (FOCS) is a tool-mounted unit. The interface with the resin during cure is a cavity machined into the autoclave tool surface and covered with a thin plate. For production use, this interface would be a one-time modification to the tool. The fiber optic sensor leads are reusable, quickly connected and disconnected from the tool, and interchangeable within the autoclave for use with any tool that is equipped with the interface modification. It is reasonable to assume that multiple sensor leads could be used during a single autoclave cure cycle to monitor several parts simultaneously by electrooptic switching of the laser excitation from one fiber lead to another.

The only anticipated recurring cost associated with use of the FOCS for production cure-monitoring is the clean-up of the interface resin cell. As an operation included in routine tool clean-up and mold release preparation, the interface preparation will require somewhat more careful attention to detail, to prevent excessive application of mold release, to assure removal of cured resin from flow-holes in the cover, and to prevent scratching of the end of the glass fiber optic clad rod. A small additional labor cost will be associated with this operation.

Future FOCS configurations, such as incorporation of optical fibers within the curing laminate, will change the recurring labor projection somewhat. The tool interface considerations will be eliminated, but the integration of the optical fibers into the prepreg layup will be required. This is not anticipated to add any significant cost to conventional layup labor cost. Since the optical fiber that would be embedded in the lay up is a relatively low cost material, no significant material cost would be incurred.

In the case of the acoustic waveguide (AWG) cure sensor, the anticipated cost associated with production use is also minor. In the current configuration, the waveguide itself is 0.02 inch diameter nichrome wire, which becomes an integral part of the cured structure. The transducers are reusable. In this program, the waveguide wires were extended through ports in the autoclave and bonded to the transducer faces with a quick-setting epoxy adhesive. This operation requires only a few minutes of labor. It is anticipated, however, that excessive sensor response attenuation will drive any future system away from this setup. Instead, it is expected that transducers and leads, capable of withstanding the temperatures and pressures of the autoclave environments, would be positioned inside the autoclave shell. Quick-attach connectors might replace the bonding operation, thus further reducing recurring labor costs.

Miniature pressure sensors are not anticipated for recurring production use, but only for development of optimum tooling, bagging and cure parameters. The current high cost of the sensors, which are not reusable, would make this practice economically unfeasible.

9.2 RECOMMENDATIONS FOR FUTURE WORK

Additional efforts are required to achieve the full potential of the Fluorescence Optrode (FOCS) and Acoustic Waveguide (AWG) sensor systems for real-time monitoring and control of composite cure processes:

- Studies of the FOCS system variables that are responsible for the lack of reproducibility found in this effort should be undertaken, in order to be able to establish more accurate quantitative relationships between sensor output values and material properties.

- The FOCS concept should be investigated for use in "smart-skin" applications, in which fiber optic sensors that are buried in the laminate are used for post-fabrication monitoring of physical property changes as well as for cure-monitoring.

- Studies should be undertaken to understand the effects of laminate environment (fiber orientations, packing, etc.) and autoclave environment (bag sealants, autoclave interface, etc.) upon AWG sensor response and attenuation.

- Evaluation of waveguide materials, such as epoxy-coated nichrome, carbon fibers, etc. may yield major improvements in AWG response repeatability and sensitivity.

- AWG improvements should be pursued, not only for cure-monitoring capability but also for their use as embedded "smart sensors" with lifetime NDE capabilities for monitoring composite mechanical properties.

REFERENCES

1. "Computer-Aided Curing of Composites," Air Force Contract No. F33615-83-C-5088, Air Force Materials Laboratory, Wright-Patterson AFB.

2. "Composite and Nonmetallic Materials," 1984 and 1985 MCAIR Independent Research and Development, MDC Reports Q0871-7 and Q0874-7.

3. Polymers and Composites, McDonnell Douglas 1983 IRAD Report Q-0866.

4. Polymers and Composites, McDonnell Douglas 1984 IRAD Report MDC Q0871-4-102.

5. Polymers and Composites, McDonnell Douglas 1985 IRAD Report MDC Q0874-4-102.

6. R. L. Levy, "Novel Fiber-Optic Sensor for Monitoring the Composite Curing Process," Polym. Mater. Sci. Eng. 54, 321 (1986).

7. R. L. Levy and S. D. Schwab, "Performance Characteristics of the Fluorescence Optrode Cure Sensor," Polym. Mater. Sci. Eng. 56, 169 (1987).

8. G. Oster and Y. Nashijima, "Fluorescence and Internal Rotation: Their Dependence on Viscosity of the Medium," J. Am. Chem. Soc. 78, 1581 (1956).

9. T. Förster and G. Hoffmann, "Effects of Viscosity on the Fluorescence Quantum Yield of a Dye System," Z. Phys. Chem. 75, 63 (1971).

10. C. J. Tredwell and A. D. Osborne, "Viscosity Dependent Internal Conversion in the Rhodamine Dye, Fast Acid Violet 2R," J. Chem. Soc. Faraday II 76, 1627 (1980).

11. R. O. Loutfy, "Fluorescence Probe for Polymerization Reactions: Bulk Polymerization of Styrene," J. Polym. Sci. 20, 825 (1982).

12. T. Hirschfeld, "Feasibility of Using Fiber-Optics for Monitoring Groundwater Contaminants," Optical Eng. 22, 527 (1983).

13. A. Novak, "A Method for Corrections of Inner Filter Effects in Measurement of Fluorescence Spectra," Coll. Czech. Chem. Commun. 43, 2869 (1978).

14. V. Alan Mode and D. H. Sisson, "Correction of Inner Filter Effects in Fluorescence Spectrometry," Anal. Chem. 46, 200 (1974).

15. R. T. Harrold, U.S. Patent No. 4,590,803, May 27, 1986, "Acoustic Waveguide Monitoring."

16. R. T. Harrold and Z. N. Sanjana, "Acoustic Waveguide Monitoring of Cure and Structural Integrity of Composite Materials," Polym. Eng. & Sci. 26, 5 (1986).

17. R. T. Harrold and Z. N. Sanjana, "Theoretical and Practical Aspects of Acoustic Waveguide Cure Monitoring of Composites and Materials," Proc. 31st. Intn'l. SAMPE Symp., p. 1313 (1986).

18. R. T. Harrold and Z. N. Sanjana, "Material Cure and Internal Stresses Monitored Via Embedded Acoustic Waveguides," Proc. 1986 Intn'l Congress on Technology and Technology Exchange, Pgh., PA, October 6-8, 1986, Paper AM-2-3.

19. R. T. Harrold and Z. N. Sanjana, "Nondestructive Evaluation of the Curing of Resin and Prepreg using an Acoustic Waveguide Sensor," Review of Progress in Quantitative Non-Destructive Evaluation, Vol. 6B, pp. 1277-1285 (1987).

20. S. Arrhenius, "Immunochemistry", Leipzig (1907).

21. J. K. Gillham, et al., "Isothermal Transitions of a Thermosetting System," J. Appl. Polym. Sci., 18, 951 (1974).

22. P. K. David, "Correlation of Arrhenius Parameters: The Electrotechnical Aging Compensation Effect", IEEE Transactions on Electrical insulation, Vol. EI-22, No. 3, June 1987.

23. T. P. L. Li and G. D. Chadderdon, "Thermal Signature and Remaining Shelf Life Prediction of Epoxies", Hybrid Circuit Technology, January 1984.

END

DATE

FILMED

DTIC

9-88